Extinction, Fixation, and Invasion in an Ecological Niche

by

MattheW Badali

A thesis submitted in conformity with the requirements
for the degree of Doctor of Philosophy
Graduate Department of Physics
University of Toronto

Abstract

Extinction, Fixation, and Invasion in an Ecological Niche

MattheW Badali
Doctor of Philosophy
Graduate Department of Physics
University of Toronto
2019

The competitive exclusion principle postulates that due to abiotic constraints, resource usage, inter-species interactions, and other factors, ecosystems can be divided into ecological niches, with each niche supporting only one species in steady state. Seemingly in conflict with this principle, remarkable biodiversity exists in biomes such as the human microbiome, the ocean surface, and every speck of soil. Despite their importance in human health and conservation biology, the long term dynamics, diversity and stability of communities of multiple interacting species that occupy similar niches are still not fully understood. Biodiversity decreases as species go extinct and increases as new species establish themselves, and both extinction and invasion are moderated by interactions with other species. Classically, the theory of niches describes biodiversity, as relatively static. More recently popular, neutral theory models biodiversity as a balance of successive extinctions and invasions.

Stochastic fluctuations allow mathematical models, like the neutral Moran model, to exhibit extinction. Stochasticity also connects neutral and niche theories, with Moran dynamics being one limit of a Lotka-Volterra model. The extinction times in the neutral and niche limits are qualitatively different, indicative respectively of exclusion and coexistence of two species, yet the transition between these limits has not been fully investigated.

I identify the nature of the transition by calculating the mean extinction time with an arbitrarily accurate technique, discovering that competing species can coexist unless their ecological niches entirely overlap, which implies that extinction and loss of biodiversity is less common than predicted by neutral models. Biodiversity is also maintained by new species entering the system, a process I represent with a single invader in the Lotka-Volterra model and repeated immigrants into the Moran model. I demonstrate that greater niche overlap leads to longer invasion times, and less likelihood of success of an invasion attempt. With the Moran model I find the critical immigration rate at which immigrants are likely to maintain their presence in the system.

Contents

List of Figures

Chapter 1

Introduction

1.1 Motivation and background

Mathematical ecology is one of the oldest discipline of mathematical biology, with its relevance dating back at least since Malthus used a model of exponential growth to argue that overpopulation would lead to widespread famine and disease, more than two hundred years ago [1]. About a century ago, Lotka [2] and Volterra [3] extended the logistic equation of Verhulst [4] and applied it to biological systems, arriving at the famous predator-prey equations. Midway through the last century, Wright [5], Fisher [6], and Moran [7] proposed urn models that demonstrate fixation and extinction in a way that is easily intuited and also treatable mathematically. Around the same time, Kimura was revolutionizing genetics by proposing models that could account for the evolution and eventual fixation or extinction of mutant alleles [8, 9]. Ecology benefited from the island biodiversity theory of MacArthur and Wilson [10]. In the last couple decades there has been debate as to the extent of neutral versus niche effects in ecological dynamics, sparked by Hubbell's unified neutral theory of biodiversity and biogeography [11]. The history of mathematical and theoretical biology, especially as applied to ecology, is punctuated by significant models like these inspiring deeper investigations of both the quantitative details and qualitative trends that the biological world might contain.

The application of mathematics to ecology opens up the possibility of addressing a variety of problems central to the field in a quantitative and predictive manner. One of the simplest problems, and one treated in this thesis, is this: what is the probability of and timescale over which a species will go extinct in an ecosystem [12, 13]? Specifically, given two competing species in a system, what is the probability of extinction of either species before the other, and the timescale over which this occurs? In an ecosystem with competing species, when all but one species has gone extinct, that final species is said to have fixated in the system.

The lifetime and extinction of species is both of theoretical interest and a pressing concern for humanity, as we exist in an epoch of unprecedented rates of extinction [14]. Conservation biology is concerned with managing and maintaining the biodiversity on Earth, to avoid these massive extinctions and potential system collapse [14–19]. Biodiversity, simply put, refers to the number of species or genetic strains in an ecosystem. I would like to highlight the issue of biodiversity, one of the stubbornly unsolved problems in modern ecology [20–23]. In 1961 Hutchinson published "The paradox of the plankton" [24], in which he speculated about an apparent contradiction: for plankton living in the upper layer of the

ocean far from shore there are few different resources on which to live, yet there is an immense diversity of different species of plankton that appear to coexist. Surely those species that reproduce the quickest or use the resources most efficiently would outcompete all others such that only the fittest would survive. This principle of competitive exclusion, sometimes called Gause's Law [25] states that "two species cannot coexist if they share a single [ecological] niche." In systems with few resources and therefore few niches, one expects that only few species will persist at any given time. The expectation is that in this homogeneous ecosystem with extreme nutrient deficiency the competition should be severe, and only a few species should persist, many fewer than the number observed.

A variety of solutions have been proposed to resolve the paradox of the plankton but there is as yet no consensus [26]. These include [20, 21, 24, 26]: the system is approaching a steady state of fewer species but very slowly; the ecosystem contains as yet undiscovered metabolic resources or factors that help differentiate their niches; environmental fluctuations or oscillations stabilize the system; spatial heterogeneity allows for local extinction but supports the great biodiversity on larger length scales; the system is stabilized by life-history traits of the plankton; the system is stabilized by the presence of predators to the plankton; there is symbiosis or commensalism between the various plankton species. This lack of consensus is a gap in the literature. While in reality each proposed solution likely contributes to some degree, a deeper understanding of each mechanism is required to evaluate their respective contributions to this problem and to others in ecology. In this thesis I address a part of the general problem by systematically investigating the extinction and coexistence of competing species in a system with parameterized overlap between their niches.

Along with the problem of the maintenance biodiversity in its own right, I have other motivations related to biodiversity as it manifests in various systems. Most obvious, and arguably most pressing to society, is the realm of conservation biology. Biodiversity is often used as an indicator of the health of an ecosystem [14–19]. A clearer understanding of the forces that maintain biodiversity could provide new and easier metrics for evaluating the health of an ecosystem, and hence the efficacy of various conservation efforts. The mechanisms of species maintenance are related to those of speciation, and an ecosystem losing stability can refer to both its collapse or the invasion of a foreign species. Invasion of a new mutant or immigrant strain or species into the system is a problem deeply intertwined with that of biodiversity maintenance [11].

Invasion is also relevant in the domain of health care. We are only recently learning, for example, about the composition of the microbiome in humans and its relation to health [27–31]. Imbalance of the microbiome composition, or invasion of a new species, can greatly impact a person's wellbeing, and a theory of whether an invasion will be successful and how long it might persist would go a long way toward diagnostics and prognostication. So too does the prediction of extinction probability and times have a number of applications. Experimentally, scientists often grow a population of one or two strains in a controlled, constrained environment to which my results are especially suited. And other than the obvious modern ecological ones, extinction times are useful in paleontology. The fossil record shows a number of species in different epochs, and these data make more sense in the light of a consistent theory of species survival and eventual decline. Similarly, extinction and fixation times are already used in the construction of phylogenetic trees [32–34]. The more accurate a theory of extinction timescales developed, the more precisely we can perform phylogenetic analyses. Mapping existent species to their common ancestors falls under the purview of coalescent theory [35]. This is part of the impact of the results presented in this thesis, in that I calculate extinction times to arbitrary accuracy, using a

controlled approximation largely neglected in the literature. Finally, with this thesis I hope to contribute to the debate of niche versus neutral theories, by showing how a Lotka-Volterra model transitions from one to the other.

1.2 Niche theories

The classic explanation for maintenance of species in an ecosystem is the theory of niches [21, 36]. The competitive exclusion principle states that in any given niche one species will eventually dominate. It is inextricably linked to the concept of an ecological niche, which Grinnell popularized more than a century ago [37]. Since then there has been debate as to its meaning and utility as a concept. Following Leibold [36], I refer to the definition of a niche according its two major uses: as the habitat or requirement niche and the functional or impact niche.

The requirement niche: Grinnell [37] defines a niche as those ecological conditions that a species can live within. These ecological conditions include environmental levels and those organisms on different trophic levels than the species, like their predators and prey, but not those on the same trophic level that might compete with them. Hutchinson [24] agrees with Grinnell, and has provided one of the most enduring conceptualizations of a niche, that of an "n-dimensional hypervolume" in the space of factors that could affect the growth or death of a species. For each factor there is some range at which the species can reproduce faster than it dies out. This is true both for abiotic factors such as temperature, and biotic factors like the concentration of predators. Sometimes these ranges are bounded by zero (eg. cannot survive with no carbon source), sometimes they are unbounded (eg. no amount of prey is too much), and sometimes they depend on the values of the other factors involved (eg. salt is fine for sea creatures so long as there is an appropriate amount of water along with it). But in the space of all these factors, Hutchinson calls the fundamental niche that volume in which the species would have a greater birth rate than death rate. He defines the realized niche as the point or subspace in this high dimensional space that the species effectively experiences, given that it is existing and potentially coexisting in an ecosystem. This also lends a natural definition of niche overlap, as the (normalized) overlap of the fundamental niches of two species [10]. The requirement niche tells us whether the coexistence point of two species is physical, according to a simple model of two species [38]. It is inherently linked to the argument that the number of limiting factors delimits the number of niches in an ecosystem [39–41].

The impact niche: The other usage of the term niche, that of a functional or impact niche, was popularized by Elton [42] and MacArthur & Levins [10]. Whereas the requirement niche focuses on what factors a species needs to live, the impact niche looks at how the species affects these factors. Their conception of a niche describes how a species influences its environment, or how that species fits in a food web; essentially, what role it plays in an ecosystem. This idea is especially attractive to those who study keystone species (those species that play a disproportionate or critical role in maintaining an ecosystem) [20, 21, 43] but is easily understood from an elementary understanding of what an ecosystem is. By way of example, in every ecosystem with flowers there is something that pollinates them. Whether the pollinator is a bird or an insect species is irrelevant; this role exists in the ecosystem, and so a species evolves to occupy this niche, to take advantage of the nectar the flower offers. The niche, in this view point, is the role the species plays in the ecosystem with regards to the other species and the environment; how it impacts the system. As per one simple model of two species, the impact niche tells us whether a coexistence point of two species is stable [44].

Both of these meanings for the word niche have their use. The literature shows attempts to resolve the discrepancies that arise when the two definitions are at odds [36, 43]. In chapter 2 I show an example derivation of the Lotka-Volterra system based on an argument of limiting factors that aligns with the requirement niche definition. However, my results hold regardless of one's definition of a niche, so long as a niche overlap parameter can be defined.

The Lotka-Volterra model can be thought of as a minimal model of niche theory [45]. The original Lotva-Volterra model was introduced around a century ago to describe the dynamics of a population of a predator and its prey. It can be seen as an extension of the Verhulst, or logistic, equation, from one to two dimensions. Throughout the thesis I shall refer to it both as a coupled logistic or Lotka-Volterra model. In its modern incarnation the generalized Lotka-Volterra model is typically written as

$$\begin{aligned} \dot{x}_1 &= r_1 x_1 \left(1 - x_1/K_1 - a_{12} x_2/K_1\right) \\ \dot{x}_2 &= r_2 x_2 \left(1 - a_{21} x_1/K_2 - x_2/K_2\right). \end{aligned} \tag{1.1}$$

The generalized Lotka-Volterra model is the accepted terminology for a dynamical system that depends linearly and quadratically on the populations modelled, with no explicit time dependence. The Verhulst or logistic model is one of these equations with its $a_{ij} = 0$. The classic Lotka-Volterra model is attained by taking the K_i's to infinity, keeping the a_{1j}/K_i ratios positive and finite, choosing r_i to be negative for the predator and positive for the prey [3, 46]. This predator prey model has oscillating dynamics about a center fixed point. I am interested in the competitive variant, where the K_i's are finite and r_i's are positive. Such a model corresponds to species that are in the same trophic level (or position in the food chain), such that two competing species can share the same predators or use the same prey as resources. More details of the Lotka-Volterra model are provided in chapter 3. Prior to the coupled logistic model that is the Lotka-Volterra model, chapter 2 treats a single species logistic model, while chapter 4 further explores the 2D generalized Lotka-Volterra model, and chapter 5 considers a Moran model with immigration. Some authors [47–50] have observed that for certain parameter values the stochastic 2D generalized Lotka-Volterra model exhibits dynamics similar to those of the Moran model [7]. They did not examine how the dynamics change as the Moran limit is approached; the transition to this limit is one of the main investigations of this thesis.

The parameters in the Lotka-Volterra equation are phenomenological and easy to understand. The turnover rate r_i, sometimes called the growth rate, reproductive ratio, or Malthusian parameter, gives the maximum growth rate a species i can achieve, specifically when first colonizing an empty system, such that the intraspecific (x_i/K_i) and interspecific $(x_j a_{ij}/K_i)$ competition terms are small. The parameter K_i is called the carrying capacity of the ecosystem, the average population the system will sustain in the absence of competitor species, given the resources available and other limiting factors present in the system. Together these two parameters, which are the only two that show up in a single species logistic equation $\dot{x} = rx(1 - x/K)$, motivate r/K selection theory, coined by MacArthur and Wilson [51]. The theory of r/K selection posits that there is a trade-off between the quantity and the quality of offspring, based on the effects of increased r or K [51]. The other parameters in the Lotka-Volterra equations are the a_{ij}'s. These parameters represent the niche overlap between the two species, or the ratio of interspecific to intraspecific competition. They can be derived from the limiting factors like resources and predators that define a niche (see [10] for one example and [52] or chapter 3 of this thesis for a different argument). There is an unresolved debate in the field as to how niche overlap should

be measured or defined [36, 53–62]. For my purposes, a_{ij} is the ratio of the effect of interspecific to intraspecific competition. The regimes of the parameter space of the deterministic Lotka-Volterra model presented are discussed in chapter 2 and in the literature [49, 63, 64].

1.3 Neutral theories

In niche models like the Lotka-Volterra model each species exists at its carrying capacity, or at an effective carrying capacity diminished by competing species extant in the ecosystem. The distribution of species abundances is predicted by the distribution of carrying capacities, in complicated models of niche partitioning or apportionment [36, 65, 66]. In contrast to niche models are neutral models, that have complete niche overlap and assume that all species share one carrying capacity for the system. Neutral models like that of Hubbell are favoured for their parsimony, the simplicity with which they can be understood simultaneous with the accuracy of their predictions [11, 43, 67, 68]. Hubbell's neutral theory of biodiversity is a minimal working model for calculating species abundance curves. Similarly, the models of Wright, Fisher, Moran, and Kimura are minimal models that show extinction (removal of a species) and fixation (removal of all but one species). Neutral models also underlie the simplest version of coalescent theory and phylogenetic tree reconstruction [33, 35], showing their use not only as minimal models but in whole sub-fields of ecology.

A neutral theory is one for which intraspecies interactions are the same as interspecies interactions, in strength and in how they affect the birth or death rates of each species. That is, an organism competes equally strongly with members of its own species as with those of other species. No species is distinguished or exceptional in a neutral theory. Thus, unless the whole system's net population is increasing or decreasing, a given organism (and hence its species) is equally likely to reproduce or die, and on average its species abundance is constant. Whether and why different species should regard each other the same as themselves is a matter of debate [11, 43, 68, 69]. It is important to clarify the difference between neutral theories and those that are simply symmetric. In a symmetric theory an exchange of labels between two species has the same effect as an exchange of population sizes. Calling the red species of figure 1.2 blue and the blue species red does not change how the system will evolve. Neutral theories are a subset of symmetric theories, since a neutral theory in which each species does not distinguish between self and others automatically allows for an exchange of species labels with no noticeable effect beyond exchanging abundances.

Despite not accounting for distinguishing features that set a species apart from others, neutral theories have been successful; in genetics Kimura predicts allele frequencies [70, 71], and in the context of ecology Hubbell's theory predicts abundance curves [11, 43, 67, 68]. Kimura was inspired by alleles rather than species, but the rationale is similar: allele frequencies fluctuate in a population, sometimes becoming common, other times rare to the point of disappearing from a population entirely. Alleles are the different variants/species of a gene, the segment of DNA that serves a single function. Most non-lethal mutations to an existing allele tend to leave its function entirely unchanged, which clearly makes for a neutral theory.

Whereas Kimura regarded allele mutations which were often synonymous and therefore neutral, Hubbell argues that different species also follow neutral behaviour and calculates the steady state abundance distribution that follows from such an assumption plus a constant influx of new species. The Hubbell model assumes that each organism from any species competes equally with all others, and

therefore as with Moran the species' probability of reproducing or dying is proportional to its fraction of the population. Hubbell predicts the distribution of species abundances, a binned plot of the number of species that belong in bins of exponentially increasing population size. Following the arguments of Hubbell, one can get an estimate of the expected biodiversity of a community, the number of species that should exist in one trophic level. The abundance distribution he predicts matches well with Fisher's phenomenological log series distribution [72, 73] and with experimental observations in a variety of biological contexts, from trees to birds to microbiomes [11]. Other authors have calculated, for a single species in a Hubbell model, how it is expected to grow and decline, and how long it will last in the system before going extinct [19, 69, 74, 75].

A similar model to that of Hubbell has those species which enter arise not from speciation but from immigration [73, 76]. Rather than being entirely new species, these immigrants are thought to come from a larger, static reservoir, so the system of interest tends to have similar species to the reservoir, as with an island that receives immigrants from a mainland population [51]. This Moran with immigration model can be thought of as a variant of Hubbell's theory; its applicability is less broad, but more apt for islands and similar small ecosystems that have their biodiversity maintained by immigration rather than the formation of new species. For the Moran model with immigration the abundance curve has been simulated [76] and the steady state probability distribution has been calculated [73], however it has not been analyzed to find its qualitatively different regimes of biological interest, nor have the extinction probabilities and times been calculated. This constitutes a gap in the literature, one which this thesis addresses.

In an ecological context, the assumption of complete neutrality whereby each species competes with all others to the same degree as intraspecies competition strains credibility. However, slight perturbations from Hubbell's theory do not significantly alter its results [68]. Furthermore, supporters claim that in some sense the different species are equivalent and behave neutrally, which is why Hubbell's theory seems to work so well in such disparate ecologies [43, 68, 69, 77].

1.4 Stochastic analysis

In the above summaries I have mentioned probability distributions, extinction times, and fluctuations, with a population having a chance to grow or shrink over time. These concepts are all stochastic in nature. In fact, stochasticity is an underlying requirement for neutral models, as I will highlight with the Moran model as an example below. Stochasticity is the technical term for randomness or noise in a system. Whereas over time the solution to, for example, a logistic differential equation simply increases continuously (and differentiably) toward its asymptote at the carrying capacity, a stochastic version allows for deviations from this trajectory, sometimes decreasing rather than steadily increasing toward the steady state, and thereafter fluctuating about the carrying capacity. Figure 1.1 shows an example of the logistic equation with noise, to provide some intuition for how fluctuations can affect a system. Depending on the system of interest, stochasticity may or may not be relevant: it is usually most important for systems with highly variable environments or small typical population sizes [34, 71, 78–82]. In the biological context, Wright and Fisher were pioneers in applying randomness and statistical reasoning. There have since been renaissances in the stochastic treatment of genetics due to Kimura and ecology due to Hubbell, and with new mathematical and computational developments it is popular today.

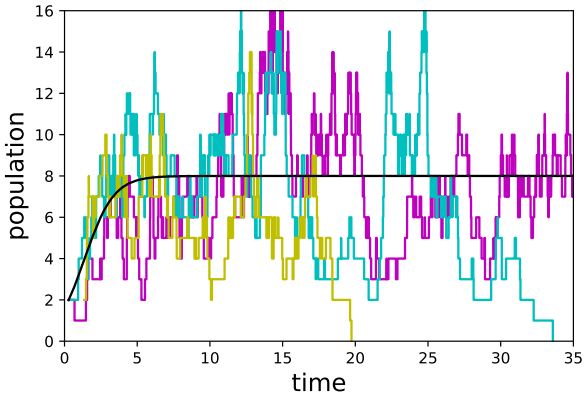

Figure 1.1: *A single logistic system with deterministic and stochastic solutions.* The smooth black line shows the deterministic solution to a one dimensional logistic differential equation (x from equation 1.1 with $a = 0$) with carrying capacity $K = 8$, which the system asymptotically approaches. The jagged lines are realizations of a 'noisy', or stochastic, version of the logistic equation, as simulated using the Gillespie algorithm. Notice that the stochastic versions tend to follow their deterministic analogue but with some fluctuations, which occasionally lead to extinction.

The Wright-Fisher model is a minimal model to show fixation and extinction, and is similar to the Moran model [7], which I will outline here for pedagogical reasons. To arrive at the classic Moran model we must first assume that no individual is better than any other in terms of reproducing faster or living longer; that is, whether an individual reproduces or dies is independent of its species and the state of the system [7]. The next assumption is that the population size is fixed, owing to the (assumed) strict competition for resources or space in the system. That is, every time there is a birth the system becomes too crowded and a death follows immediately. Alternately, upon death there is a vacancy in the system that is filled by a subsequent birth. In the classic Moran model each pair of birth and death event occurs at a discrete time step. (The similar Wright-Fisher model, where each step is longer and involves replacing each individual in the system, has the same long time dynamics [34].) This assumption of discrete time can be relaxed without a qualitative change in results, as will be reviewed in chapter 5. The Moran model is most appropriate for modelling a system of asexually reproducing organisms, like bacteria in an enclosed space.

Figure 1.2 gives a sketch of the possible outcomes each time step of a Moran model. For each birth or death event the participating species is chosen with a chance proportional to its abundance in the system. Since a species is equally likely to increase or decrease each time step, the model is akin to an unbiased random walk. And since each event has an equal probability of happening for a given species, the frequency of that species tends to stay constant on average [7, 70]. However, due to the randomness inherent in the model, the species' frequency in fact fluctuates - this is stochasticity. This fluctuation is not indefinite; there are two states from which the system cannot exit and thus only accumulate in probability of occurrence. These static states are extinction and fixation: the species has no chance of reproducing when at zero population (extinction) and does not change abundance when it is the only species in the system (fixation) as it constantly is both reproducing and dying with unit probability each time step. Both of these cases are absorbing states, so called since once the system reaches either it will stay in that state indefinitely.

The natural mathematical tool to describe stochastic systems like this is a probability distribution

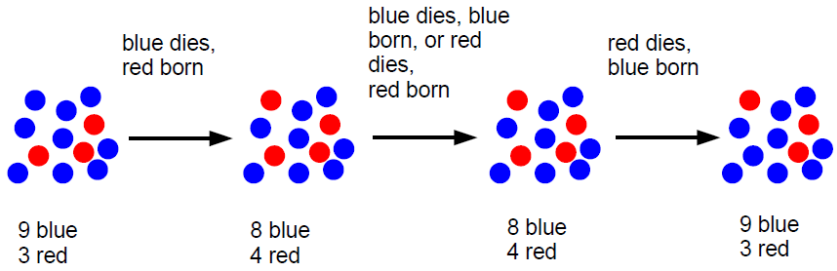

Figure 1.2: *Example Time Steps of the Moran Model.* Here is a sample Moran model with $K = 12$ individuals, initially $n = 3$ of which are red. In the first time step, a red individual is chosen to reproduce (which would happen with probability $n/K = 3/12$) and a blue one dies (probability $9/12$). This increases the number of red individuals in the system. Other possibilities each time step are that the number of reds remains the same or decreases. There is a non-zero chance that in as few as three steps a colour will have fixated in the system. Over time the probability of fixation increases such that it is almost certain the system will fixate eventually. Once only one colour remains in the system the chance that a different colour reproduces (and is thus introduced into the system) is zero, since there are none of that different colour around to reproduce.

over the states. The evolution of the probability distribution is given by a continuity equation called the master equation [78, 82, 83]. As there is a probability of being in each state at a given time, there is a distribution of times when the system reaches fixation or extinction. The mean of this distribution is one of the main objects of study of this thesis. More generally in the field of stochastic analysis it is known as a mean first passage time, the mean time before a system first reaches some predefined state or collection of states. The mean first passage time gives an estimate of the time two species will coexist in a system (or the inverse of the mean fixation rate of the system).

Stochasticity originates from two main causes. It can arise from the extrinsic fluctuations of the environment [84, 85], in that limiting factors like resource availability or temperature fluctuate over time. It is also intrinsic to any system with a finite size or integer state space. A deterministic system like the logistic one shown in the black line of figure 1.1 has a continuous solution, but a real population cannot vary continuously between integers; rather, it is discretized. Constraining the system to integer values, and the inherent randomness in the birth and death times of the individuals, leads to demographic noise [47–50, 86–90]. Demographic stochasticity is the focus of my thesis. Chapter 2 deals with the inclusion of demographic fluctuations in a deterministic equation. Each stochastic model has a deterministic analogue when fluctuations are negligible, but many stochastic models lead to the same deterministic equation [78, 82, 91–93]; prior to my research presented in chapter 1 a comprehensive investigation of the single species logistic model with demographic noise had not been conducted.

It is accepted in the literature that demographic noise in a system whose deterministic analogue has a stable fixed point leads to extinction times scaling exponentially in the system size if the initial condition is near that fixed point [88, 94–98]. That is, if K is the constant or mean system size, then demographic fluctuations lead to:

$$\tau \propto e^{cK} \tag{1.2}$$

for some constant c. This scaling is most readily observed in the logistic system [86, 91, 99–103], covered in chapter 2. Environmental noise in the logistic system has polynomial scaling of the mean extinction time [80, 99]:

$$\tau \propto K^d \tag{1.3}$$

for some constant d. Importantly for this thesis, polynomial dependence on system size is also found when there is no fixed point in the deterministic analogue, or one of neutral stability, like the Moran model [88, 104]. When the deterministic fixed point is unstable extinction happens even in the deterministic limit, and is logarithmic when starting from the fixed point [88, 95, 105]:

$$\tau \propto \ln(K). \tag{1.4}$$

These scalings give the time for the system to start near a fixed point and hit a boundary (which could be a fixed point, absorbing state, or some other boundary). In all these cases K is the system size, typically taken to be some measure of the magnitude of the fixed point when relevant. Often this fixed point is the carrying capacity. For those systems where the fixed point is stable, the extinction time also does not tend to depend on the initial conditions [49], as the deterministic draw to the fixed point is greater than the destabilizing effects of noise, and it is only a rare fluctuation that leads to extinction. A mean time to extinction that is exponential in the population size is commonly considered to imply stable long term existence for typical biological examples, which have large numbers of individuals [80, 106]. A sub-exponential extinction time implies exclusion of a species, and a reduction of the biodiversity of the ecosystem. It has recently been shown that the Lotka-Volterra model, which has exponential scaling, shows Moran-like dynamics in a certain parameter limit, including algebraic dependence of the mean fixation time on system size [47–50]. There is a gap in the literature in that the transition between these two limits has not been carefully examined.

Stochastic equations are generally hard to solve, with a solution only reliably being found for one dimensional systems of birth-death processes [78, 82, 107]. The dimensionality, in an ecological context, is given by the number of distinct species or strains being modelled. Particular realizations of solutions to the master equation are found via the Gillespie algorithm, also knows as the stochastic simulation algorithm [108, 109]. For most of my research I calculate the mean time to extinction exactly, or at least to arbitrary accuracy, following a textbook formulation that involves inverting the transition matrix [78, 91, 110, 111]. There also exist many approximation techniques to deal with stochastic problems, which I discuss in the next chapter. How these approximations fail when estimating the mean extinction time of a simple system like a single species logistic model has not previously been investigated; this investigation constitutes half of the next chapter.

1.5 Structure of thesis

The major questions of this thesis are: How should the probability and mean time to extinction be approximated? Inspired by problems of biodiversity, what is the mean time to extinction of two competing species? Conversely, what is the probability and timescale of invasion of a second species into an ecosystem occupied by a first? I do not guarantee answers to all of these questions, but my research contributes to their understanding. Specifically, there are a few gaps in the literature that I address:

- In a one dimensional stochastic logistic model at least four constants are necessary to parameterize the system. Dependence of the extinction time on rate constant and carrying capacity is well known [86, 91, 92, 98, 105, 112, 113]; one of the other parameters has not been investigated [45].
- The two dimensional stochastic coupled logistic model, also known as the Lotka-Volterra model, reproduces Moran-like dynamics in one parameter limit [47–50]. How the system transitions from

these two qualitatively different regimes is not currently known.

- Invasion into the Lotka-Volterra model has only been previously considered in the Moran limit [110, 114–116] or into a one dimensional logistic model [105]. An exploration of invasion probability and time with niche overlap has yet to be accomplished.

- With speciation the Moran model gives the Hubbell model [11, 69]; with immigration it gives an island model [10] that has remained mostly unconsidered [73], especially in biological interpretation and with regards to its dynamics.

The structure of the thesis follows the above points, with one chapter addressing each of the four points, and a final chapter drawing conclusions about the bigger questions.

First, I use the exact techniques mentioned above and introduced more completely in the next chapter to investigate a single species logistic system, appraising the effect of intraspecies competition on the birth or death rates and how this affects the mean time to extinction. I show that intraspecies interactions shorten the time until extinction when they lead to increased death rates rather than reduced birth rates. The simple system considered in this chapter also affords a thorough comparison of the common approximation techniques to stochastic problems. I show that neither of the two most common approximation techniques, the Fokker-Planck and WKB approximations, accurately captures the exponential scaling and algebraic prefactor of the mean extinction time with system size. Despite its continued use, the failure of the Fokker-Planck technique is well known [80, 98, 101, 117]; this is not the case for the WKB technique. The exact techniques and the approximations together make up chapter 2, regarding a one dimensional system. This chapter is being prepared as a paper for publication [13].

The two dimensional generalized Lotka-Volterra system is the subject of chapter 3. It allows me to study biodiversity maintenance as I probe how long two species will coexist, as characterized by the mean time to fixation in the system. It was already known that the overlap of their ecological niches is the parameter that controls the transition between effective coexistence and rapid fixation. I determine that two species will effectively coexist unless they have complete niche overlap, even if they have only a slight niche mismatch. Along with the mean time to fixation, my analysis uncovers a typical route to fixation, or rather a lack of a typical route, the discussion of which wraps up this chapter.

The next chapter, chapter 4, extends the scope of this thesis to invasion of a new species into an already occupied niche. I calculate the probability of a successful invasion as a function of system size and niche overlap. Then the mean invasion time conditioned on the success of the invasion attempt is analyzed. I discover that the closer the invader is to having complete niche overlap with the established species, the less likely it is to successfully invade, and the longer an invasion attempt will take before it is resolved. Chapters 3 and 4 together form another paper being reviewed for publication [12].

Once these timescales are developed, I regard the Moran/Hubbell model modified to account for repeated invasions of the same species in Chapter 5. I identify the critical value of the immigration rate above which a species will have a moderate population size and below which the population is either large or largely absent in its contribution to the abundance distribution. I also reveal how immigration acts to stabilize a species in a population, such that the time before it first reaches either extinction or fixation is lengthened.

In the conclusions chapter I address some of the big questions I have raised. Regarding biodiversity maintenance, I infer when two species will coexist in a Lotka-Volterra model, and discover that even a small departure from Hubbell's assumption of neutrality drastically complicates his predictions. So long

as there are slight differences in their niches the many species of plankton can coexist. My examination of invasion into the Lotka-Volterra model and my analysis of the Moran model with immigration reinforce that abundance curves cannot be predicted by Hubbell's simple model if there is niche mismatch. The final, Discussion chapter is also where I explore experimental tests, applications and extensions of the results arrived at in this thesis, and suggest next steps for this research, both continuations and implementations to novel situations.

Chapter 2

Extinction: Transition from One Species to Zero

This chapter is based on a paper written by myself, Jeremy Rothschild, and our supervisor Anton Zilman, which is currently being prepared for submission [13].

2.1 Introduction

Interactions are what make physics interesting. So too in biology, interactions between organisms lead to more interesting, and biologically realistic, situations. Later chapters of this thesis will look at interactions between different species. First it will be useful to consider self interactions, that is to say interactions between members of the same species. The inclusion of intraspecies interactions into a model of one species already leads to successful biological models [4, 11, 80, 91, 112, 118–124], of use in that they curb unlimited grown and lead to stable populations [4, 80]. Biologically, interactions mean that the birth or death rate of an organism is influenced by the number of other organisms present in the system. Specifically, the per capita birth rate can be reduced by the presence of competitors, for instance if the competitors reduce the resource abundance and growth is slowed [125, 126]. Alternatively, the per capita death rate can be increased by neighbours, perhaps due to secreted factors like toxins or waste products introduced by those neighbours [121, 127, 128]. The biological reality determines how this shows up in a mathematical model that captures the growth and decay of the population. In either case the interactions are modelled mathematically as a nonlinear term in the equations [80, 91, 92, 100, 102, 118, 119, 121]. The oldest model of intraspecies interactions is named for Verhulst [4], and is also called the logistic equation. The logistic equation has seen wide use in a number of biological contexts [11, 80, 91, 112, 118–124].

While the logistic model has been widely employed, it has not been thoroughly studied in a stochastic context. Specifically, applying demographic stochasticity to a logistic model involves four parameters (basal per capita birth and death values and the magnitude of interaction effects on each). To the best of my knowledge no one has done an exhaustive study of the effect of all four parameters on stochastic quantities like the mean time to extinction, despite the solution being entirely tractable. One subtlety with the stochastic problem is that the mapping from deterministic to stochastic dynamics is not unique; many stochastic models give the same deterministic limit as noise becomes negligible, since

the deterministic dynamics are given by the difference between birth and death rates [78, 82, 91–93]. Some of the parameters that define the stochastic model do not show up in the deterministic limit; in a sense they are "hidden" parameters. This highlights the limitation of only using deterministic theories such as the logistic differential equation; not only do they not allow extinction, they lose some details of a more accurate representation of the physical system. For it is sensible to model each of the birth and death rate with a per capita value, and model the decrease or increase of these basal rates due to intraspecies competition each with another parameter. Of these four parameters, only two show up in the deterministic logistic equation. Whereas the effects of carrying capacity and basic reproductive ratio on the mean time to extinction are known (scaling exponentially and proportionally, respectively) [94, 95, 99], the effect of the other two parameters are not well characterized. Using the metrics of the quasi-stationary probability distribution function (QSD) and the mean time to extinction (MTE) I will show that the allocation of linear and nonlinear contributions between the birth and death rate, as given by these two parameters, has a drastic effect. Specifically, those species with larger birth and death rates are likely to go extinct quicker than those with smaller birth and death rates, even if their basic reproductive ratios are the same. Regarding intraspecies interactions, I will show that extinction is more rapid when interactions increase the death rate rather than slow the birth rate despite having the same effect on average.

I will also use the simple system of a logistic model with demographic noise to evaluate some of the more common approximation techniques used in the literature. The Fokker-Planck equation, for example, has a long history of use, and despite it being known to fail [101, 117], is still a popular choice today [48–50, 70, 83, 94, 95, 98, 99, 106, 110, 111, 129–131]. Also known as the backward Kolmogorov equation, it approximates the master equation with a partial differential equation for the probability distribution for continuous (time and) population density, rather than the discretized population state space on which the master equation acts [78, 82]. A more recently developed approximation technique is the WKB method [80, 86, 101, 103, 123], which also considers a continuous state space, and defines a conjugate variable to the population size, such that the system evolves in this expanded space. The WKB method generally compares to simulations more favourably than the Fokker-Planck equation [98], but is also known to be occasionally incorrect [102].

2.2 One species logistic model

The simplest model of an isolated population has linear birth and death terms (that is, the per capita birth and death rates are constant: $b_n/n = \beta$, $d_n/n = \mu$). The difference between per capita birth and death gives a rate constant r, the Malthusian or exponential growth rate, such that the deterministic per capita growth would be $\frac{1}{n}\frac{dn}{dt} = r$. This model is a classic but gives the outcome of population explosion if $r > 0$ [1]. Even in the stochastic case there is a finite probability of population explosion, and the mean diverges [78]. To mathematically curb this infinite growth, and to biologically allow for intraspecies interactions, a non-linear term is required. A quadratic is the simplest non-linearity, so it serves as a popular choice for modelling intraspecies interactions, giving the equation

$$\frac{dn}{dt} = r\,n\left(1 - \frac{n}{K}\right), \tag{2.1}$$

in the deterministic case [80, 91, 92, 100, 102, 118, 119, 121]. One interpretation is that the rate constant is inhibited by the density of the population, hence a decrease by n/K. The parameter K is the carrying capacity, a phenomenological measure of the system size. Many dynamical systems can be approximated by a Taylor series expansion at a population small relative to the characteristic system size, such that they recover the logistic equation. For example, if exponential growth is inhibited by Michaelis-Menten kinetics such that $\frac{1}{n}\frac{dn}{dt} = r\left(1 - \frac{\gamma n}{n+\tilde{K}}\right)$, at small population the dynamics are the same as the logistic equation with $K = \tilde{K}/\gamma$. Extinction occurs when the system reaches $n = 0$, an absorbing state.

Deterministically, the origin is an unstable fixed point of the logistic equation, whereas there is a stable fixed point at $n^* = K$. Common practice in dynamical systems analysis is to rescale variables to remove parameters and simplify the system. Since we are dealing with continuous time we can remove the rate constant from our equation, by henceforth rescaling the time by $1/r$. Similarly, in the deterministic equation 2.1 we could rescale n by K and have no remaining parameters. However, in the stochastic version we cannot apply this latter rescaling to eliminate K, because of the implicit population scale of ± 1 organism for each birth/death event. The integer number of organisms in systems with demographic noise has an implicit population scale of 1. See figure 2.1.

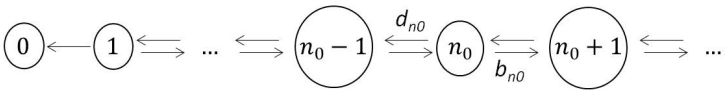

Figure 2.1: *Each realization of a birth-death process is a random walk on a lattice.* Each node of the lattice corresponds to a population size. Birth jumps the system one node to the right and death moves it one left, toward the absorbing state at zero population. A system with one species only need a one dimensional lattice; each additional species requires an additional dimension to represent the combination of populations for each species. The master equation describes how a probability distribution on the lattice evolves in time.

The system being constrained to integer populations gives a clear example of why the deterministic analysis is insufficient. Instead of the continuous, fractional populations of equation 2.1, one must define birth and death rates. As is standard, I assume that each birth event is independent and distributed exponentially with a probability $b_n\,dt$ of occurring in each infinitesimal time interval dt, and similarly for death events [78, 79, 82]. The Markov property underlying most stochastic processes studied, including those in this thesis, is that future events only depend on the present state [78, 79, 82], hence a birth event happening with the same probability in each time interval, given that the state is the same at the start of each of those intervals. In this chapter I use the birth rate

$$b_n = \begin{cases} r\,(1+\delta)\,n - \frac{r\,q}{K}n^2 = r\,n\left(1+\delta-q\frac{n}{K}\right) & \text{for } 0 \le n < N \\ 0 & \text{for } n \ge N \end{cases} \tag{2.2}$$

(see equation 2.5 below for the definition of N) and the death rate

$$d_n = r\,\delta\,n + \frac{r(1-q)}{K}n^2 = r\,n\left(\delta + (1-q)\frac{n}{K}\right). \tag{2.3}$$

Such a parameterization, with the four parameters, is novel. Denoting $P_n(t)$ as the probability that the

population is composed of n organisms at time t, these rates are used in the master equation

$$\frac{dP_n}{dt} = b_{n-1}P_{n-1}(t) + d_{n+1}P_{n+1}(t) - (b_n + d_n)P_n(t). \tag{2.4}$$

In addition to r and K, the stochastic rates of equations 2.2 and 2.3 have two additional parameters: $q \in [0, 1]$ shifts the nonlinearity between the death term and the birth term, whereas the parameter $\delta \in [0, \infty)$ establishes a scale for the contribution of linear terms in both the birth and death rates. I include the parameter δ to account for the stochastic relevance of the absolute values of the per capita birth and death rates; in the deterministic limit only their difference r affects the dynamics of the system; in reality δ is typically smaller than one [132]. Parameter q describes where the intraspecies inhibition acts: a q near unity implies competition for resources and a decreased effective birth rate, whereas a low q near zero reflects more direct conflict, with intraspecies interactions resulting in greater death rates of organisms. In reality most systems will lie somewhere between $q = 0$ and $q = 1$, as the effects of crowding and competition will both reduce birth and increase death rates. Note that so long as $q \leq 1$ the death rate is positive semi-definite for the domain of interest. It can be readily checked that $b_n - d_n$ recovers the right-hand side of equation 2.1 where, as per design, the new parameters q and δ do not appear. The choice of these parameters specifies a particular model and has consequences for the QSD and MTE.

The model described above has one other notable feature. Except at $q = 0$, there is a population at which the competition brings the effective birth rate to zero. This is the maximum size the population can achieve, and I define this cutoff as

$$N = \left\lfloor \frac{1+\delta}{q} K \right\rfloor, \tag{2.5}$$

where $\lfloor \cdot \rfloor$ is the floor function, rounding down to the nearest integer. Therefore I limit the calculations to the biologically relevant range $n \in [0, N]$. Already it is evident that the parameters δ and q have an effect on the system, as different values of the parameters will naturally define a range of states accessible in the model. At $n = 0$ both the birth and death rates go to zero, as they should, for it to be an absorbing state.

2.3 Quasi-stationary probability distribution function

The evolution of the distribution in the single birth and death process is captured in the master equation 2.4 [78, 82]. Note that ultimately at large times the probability of being at population size $n \neq 0$ decays to zero, as more and more of the probability gets drawn to the absorbing state. However, the approach to the true steady state is slow (on the order of the MTE; see next section below). Prior to reaching extinction, the system tends more rapidly toward a quasi-stationary distribution. That is, after some decorrelation time, the system reaches a state that changes very little as it slowly leaks probability into the absorbing state at extinction.

I want to solve this conditional probability distribution function P_n^c: the probability distribution of the population conditioned on not being in the steady extinct state. It is found by renormalizing the probability of being at each state n by the total probability that the system has not yet gone extinct [78]:

$$P_n^c \equiv \frac{P_n}{1 - P_0}. \tag{2.6}$$

The dynamics of this conditional distribution are described by a slightly different master equation than equation 2.4 [78]:

$$\frac{dP_n^c}{dt} = b_{n-1}P_{n-1}^c + d_{n+1}P_{n+1}^c - \big(b_n + d_n - P_1^c d_1\big)P_n^c. \tag{2.7}$$

After an initial transient period, this conditional probability will stabilize to a steady $\tilde{P}_n^c$ for which $d\tilde{P}_n^c/dt = 0$. The steady state of this distribution is referred to as the quasi-stationary distribution (QSD), not to be confused with the true stationary distribution of the population which is $\tilde{P}_n(t \to \infty) = \delta_{n,0}$, extinction.

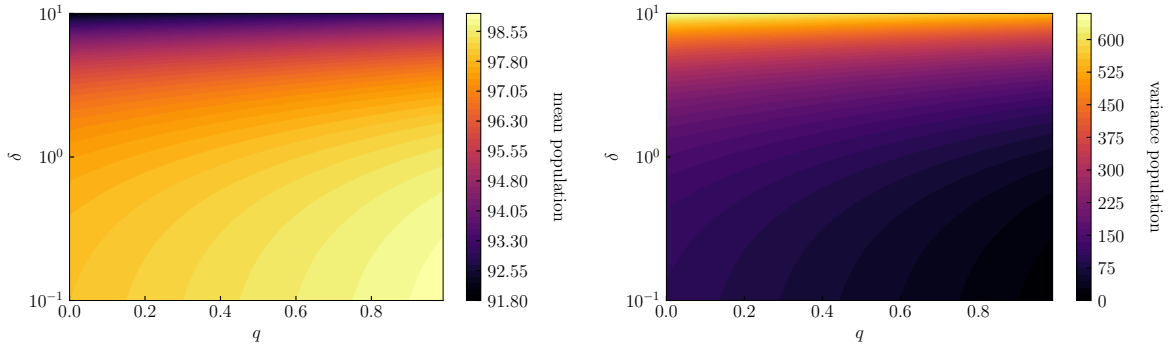

Figure 2.2: *Characterizing the quasi-stationary probability distribution function for varying basal death rate δ and competition mechanism parameter q.* Lightness indicates an increased mean or variance in the left and right panels respectively. Carrying capacity $K = 100$. *Left:* The QSD has decreasing mean with increased δ or decreased q. *Right:* The QSD has increasing variance with increased δ or decreased q.

To calculate the QSD I employ the following textbook algorithm [78]: at steady state equation 2.7 can be rearranged to relate $\tilde{P}_{n+1}$ to $\tilde{P}_n$ and $\tilde{P}_{n-1}$

$$\widetilde{P}_i^c = \frac{-\widetilde{P}_{i-2}^c b_{i-2} + (b_{i-1} + d_{i-1})\widetilde{P}_{i-1}^c - \widetilde{P}_{i-1}^c \widetilde{P}_1^c d_1}{d_i}. \tag{2.8}$$

Given that $b_0 = 0$ there is a lower cutoff and so the whole distribution can be written in terms of $\tilde{P}_1$, which is then solved by normalization of the total probability to unity. The outcome of this algorithm constitutes the novelty of this section, and is seen in figure 2.2 for different values of q and δ. For an example of the probability distribution function itself, see the left panel of figure 2.6; the distribution appears to be well characterized by its mean and variance. Increasing the value of δ shifts the mean slightly toward 0 and spreads the distribution out, increasing its variance. In biological terms, having large birth and death rates leads to frequent deviations from the carrying capacity compared to small birth and death rates with an equivalent reproductive rate r. Decreasing q has a similar but lesser effect to increasing δ. Intraspecies interactions that reduce birth rate tend to cause the population to stagnate near the carrying capacity, with only small stochastic fluctuations. When these interactions are a cause of death it makes the system less stable, with larger fluctuations, hence a greater variance.

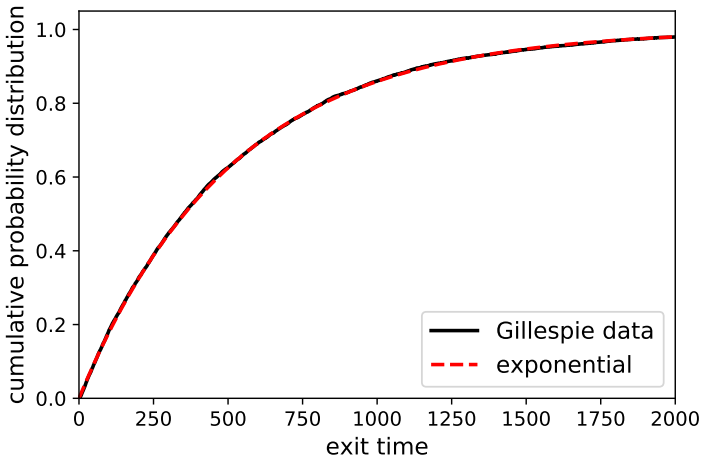

Figure 2.3: *The extinction time cumulative distribution of a single species logistic model is dominated by a single exponential tail.* Except at early times, the bulk of the cumulative distribution function is modelled by an exponential distribution with the same mean, shown in the red dotted line. The $10,000$ data are generated using using the Gillespie algorithm for $K = 8$, $\delta = q = 0$, starting from the carrying capacity. Similar results are seen for various values of δ and q. For higher carrying capacities the assumption of exponentially distributed times becomes even more accurate.

2.4 Exact mean time to extinction

As described earlier, the system ultimately goes to the absorbing extinct state $n = 0$, with some distribution of (first passage) extinction times. In many cases, including the single logistic model, the MTE characterizes the entire distribution of exit times [107, 133], which are observed to look roughly exponential, as shown in figure 2.3. Because the absorbing point is deterministically repelling and, as the QSD shows, the system spends most of its time near the deterministic fixed point at $n = K$, extinction events are rare, far from equilibrium. These extinction attempts can be considered as almost independent, since the autocorrelation time is so much shorter than the time between attempts [95, 107]. The system has repeated, independent events that occur with at a constant rate; it is Poissonian, hence the distribution of extinction times is exponential and described by its mean, the MTE [94, 95, 99, 107]. Another way to get intuition into the exit times being roughly exponentially distributed is to rewrite the master equation 2.4 in vector form as $\partial_t \vec{P} = \hat{M}\vec{P}$, which is solved by $\vec{P}(t) = e^{\hat{M}t}\vec{P}(0)$. The probability of being in each state, and relevantly the absorbing state, is a sum of exponentials (in a basis which diagonalizes the transition matrix $\hat{M}$), and at long times this is dominated by the single longest lasting exponential term.

For one-species systems it is well known how to exactly solve the MTE for a birth-death process. The mean time of extinction starting from a population of size n is [78, 134]

$$\tau(n) = \sum_{i=1}^{N} q_i + \sum_{j=1}^{n-1} S_j \sum_{i=j+1}^{N} q_i, \tag{2.9}$$

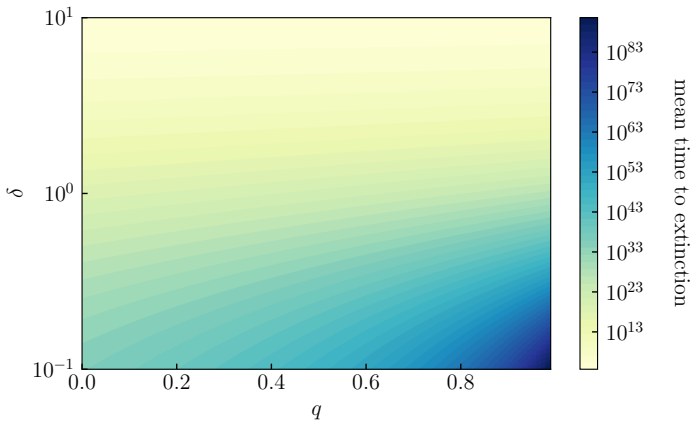

Figure 2.4: *Exploring the mean time to extinction (from equation 2.9) in the parameter space.* The parameter q shifts the nonlinearity between the birth and death rates: for $q = 0$ the nonlinearity is purely in the death rate, for $q = 1$ nonlinearity appears only in birth. The birth and death rates are increased simultaneously with δ. Extinction occurs more rapidly as δ increases or q decreases, as the system effectively becomes more noisy.

where

$$q_1 = \frac{1}{d_1} \tag{2.10}$$
$$q_i = \frac{b_{i-1}\cdots b_1}{d_i d_{i-1}\cdots d_1} = \frac{1}{d_i}\prod_{j=1}^{i-1}\frac{b_j}{d_j}, \qquad \text{for } i > 1$$

and

$$S_i = \frac{d_i \cdots d_1}{b_i \cdots b_1} = \prod_{j=1}^{i}\frac{d_j}{b_j}. \tag{2.11}$$

If N does not exist or is negative the sum instead goes to infinity. These equations come from noting $\tau(0) = 0$, $\tau(1) < \infty$, and iterating the difference equation [78, 134]

$$\tau(n) = \frac{1}{b_n + d_n} + \frac{b_n}{b_n + d_n}\tau(n+1) + \frac{d_n}{b_n + d_n}\tau(n-1), \tag{2.12}$$

which itself comes from noticing that from state n the system will either go to state $n+1$ (with probability $\frac{b_n}{b_n+d_n}$) or state $n-1$ (with probability $\frac{d_n}{b_n+d_n}$), and the mean time for either of these jumps is $\frac{1}{b_n+d_n}$. Thus the mean time to extinction from neighbouring states are related, which leads to this recurrence relation.

Combining equations 2.2 and 2.3 with the solution for the mean time to extinction 2.9 I obtain a complicated analytical expression in the form of a hypergeometric sum, given in the appendix. Little intuition can be gained from the mathematical expression, but the numerical results of the MTE, as shown in figure 2.4, are more interpretable. A typical trajectory starting from n goes first to the deterministic fixed point K and fluctuates about that point before a large fluctuation leads to its extinction. Since the time for the population to reach carrying capacity is insignificant compared to the extinction time, the MTE is largely independent of the initial population [49], and I write $\tau(n) \approx \tau(K) \equiv \tau_e$ for all n here and for most of this thesis. This approximation only fails for small n [49]. It is well known that

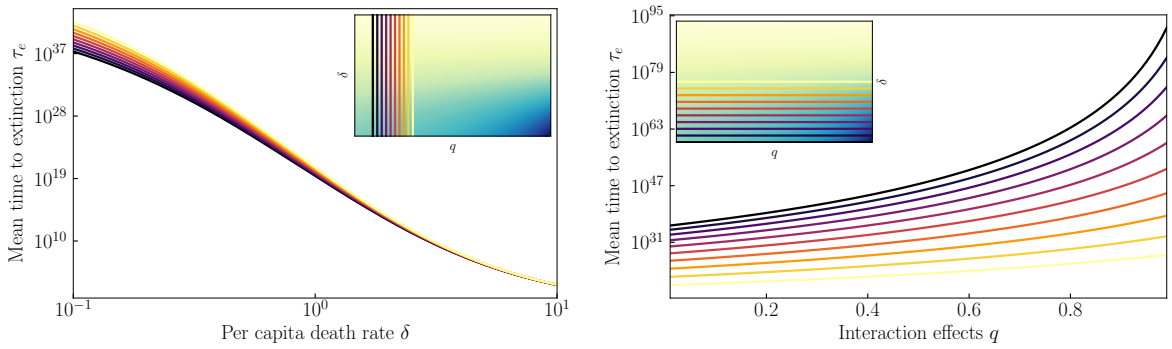

Figure 2.5: *Mean time to extinction for varying basal death rate δ and competition mechanism parameter q.* Each line represents a slice in figure 2.4. Lightness of the line indicates an increase of q or δ in the left and right panels respectively. Carrying capacity $K = 100$. *Left:* Vertical slices of the heat map show that increasing δ decreases τ for different values of q. *Right:* Horizontal slices of the heat map show that increasing q increases τ for different values of δ.

τ_e scales as e^K [80, 95] and this is indeed what I observe (for an example see the appendix or the right panel of figure 2.6 below). Similarly the times I report have all been rescaled by r and so are measured in generations, such that the real times are $r\tau_e$. What is less well known, the novelty of this research, is the dependence on the additional parameters δ and q. Figure 2.5 shows that the MTE depends on the values of δ and q, parameters that appear in the births and deaths but do not appear in the deterministic equation.

Increasing the scaling of the linear terms δ in birth and death rates has a tendency to decrease τ_e. A decrease in τ_e is also observed as q is decreased, shifting the nonlinearity from the birth to the death rate. Just as increasing both the birth and death rates (via increased δ or decreased q) broadens the QSD, so too does it decrease the MTE. Note that the effect of q is magnified for smaller values of δ and weaker for larger values of δ; that is, the intraspecies interactions modelled by the quadratic term matter more when the basal birth and death rates are both relatively low. Again I remind the reader that in all of the above calculations the same average dynamics $b(n) - d(n)$ were maintained. A more detailed interpretation and justification of these results appears in the discussion section below, but the simple explanation is that those changes which act to broaden the QSD also increase the probability of being near, and therefore more quickly reaching, extinction. Having larger δ or smaller q implies larger birth and death rates (either in the basal rates or in the effect of intraspecies interactions, respectively), hence a system with greater fluctuations and less stability. It bears noting that the effects of the additional parameters δ and q on the MTE can be quite drastic. In the limit of $\delta = 0$ and $q = 1$ there is no death, $d_n = 0 \ \forall n$, and the system simply grows to the carrying capacity and rests there, never going extinct.

2.5 Approximation techniques

As shown above, for a one-species model it is possible to write down a closed form solution for the MTE τ_e. However, finding a solution for the mean time to extinction given multiple populations, and therefore higher dimensions, is not as trivial. Nor can an analytic expression be found, even for a single species. Many approximations have been developed to accommodate these complications. These approximations make analytic calculations possible or reduce numeric computing runtime significantly;

therefore it is important to know which of these tools to use and when they are applicable. Unfortunately the most popular approximation is known to fail in some situations [101, 117], and an exhaustive test with the approximations I highlight below has not been performed (but see [98, 100]). Using the same model system of a single logistic species I shall evaluate the Fokker-Planck equation, the Gaussian approximation to the Fokker-Planck equation, the WKB method, and some numerical methods. I have not invented these methods, but I apply them in the context of this stochastic logistic model with the full four parameters needed to characterize its quadratic nature. Comparing these approximations to the above exact results will grant insight into their utility.

In one and more dimensions the MTE can be solved to arbitrary accuracy numerically. Specifically, the Gillespie or stochastic simulation algorithm [108, 109] generates particular realizations of a stochastic process that, taken in aggregate, obey the evolution of the probability distribution as given by the master equation 2.4. The Gillespie algorithm is often used by researchers to verify their approximations [48–50, 81, 88, 135, 136], and I do the same here. Unfortunately, as I referenced above, the MTE tends to scale exponentially with the system size, and the Gillespie algorithm tends to have a computational time proportional to the system time [108], and so it quickly becomes unusable for systems of large size. The transition matrix inverse method alluded to in the introduction chapter and used in subsequent chapters of this thesis calculates the MTE to arbitrary accuracy. Essentially, equation 2.12 can be written in matrix form as [78, 83]

$$\hat{M}^T\vec{T} = -\vec{1} \tag{2.13}$$

with $\left(\vec{T}\right)_n = \tau(n)$ and elements of $\hat{M}$ being the birth and death rates into and out of each state. If N exists the matrix is finite and can be inverted; if not, a cutoff is introduced to make $\hat{M}$ finite [110, 111, 137]. This is the arbitrarily precise technique I use in chapters 3 and 4 of this thesis. Since it involves inverting a matrix of size proportional to the system size to the power of the number of species it can be taxing on a computer's RAM. A cruder yet faster and less RAM-intense numerical approximation is to take the negative reciprocal of the smallest magnitude eigenvalue [107]:

$$\tau_e \approx -1/\lambda_1. \tag{2.14}$$

This corresponds to keeping only the longest-lived term in the sum of exponentials $\vec{P}(t) = e^{\hat{M}t}\vec{P}(0)$ (see the discussion regarding figure 2.3). For this chapter, all of these numerical methods (Gillespie algorithm, matrix inverse method, and smallest eigenvalue) give results indistinguishable from the exact summation of equation 2.9 and so they are not included in any figures. etimedistr

The first approximation I will regard is the Fokker-Planck (FP) equation, which approximates the discrete populations as continuous. Starting from the master equation 2.4 one employs the Kramers-Moyal expansion [82]. The Pawula theorem says that when employing the Kramers-Moyal expansion the only valid orders to stop the expansion are at two terms or infinite [79]. The expansion requires the definition of a density $x = n/K$ and that the rates w_n can be written in a form $w_n/K = w(x)$, eventually arriving at:

$$\partial_t p(x,t) = -\partial_x\Big((b(x) - d(x))p(x,t)\Big) + \frac{1}{2K}\partial_x^2\Big(\big(b(x) + d(x)\big)p(x,t)\Big). \tag{2.15}$$

Instead of the master equation's difference differential equation for the probability P_n, equation 2.15 is a partial differential equation for the probability density $p(x)$. The first term on the right-hand side is often called the drift term and reduces to the deterministic dynamics when fluctuations are neglected

[82]. The second term is the diffusion term and describes the effect of stochasticity on the system. There is a one-to-one correspondence between Fokker-Planck and Langevin equations, which are stochastic differential equations [82]. Equation 2.15 can be solved directly to get the MTE [82, 83]:

$$\tau(n) = 2K \int_0^n dy \frac{1}{\phi(y)} \int_y^\infty dz \frac{\phi(z)}{B(z)}, \tag{2.16}$$

where $\phi(x) = \exp\left[\int_0^x dy\, 2A(y)/B(y)\right]$, $A(y) = b(y) - d(y)$, and $B(y) = b(y) + d(y)$. I have calculated these integrals numerically where possible, but it is prone to computational problems of convergence at large K. To find the QSD the left-hand side of equation 2.15 is set to zero, resulting in the steady state probability density [82]

$$\ln p(x)^{ss} \propto \frac{2K(b(x) - d(x)) - \partial_x(b(x) + d(x))}{(b(x) + d(x))}. \tag{2.17}$$

By analogy with Boltzmann statistics, the negative of the right-hand side of the above equation is sometimes referred to as a pseudo-potential [130, 138–140], although in higher dimensions it cannot be defined [12, 139], as will be further discussed in the next chapter.

The Fokker-Planck equation can be further simplified by linearizing the birth and death rates about a stable (deterministic) fixed point x^*. The drift term is replaced with $(x - x^*)\partial_x(b(x) - d(x))|_{x=x^*}$ (since by definition $(b(x) - d(x))|_{x=x^*} = 0$) and the diffusion with $(b(x) + d(x))|_{x=x^*}$. We only expect this approximation to hold near the fixed point. The solution is

$$p(x) = \frac{1}{\sqrt{2\pi\sigma^2}} \exp\Big\{ - \frac{(x - x^*)^2}{2\sigma^2} \Big\}, \tag{2.18}$$

a Gaussian centred at the fixed point with variance $\sigma^2 = K \frac{-(b(x)+d(x))|_{x=x^*}}{2\partial_x(b(x)-d(x))|_{x=x^*}}$. As described earlier, the quasi-stationary probability distribution leaks from P_n, a non-extinct population, to P_0. And since this is a single step process (with the population only changing by one individual per event), the only transition from which it can reach the absorbing state is through a death at P_1: all population extinctions must go through this sole state. The flux of the probability to the absorbing state is thus given by the expression $d_1 P_1$, hence the MTE can be approximated from the QSD [103]:

$$\tau_e \approx \frac{1}{d_1 P_1} \tag{2.19}$$

Based on the flux into the zero state, the Gaussian approximation to the Fokker-Planck equation has an MTE of [79]

$$\tau_e \approx 2\sqrt{2\pi\sigma^2}\, (\partial_x(b(x) + d(x))|_{x=0})^{-1} \exp\Big\{ \frac{(x^*)^2}{2\sigma^2} \Big\}. \tag{2.20}$$

Another method frequently utilized is the WKB approximation [80, 86, 87, 96, 98, 101–103, 123]. Generally, the WKB method involves approximating the solution to a differential equation with a large parameter (such as K) by assuming an exponential solution (an ansatz) of the form [103]

$$p(x) \propto \exp\left\{ K \sum_{i=0}^{\infty} \frac{1}{K^i} S_i(x) \right\}. \tag{2.21}$$

Starting from the Fokker-Planck equation 2.15, one can immediately apply the ansatz in the probability density and solve the subsequent differential equations to different orders in $1/K$[103]. To leading order,

only

$$S_0(x) = \int_{x=0}^{1} dx \ln\left(\frac{b(x)}{d(x)}\right) \tag{2.22}$$

is needed. This method is sometimes referred to as the real-space WKB approximation, wherein we obtain a solution for the quasi-stationary probability distribution. Another method, known as the momentum-space WKB, is to write the evolution equation of the generating function of $p(x)$, the conjugate of the master or FP equation, and then apply the exponential ansatz [86, 103]. The momentum-space WKB has been shown to err from real-space WKB [80, 103], and it seems the real-space WKB method is now more popular [80, 87, 96, 98, 102, 103, 123]. The quantity $S_0(x)$ can be interpreted as the action in a Hamilton-Jacobi equation [103]. As before, the MTE can be calculated from the QSD equation 2.21 using equation 2.19.

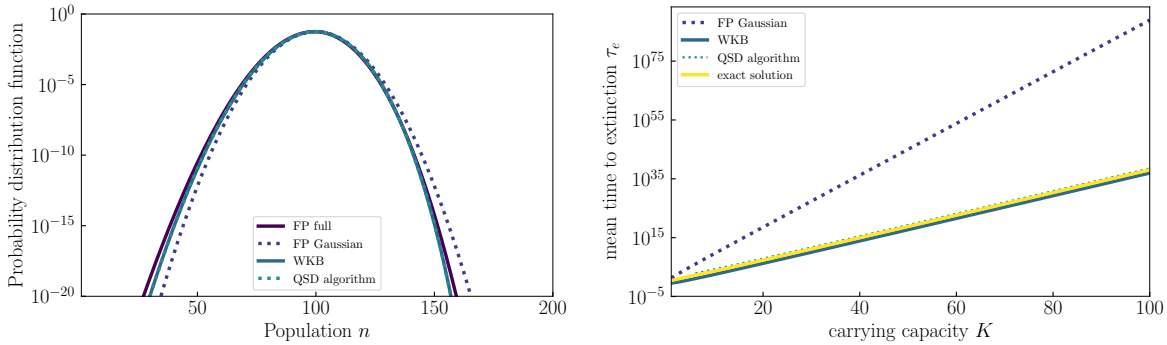

Figure 2.6: *Approximation techniques for calculating the QSD and MTE.* Carrying capacity $K = 100$, $\delta = 0.4$ and $q = 0.7$. *Left:* The quasi-stationary probability distribution function is calculated using the QSD algorithm, and approximated with the Fokker-Planck equation, Fokker-Planck Gaussian approximation, and WKB method. The WKB method gives the best match with the correct QSD algorithm solution. All of the methods correctly capture the QSD near the deterministic fixed point, but start to diverge away from the deterministic fixed point $n^* = K$. *Right:* The mean time to extinction is calculated exactly using equation 2.9. Except for the regular Fokker-Planck solution, the same approximations as in the left panel are used, as is the QSD in conjunction with equation 2.19. WKB stays closest to the true solution.

The left panel of figure 2.6 gives an instance of the quasi-stationary distribution as a function of n for a choice of the parameters q, δ and K for each technique. Note that with this scale of the figure the WKB approximation and the quasi-stationary algorithm are not distinguishable by eye, though there are indeed slight differences. In general, the ability of the techniques to successfully approximate the quasi-stationary distribution and mean time to extinction depends heavily on the region of parameter space. Regarding figures similar to the right panel of figure 2.6 (shown in the appendix) reveals that WKB works well when δ is small, but is off by a significant factor for large δ. The regular Fokker-Planck approximation involves numerical integration and shows convergence issues except at low K and so is not plotted, but based on the low K results it shows an opposite trend to WKB, working well at high δ but not at low. The Gaussian approximation to the Fokker-Planck equation always performs poorly. Figure 2.7 shows the success of these techniques as δ is varied, for a low carrying capacity.

The best candidate in most regimes appears to be the WKB approximation. It generalizes to multiple dimensions without conceptual difficulty. Mathematically, at higher dimensions WKB necessitates solving a Hamiltonian system, in order to find the most probable route to extinction along which to

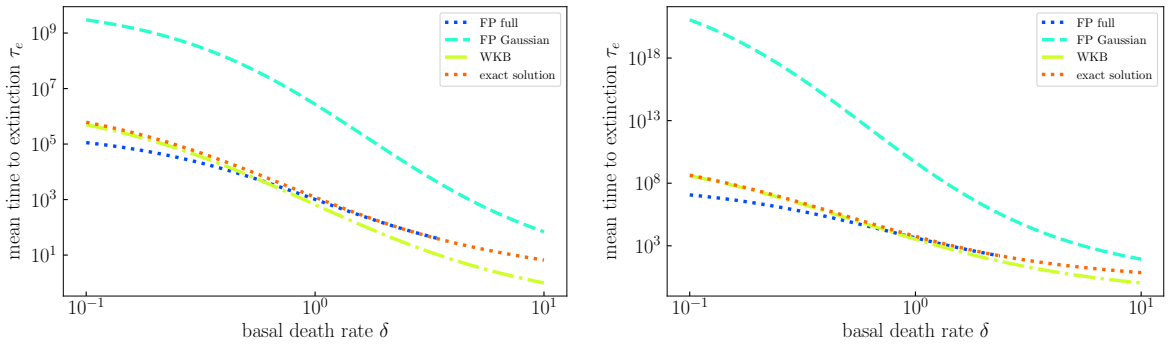

Figure 2.7: *Approximation techniques as they depend on basal death rate.* Carrying capacity $K = 16$, δ varying, and $q = 0.2$ (left) or 0.7 (right). At low δ, the WKB approximation performs well, but its performance worsens as δ is increased. Numerical solution of the Fokker-Planck equation shows the opposite result, being off from the true solution at low δ and only matching it as δ increases.

integrate equation 2.22; an analytic solution cannot be derived in general, and a symplectic integrator is necessary to find the numeric trajectory [141]. In this one-dimensional case I find an analytic expression for the mean time to extinction using the WKB approximation of equations 2.21 and 2.22, evaluated using the birth and death rates 2.2 and 2.3, and the flux equation 2.19:

$$\begin{aligned}\tau_{\text{WKB}} =& \frac{\sqrt{2\pi K}}{\delta + (1-q)/K}\left(\frac{K(1+\delta)-q}{K\delta+(1-q)}\right)\sqrt{\frac{(1+\delta-q)^2}{\delta q + (1-q)(1+\delta)/K}} \\ &\times \exp\left\{K\left(\frac{1+\delta}{q}\ln\left[\frac{K(1+\delta)-1}{K(1+\delta-q)}\right] + \frac{\delta}{1-q}\ln\left[\frac{K\delta+(1-q)}{K(1+\delta-q)}\right]\right)\right\}.\end{aligned} \tag{2.23}$$

We can contrast this with a further approximation to the Fokker-Planck solution of equation 2.16, with a Laplace method/saddlepoint approximation expanding ϕ and $1/\phi$ about 0 and K [78, 101, 138]:

$$\tau_{FP} \approx \sqrt{\frac{4\pi(1+2\delta)^2}{K(1+\delta-q)}}e^{K\left(4(1+\delta-q)\ln 2(1+\delta-q)-2(1-2q)\right)/(1-2q)^2}. \tag{2.24}$$

Both formulae are dominated by their exponential dependence on K. This is to be expected, as it matches with the research community's intuition that systems with a deterministically stable fixed point scale as $\tau \propto e^{cK}$ [88, 94–98]. The qualitative behaviour of the MTE is most affected by the coefficient c. While I have not found a simple closed analytical form for the exact solution of the MTE in general, the asymptotic scaling for $\delta, q = 0$ is known to increase as $\tau_e \propto \frac{1}{K}e^K$ [95, 113], with $c = 1$. The approximated Fokker-Planck solution has $c = \left(4(1+\delta-q)\ln 2(1+\delta-q)-2(1-2q)\right)/(1-2q)^2$, giving $c = 4\ln 2 - 2 \approx 0.7$ for $\delta, q = 0$, slightly underestimating the scaling. The lowest order of a Taylor expansion in δ and q of the WKB solution, as calculated using Mathematica, gives a coefficient of $c = 1 - 1/K$, which nicely matches the expected limit. The prefactor of the WKB solution that is algebraic in K does not match with the true limit [12, 13, 102], but it is less dominant than the exponential term. See the appendix for the calculation with $\delta, q = 0$.

2.6 Discussion

Why should the parameters δ and q matter if they do not show up in the no fluctuation, deterministic dynamics of equation 2.1? The parameter δ gives a scale for the linear per capita birth and death rates individually (rather than their difference r). This scaling differentiates systems with low birth and death rates from those with high turnover, even when the two models would have the same average dynamics. Whereas the deterministic dynamics includes only the difference of birth and death and will not distinguish between populations with high or low turnover, the magnitude of the birth and death rates affect stochastic processes like extinction. For example, the probability of extinction of a system with linear birth and death rates ($b_n = \beta n$ and $d_n = \mu n$) starting from population n_0 goes as $(\beta/\mu)^{n_0}$ [78]. In this context, the model with high turnover will differ from one with low turnover as the ratio b_n/d_n will depend on the scale, that is to say, on δ. In bacterial systems it seems that δ is typically small compared to one [132].

Additionally, q determines whether intraspecies interactions have a greater effect on birth or death. It moves the quadratic dependence between the two rates. By having the nonlinearity in the birth, one is assuming that the competition, modelled by the quadratic term, slows down the birth rate, for instance in the form of quorum sensing [125] or adaptation to resources [126]. If it were present in the death the supposition is that the competition instead kills off individuals, for example with illness spreading more rapidly in denser populations [121] or an increase in secreted toxins [127, 128]. The parameter q is not typically measured, though I expect it to be between zero and one in most biological populations, as competition for resources slowing down birth rates and waste production increasing death rates are common to most systems. Although I have worked with a $q \in [0, 1]$, there is no mathematical reason why q could not take values outside this range. Negative values of q would increase both rates, with a physical meaning that the density dependence would in fact be beneficial for the birth rates, as in the Allee effect [21, 103], and of even greater contribution to the death rates. Any $q > 1$ has the opposite effect of negatively impacting both rates, signifying that population density would reduce both the birth and death rates.

Figure 2.4 summarizes the numerical results of equation 2.9 into a heat map of the mean time to extinction as a function of the two additional parameters q and δ. For the range of q and δ explored, I find that the MTE changes similarly upon decreasing q and increasing δ, although it depends more sensitively on δ. Though it is not trivially apparent from the form of the exact analytical solution 2.9 that the linear contribution to the rates should be more significant, one can get some intuition. At small populations, the linear term is of order δ (for $\delta \geq 1$ - otherwise it's order one) and the quadratic terms is of order q/K, hence the linear term dominates the small population end of the distribution, as K is typically large. The MTE comes from the small population dynamics (see equation 2.19) and so the greater order term will have a stronger effect. These relative orders also explain why the effect of q on the MTE is strongest when δ is small and almost negligible for large δ.

The qualitative features of my results can be readily intuited by considering the effect each of these parameters has on the quasi-stationary probability distribution; see figure 2.2. A broader probability distribution function corresponds to a shorter MTE, as probability more readily leaks from the quasi-steady state solution to extinction. I find that decreasing δ narrows the distribution and slightly shifts the mode away from $n = 0$. Both of these trends act to lengthen the extinction time. As observed earlier, the reverse is true for varying q: narrower QSDs are observed when q is instead increased. For a population that has greater variance about the carrying capacity, states farther from the fixed point

will be explored more frequently, increasing the probability that the system will stochastically go extinct earlier. My results give the mean extinction time of a single, self-interacting logistic species, for all coefficients for first and second order terms, an exploration of which had not previously been performed, to my knowledge.

Varying the parameters has another effect on the probability distribution, as the parameters determine the maximum population size N, restricting the possible states to those less than the population cutoff. By setting manual cutoffs in the numerical analysis and comparing the results to the true MTE I have checked that this change in maximum population size has no noticeable effect on the MTE.

How can the MTE be probed in a lab setting? For experimentalists the difficulty of measuring a birth or death rate alone, as it changes with something like population density, varies with the system of interest. However, as previously discussed, measuring the average dynamics alone is insufficient. In a bacterial species the birth rate can be inferred by the uptake and usage of radioisotope-doped nucleotides in nucleic acid synthesis [142]. The death rate is easily inferred from the birth rate and the average dynamics, or it too can be measured using radioisotopes [132]. In principle these rates could be compared to the MTE of an experimental system, but in practice for most biological systems the carrying capacity is large, making the MTE prohibitively long. For example, assuming $\tau_e \sim e^K/K$, the famous Lenski experiment [143] which cultures 5×10^8 bacteria each day and 6.64 generations a day will not reach its MTE for another 10^{10^8} years. Obviously a smaller carrying capacity would be required to reasonably measure the MTE. The QSD could be probed by either running many experiments in tandem or running one experiment for a long time (but not so long as the MTE) and repeatedly taking measurements, so long as the interval between measurements is longer than the autocorrelation time [107].

The use of approximations is widespread and necessary when using mathematics to model real systems. I find that all approximations considered in this chapter accurately capture the QSD near the deterministic fixed point. Regarding the MTE, the WKB approximation fares best, though it does incorrectly calculate the algebraic prefactor [12, 13, 102]. The Fokker-Planck equation appears to fare well for large δ and low K, presumably because the absorbing state is effectively "near" the stable fixed point $n^* = K$ when the variance is so large, as is the case for large δ. I also remind readers that inverting the transition matrix, as will be done in the following chapters, gives numerical results practically identical to the analytic solution.

Historically the choice of model seemed to be one of taste or mathematical convenience [80, 91, 92, 100, 102, 118, 119, 121], so long as the deterministic limit was as desired. In this chapter I have shown that those parameters hidden from the deterministic dynamics nevertheless have significant qualitative and quantitative effects on stochastic processes like extinction, as characterized by the MTE. A species survives longest when both its birth and death rates are low, and intraspecies interactions act to inhibit birth rather than intensifying death rates. In light of my conclusion that the stochastically relevant but "hidden" parameters matter, one must carefully ensure that a model, at a stochastic rather than deterministic level, is accurately informed by the biology being emulated.

Chapter 3

Fixation: Transition from Two Species to One

This chapter, along with the next one, is based on a paper written by me and my supervisor Anton Zilman, which is currently under revision for The Proceedings of the Royal Society Journal [12].

3.1 Introduction

The previous chapter treated the tractable problem of a single species experiencing only intraspecies interactions. Adding a second species complicates both the mathematics and the biology, but offers a step toward possible resolutions to the problem of biodiversity. A community of interacting species is built up of pairwise competition, to lowest order; if two species with overlapping niches can coexist, it gives credence to biodiversity in ecosystems with low numbers of niches. Competitive exclusion suggests that only one species will persist in each ecological niche [25, 144, 145], but ecosystems like the ocean surface seem to have more species than there are niches [24]. Niche and neutral models both address this "paradox of the plankton" but a resolution remains elusive. Further study is required, and I present my contributions in this chapter.

Deterministically, ecological dynamics of mixed populations have commonly been described using a dynamical system of the numbers of individuals of each species and the concentrations of the limiting factors [39–41]. Steady state coexistence typically corresponds to a stable fixed point in such dynamical system, and the number of stably coexisting species is typically constrained by the number of limiting factors. In some cases, deterministic models allow coexistence of more species than limiting factors, for instance when the attractor is a limit cycle rather than a point [41, 146]. Particularly pertinent for this chapter is the case when the interactions of the limiting factors and the target species have a redundancy that results in the transformation of a stable fixed point into a marginally stable manifold of fixed points. Then the stochastic fluctuations in the species numbers become important [3, 41, 61, 147–149]. I will return to the mathematical formulation of these concepts later.

Stochastic effects, arising either from the extrinsic fluctuations of the environment (treated, for example, in [84, 85]) or the intrinsic stochasticity of individual birth and death events within the population (treated, for example, in [47–50, 86–90]), modify the deterministic picture. As in the previous chapter, I focus on this latter type of stochasticity, known as demographic noise. Demographic noise causes fluctu-

ations of the populations abundances around the deterministic steady state until a rare large fluctuation leads to extinction of one of the species [47, 49, 150]. In systems with a deterministically stable coexistence point, the mean time to extinction is typically exponential in the population size [80, 91, 96, 102], as was seen in the previous chapter. Exponential scaling is commonly considered to imply stable long term coexistence for typical biological examples with relatively large numbers of individuals [80, 106].

By contrast, in systems with a neutral manifold that restore fluctuations off the manifold but not along it, mean extinction timescales as a power law with the population size, indicating that the coexistence fails in such systems on biologically relevant timescales [7, 47, 70, 85]. This type of stochastic dynamics parallels the stochastic fixation in the classical Moran-Fisher-Wright model that describes strongly competing populations with fixed overall population size [5–7, 32, 33, 150–152].

As is reviewed below, a broad class of dynamical models of multi-species populations interacting through limiting factors can be mapped onto the generalized Lotka-Volterra model. Lotka-Volterra models allow one to conveniently distinguish between various interaction regimes, such as competition or mutualism, and which have served as paradigmatic models for the study of the behavior of interacting species [3, 47–50, 61, 76, 88–90, 147, 148]. Remarkably, the stochastic dynamics of LV type models is still incompletely understood, and has recently received renewed attention motivated by problems in bacterial ecology and cancer progression [49, 90, 127, 151–153]. There has also been the observation that for certain parameter values that the stochastic 2D generalized Lotka-Volterra model exhibits similar dynamics to the Moran model [47–50]. How the system transitions from the typical LV results of MTE scaling exponentially with system size to the algebraic times of the Moran model is the main result of this chapter. The results outline the conditions of niche overlap and carrying capacity that allow two species to coexist (and conversely, those that will lead to relatively quick fixation).

In this chapter, I analyze a model of two competing species with the emphasis on the transition from deterministic coexistence to stochastic fixation. I use the master equation and first passage formalism that enables numerically solution to arbitrary accuracy in all regimes. First I will provide a mathematical argument for competitive exclusion, a derivation of the competitive LV model, and an examination of the Lotka-Volterra regimes of deterministic stability, all of which are summarized from the literature and included for context. Then I will introduce the stochastic description of the LV model and analyze fixation times as a function of the niche overlap between the two species. These results will be compared to known analytic limits, included here for completeness. I will make further comparisons to the Fokker-Planck and WKB approximations before concluding with a general discussion of the results.

3.2 Long-term stability of deterministic interacting populations

This section is a summary of some work by McGehee and Armstrong [39–41]. I include it for pedagogical purposes, as it gives a mathematical argument for competitive exclusion constraining the number of species to the number of different limiting factors which might define a niche.

Quite generally, the dynamics of a system of N asexually reproducing species that interact with each other only through M limiting factors (such as food, soluble signaling and growth/death factors, toxins, metabolic waste) and experience no immigration can be described by the following system of equations for the species $x_1, ..., x_N$ and the limiting factor densities $f_1, ..., f_M$ [39–41]:

$$\dot{x}_i = \beta_i(\vec{f})x_i - \mu_i(\vec{f})x_i, \tag{3.1}$$

where $\vec{f}$ is the state of all factors that might affect the per capita birth rate $\beta_i(\vec{f})$ and the death rate $\mu_i(\vec{f})$ of the species i.

The density of a factor j in the environment, f_j, follows its own dynamical production-consumption equation

$$\dot{f}_j = g_j(\vec{f}, \vec{x}) - \lambda_j(\vec{f}, \vec{x}) f_j \tag{3.2}$$

where g_j is a production-consumption rate that includes both the secretion and the consumption by the participating species as well any external sources of the factor f_j, and λ_j is its degradation rate. Alternatively, for some abiotic constrains such as physical space or amount of sunlight, the concentration of the factor f_j can be set through a conservation equation of a form [40, 41] $f_j = c_j(\vec{f}, \vec{x})$.

The fixed points of the $N + M$ equations (3.1) and (3.2) determine the steady state numbers of each of the N species and the corresponding concentrations of the M limiting factors. However, the structure of equations (3.1) imposes additional constraints on the steady state solutions: at a fixed point $\beta_i(\vec{f}) = \mu_i(\vec{f})$ for each of the N species, which determines the steady state concentrations of the M limiting factors $\vec{f}$. However, if $N > M$, the system (3.1) of N equations is over-determined and typically does not have a consistent solution, unless the fixed point populations of $N - M$ of the species are equal to zero [39–41, 149, 154]. This reasoning provides a mathematical basis for the competitive exclusion principle, whereby the number of independent niches is determined by the number of limiting factors, and a system with M resources can sustain at most M species in steady state.

Nevertheless, as mentioned in the introduction, the number of species at the steady state can exceed the number of limiting factors, when the N equations for the species are not independent and thus provide less than N constraints on the solutions. In this case, at steady state the populations of the non-independent species typically converge onto a marginally stable manifold on which each point is stable with respect to off-manifold perturbations but is neutral within the manifold [40, 47, 88, 148, 155]. I return to this point in the following sections within the discussion of the Lotka-Volterra model.

3.3 Minimal model of interacting species and a derivation of 2D Lotka-Volterra model

As a minimal example, in this section I introduce a model of two interacting species whose dynamics is constrained by two secreted factors. The idea is not novel, but it is instructive in understanding how niche overlap relates to the conditions of exclusion and neutrality. Each species x_i has basal per capita birth rate β_i, death rate μ_i, and each generates the secreted soluble factors t_j at rates g_{ji}. For my purposes, a species is a collection of organisms with the same mean birth and death rates, that are distinguishable from members of other species. Each factor t_i is degraded at a rate λ_i, and affects the death rate of each bacterium linearly with the efficacy e_{ij}. Positive e_{ij} may correspond to metabolic wastes, toxins or anti-proliferative signals [127, 128, 156–159], while negative e_{ij} would describe growth factors or secondary metabolites [157, 160, 161]. The model kinetics is encapsulated in the following equations for the turnover of the species numbers:

$$\begin{aligned} \dot{x}_1 &= \beta_1 x_1 - \mu_1 x_1 - e_{11} t_1 x_1 - e_{12} t_2 x_1 \\ \dot{x}_2 &= \beta_2 x_2 - \mu_2 x_2 - e_{21} t_1 x_2 - e_{22} t_2 x_2, \end{aligned} \tag{3.3}$$

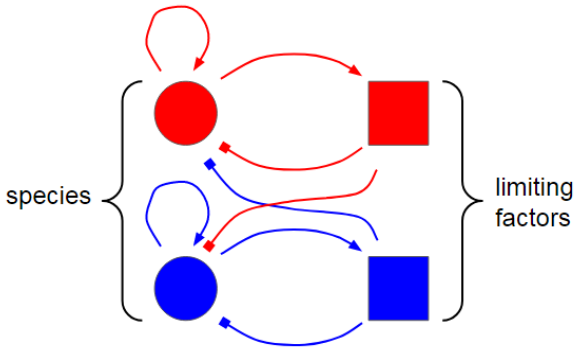

Figure 3.1: *A simple two species two resource model that derives the Lotka-Voltera model.* Each of the two species (here, red and blue circles) reproduces (arrows to self) and produces a toxin (arrows to limiting factors, respectively red and blue squares) which inhibits its own growth (square-ending lines to self) and the growth of the other (square-ending lines to other colour).

and the equations for the production and the degradation of the secreted factors:

$$\begin{aligned} \dot{t}_1 &= g_{11}x_1 + g_{12}x_2 - \lambda_1 t_1 \\ \dot{t}_2 &= g_{21}x_1 + g_{22}x_2 - \lambda_2 t_2. \end{aligned} \tag{3.4}$$

Figure 3.1 gives a pictoral representation of the interactions of the two species (cirlces) and their associated toxins (squares), albeit with $g_{12} = g_{21} = 0$.

It is useful to recast equations (3.3), (3.4) defining vectors $\vec{x} = (x_1, x_2)$ and $\vec{t} = (t_1, t_2)$, so that

$$\dot{\vec{x}} = \hat{R}\hat{X}\left(\vec{1} - \hat{E}\vec{t}\right) \quad \text{and} \quad \dot{\vec{t}} = \hat{L}\left(\hat{G}\vec{x} - \vec{t}\right), \tag{3.5}$$

where we have the matrices $\hat{X} = \begin{pmatrix} x_1 & 0 \\ 0 & x_2 \end{pmatrix}$, $\hat{L} = \begin{pmatrix} \lambda_1 & 0 \\ 0 & \lambda_2 \end{pmatrix}$, $\hat{R} = \begin{pmatrix} r_1 & 0 \\ 0 & r_2 \end{pmatrix} \equiv \begin{pmatrix} \beta_1 - \mu_1 & 0 \\ 0 & \beta_2 - \mu_2 \end{pmatrix}$, $\hat{G} = \begin{pmatrix} g_{11}/\lambda_1 & g_{12}/\lambda_1 \\ g_{21}/\lambda_2 & g_{22}/\lambda_2 \end{pmatrix}$, and $\hat{E} = \begin{pmatrix} e_{11}/r_1 & e_{12}/r_1 \\ e_{21}/r_2 & e_{22}/r_2 \end{pmatrix}$.

In many experimentally relevant systems, such as communities of microorganisms and cells, the timescale of production, diffusion, and degradation of secreted factors is on the order of minutes [162], whereas cell division and death occurs over hours [143, 163], and the dynamics of the turnover of the secreted factors can be assumed to adiabatically reach a steady state $\vec{t}^*$ given by $\vec{t}^* = \hat{G}\vec{x}$ [85, 103, 149]. In this approximation the dynamical equations for the species number reduce to

$$\dot{\vec{x}} = \hat{R}\hat{X}\left(\vec{1} - (\hat{E}\hat{G})\vec{x}\right). \tag{3.6}$$

Written explicitly, this becomes the familiar generalized two-species competitive Lotka-Volterra system [48–50, 52, 88, 147, 164, 165]:

$$\begin{aligned} \dot{x}_1 &= r_1 x_1 \left(1 - \frac{x_1 + a_{12}x_2}{K_1}\right) \\ \dot{x}_2 &= r_2 x_2 \left(1 - \frac{a_{21}x_1 + x_2}{K_2}\right), \end{aligned} \tag{3.7}$$

where $\frac{1}{K_i} = \frac{e_{ii}g_{ii}}{r_i\lambda_i} + \frac{e_{ij}g_{ji}}{r_i\lambda_j}$ and $\frac{a_{ij}}{K_i} = \frac{e_{ii}g_{ij}}{r_i\lambda_i} + \frac{e_{ij}g_{jj}}{r_i\lambda_j}$. The turnover rates r_i set the timescales of the birth and death for each species, and K_i are known as the carrying capacities. The interaction parameters a_{ij} provide a mathematical representation of the intuitive notion of the niche overlap between the species [10, 59, 60, 62]. When $a_{ij} = 0$, species j does not affect the species i, and they occupy separate ecological niches. At the other limit, $a_{ij} = 1$, the species j compete just as strongly with species i as species i does within itself, and both species occupy same niche. I refer to the a_{ij} as the niche overlap parameters.

The number of deterministically viable species is typically constrained by the number of limiting factors [41], as described in the previous section. Namely, if both matrices $\hat{E}$ and $\hat{G}$ are non-singular and invertible, the solutions to equation (3.5) are that one (or both) of the species is zero or else $\vec{x}^* = (EG)^{-1}\vec{1}$. The latter solution corresponds to the coexistence of the two species.

When the matrix $(\hat{E}\hat{G})$ is singular ($a_{12}a_{21} = 1$), the coexistence fixed point $\vec{x}^* = (EG)^{-1}\vec{1}$ does not exist, and the equations (3.5) are satisfied only if the population of one (or both) of the species is zero. Biologically, this condition corresponds to the complete niche overlap between two species, whereby only one species can survive in the niche. (Of note, exclusion of one species by the other can also occur in non-singular cases, as discussed in the next section.) Nevertheless, even in the complete niche overlap case, multiple species can deterministically coexist within one niche if the matrix $(\hat{E}\hat{G})$ possesses a further degeneracy, $K_1/K_2 = a_{12} = 1/a_{21}$, corresponding to an additional symmetry in the interactions of the species with the constraining factors, as illustrated in the next paragraph.

These mathematical notions can be understood in a biologically illustrative example, when the matrix $\hat{E}$ is singular, so that $\det(\hat{E}) = 0$. Any singular 2×2 real matrix can be written in the general form $\hat{E} = \begin{pmatrix} \alpha & \alpha\beta \\ \alpha\gamma & \alpha\beta\gamma \end{pmatrix}$, where α, β and γ are arbitrary real numbers [166]. In this case equation (3.3) becomes

$$\begin{aligned} \dot{x}_1 &= r_1 x_1\big(1 - \alpha\,(t_1 + \beta t_2)\,\big) \\ \dot{x}_2 &= r_2 x_2\big(1 - \gamma\alpha\,(t_1 + \beta t_2)\,\big), \end{aligned} \tag{3.8}$$

so that both secreted factors effectively act as one factor with concentration $t \equiv t_1 + \beta t_2$. With $\gamma \neq 1$ this corresponds to the classic notion of two species and only one limiting factor. The two equations cannot be simultaneously satisfied and the only solution of equations (3.8) is either $x_1 = 0$ or $x_2 = 0$ (or both). This is one example of competitive exclusion due to competition within a single niche. Finally, when $\gamma = 1$ (corresponding to $a_{12} = 1/a_{21} = K_1/K_2$), both the species and the secreted factors are functionally identical, and the equations (3.8) allow multiple solutions lying on the line in phase space defined by $\vec{x}^* = \hat{G}^{-1}\vec{t}^*$ and $1 = \alpha\,(t_1^* + \beta t_2^*)$ [40, 48]; in this case many different mixtures of the two species can be deterministically stable, depending on the initial conditions. However, as discussed in the next section, this line of fixed points is unstable with respect to perturbations along the line, and stochastic effects become important. These derivations above provide a mathematical definition and a biological illustration of the niche overlap between two interacting species, and can be extended to a general case of N species interacting via M factors, as shown in the Supplementary Information. In the next two sections, I study how the niche overlap affects the stability of the species coexistence in deterministic and stochastic cases.

3.4 Deterministic stability of the Lotka-Volterra model

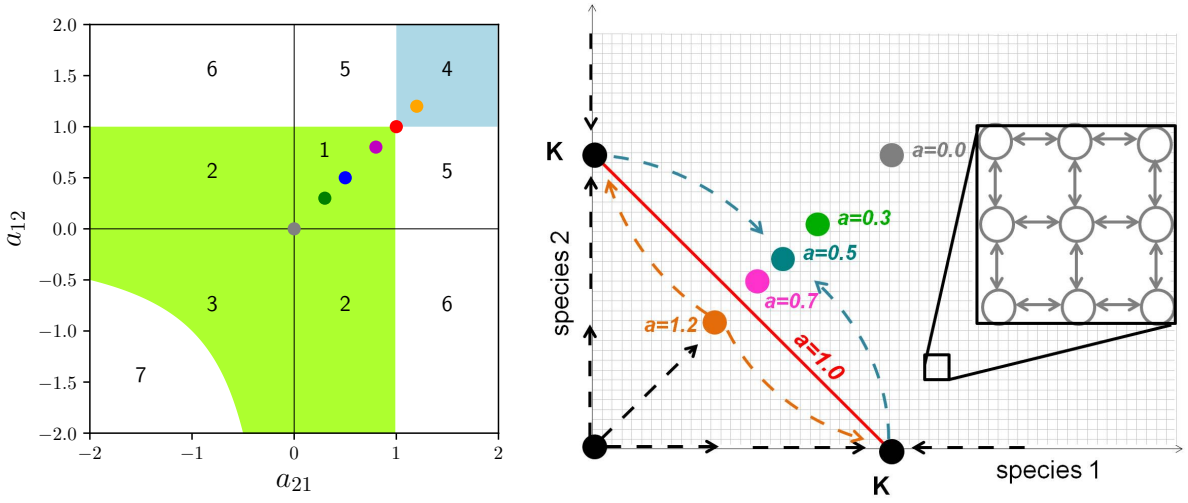

Figure 3.2: *Left: stability phase diagram of the coexistence fixed point for* $K_1 = K_2 = K$. The coexistence fixed point $C = \left(\frac{K_1 - a_{12}K_2}{1-a_{12}a_{21}}, \frac{K_2 - a_{21}K_1}{1-a_{12}a_{21}}\right)$ is stable in the green region and unstable in the blue region; in the white regions it is non-biological (negative). Colored dots indicate the parameter range studied in the paper. The numbered regions correspond to different biological regimes; see text. For the degenerate case $a_{12} = a_{21} = 1$, indicated by the red dot, the coexistence fixed point is replaced by a line of marginal stability, shown in the right panel. *Right: phase space of the coupled logistic model.* Colored dots show C at the indicated values of the symmetric niche overlap a. The fixed point is stable for $a < 1$. At $a = 0$ the two species evolve independently. As a increases, the deterministically stable fixed point moves toward the origin. At $a = 1$ the fixed point degenerates into a line of marginally stable fixed points, corresponding to the Moran model. The dashed lines illustrate the deterministic flow of the system: blue is for $a = 0.5$, and orange for $a = 1.2$. Having an asymmetry $r_1 \neq r_2$ deforms the dynamical flows but not position of C. The zoom inset illustrates the stochastic transitions between the discrete lattice states of the system. Fixation occurs when the system reaches either of the axes. See text for details.

In this section, which is a summary of the deterministic 2D Lotka-Volterra literature [49, 63, 64], I examine the behaviour of the deterministic equations 3.7, herein referred to as the coupled logistic or Lotka-Volterra equations, which have four fixed points:

$$O = (0,0) \quad A = (0,K_2) \quad B = (K_1,0) \quad C = \left(\frac{K_1 - a_{12}K_2}{1-a_{12}a_{21}}, \frac{K_2 - a_{21}K_1}{1-a_{12}a_{21}}\right). \tag{3.9}$$

The origin O is the fixed point corresponding to both species being extinct, and is unstable with positive eigenvalues equal to r_1 and r_2 along the corresponding on-axis eigendirections. The single species fixed points A and B are stable on-axis (with eigenvalues $-r_1$ and $-r_2$, respectively), but are unstable with respect to invasion if point C is stable, reflected in the positive second eigenvalue equal to $r_2(1 - a_{21}K_1/K_2)$ and $r_1(1-a_{12}K_2/K_1)$, respectively. Fixed point C corresponds to the coexistence of the two species and is stable in the green shaded region in the left panel of figure 3.2, which shows the stability diagram of the system for $K_1 = K_2$ [49, 63, 64].

The different regions of the phase space in figure 3.2 are known to have biological interpretations [56, 63, 64]. Parasitism, or predation/antagonism, occurs in regions 2 and 6 of (a_{12}, a_{21}) space, where $a_{12}a_{21} < 0$, with one species gaining from a loss of the other. In the strong parasitism regime (region 6), where

the positive a_{ij} is greater than one, the parasite/predator drives the prey to extinction deterministically, and the only stable point is the predator's fixed point (A or B). Conversely, weak parasitism (region 2) allows coexistence of both species despite the detriment of one to the benefit of the other [49, 63, 64].

The regions with both $a_{ij} < 0$ correspond to mutualistic/symbiotic interactions between the species [49, 63, 64]. Weak mutualism (region 3) is mathematically similar to weak competition in that it results in stable coexistence. Strong mutualism (region 7) results in population explosion. Detailed study of this regime lies outside of the scope of the present work (but see [167]).

The quadrant with both $a_{12} > 0$ and $a_{21} > 0$ corresponds to the competition regime. At strong competition with either a_{12} or a_{21} greater than one (regions 4 and 5 in the left panel in figure 3.2), either one of the species deterministically outcompetes the other (region 5) or the system possesses two single-species stable fixed points A and B with separate basins of attraction (region 4). The complete niche overlap regime of the underlying model of equations (3.5) and defined by $\det[\hat{E}\hat{G}] = 0$ is contained within region 4, and is given by the line $a_{12}a_{21} = 1$. These regimes correspond to the classical competitive exclusion theory, together with the strong parasitism case (region 6). By contrast, weak competition (region 1) where both $0 < a_{ij} < 1$ results in the stable coexistence at the mixed point C. In the special case $a_{12} = a_{21} = 1$ (shown by the red dot) the stable fixed point degenerates into a neutral line of stable points, defined by $x_2 = K - x_1$, as shown in the right panel of figure 3.2. Each point on the line is stable with respect to perturbations off line, but any perturbations along the line are not restored to their unperturbed position [40, 155]. This line correspond to the singular case, discussed in the previous section, where the two species are functionally identical with respect to the action of the secreted factors (*eg.* $e_{11}/r_1 = e_{12}/r_1$ and $e_{22}/r_2 = e_{21}/r_2$ in equations (3.5)). The stochastic dynamics along this line correspond to the classical Moran model as discussed below, and in the following I refer to this line as the Moran line.

The right panel of figure 3.2 shows the phase portrait of the system, in the symmetric case of $K_1 = K_2 \equiv K$, $r_1 = r_2 \equiv r$, and $a_{12} = a_{21} \equiv a$, where neither of the species has an explicit fitness advantage. This equality of the two species, also known as neutrality, serves as a null model against which systems with explicit fitness differences can be compared. In this thesis, I focus on species coexistence in the weak competition regime, finding the scaling of the mean time to fixation due to stochasticity. The asymmetric case is also treated, with results qualitatively similar to the symmetric case.

3.5 The stochastic Lotka-Volterra model

This section introduces the stochastic Lotka-Volterra model I analyze, which is the same used by some others [47, 48, 89]. However, the technique I use is more precise than what has been used in this literature, so my data are new.

Stochasticity naturally arises in the dynamics of the system from the randomness in the birth and death times of the individuals - commonly known as the demographic noise [79, 86, 168, 169]. Competitive interactions between the species can affect either the birth rates (such as competition for nutrients) or the death rates (such as toxins or metabolic waste), and in general may result in different stochastic descriptions [13, 100], as was discussed in the previous chapter. In this chapter, I follow others [47, 48, 89] in considering the case where the inter-species competition affects the death rates, so that the per capita

birth and death rates b_i and d_i of species i are:

$$\begin{aligned} b_i/x_i &= r_i \\ d_i/x_i &= r_i \frac{x_i + a_{ij}x_j}{K_i}. \end{aligned} \tag{3.10}$$

In terms of the previous chapter, this corresponds to choosing $\delta = 0$ and $q = 0$. Certainly different choices of δ and q would give different quantitative results, but the purpose of this chapter is not to investigate the effect of these parameters in the two-dimensional system but to find the transition between the qualitatively different results of the niche and neutral regimes of the Lotka-Volterra model. In the deterministic limit of negligible fluctuations the model recovers the mean field competitive Lotka-Volterra equations (3.7) [47]. As before, I renormalize the time by r, such that all times are implicitly expressed in units of $1/r$.

The system is characterized by the vector of probabilities $P(s,t|s^0)$ to be in a state $s = \{x_1, x_2\}$ at time t, given the initial conditions $s^0 = (x_1^0, x_2^0)$: $\vec{P}(t) \equiv \big(\dots, P(s,t|s^0), \dots\big)$ [137]. The forward master equation describing the time evolution of this probability distribution is [79]

$$\frac{d}{dt}\vec{P}(t) = \hat{M}\vec{P}(t), \tag{3.11}$$

where $\hat{M}$ is the (semi-infinite) transition matrix. I do not include the absorbing states in my transition matrix, and the master equation 3.11 as written does not preserve probability, as some of it leaks into fixation.

Because the approximate analytical and semi-analytical solutions of the master equation (3.11) often do not provide correct scaling in all regimes ([13, 101, 103, 117]; see also the previous chapter), I analyze the master equation numerically in order to recover both the exponential and polynomial aspects of the mean time to fixation. To enable numerical manipulations, I introduce a reflecting boundary condition at a cutoff population size $C_K > K$ for both species to make the transition matrix finite [137, 170] and enumerate the states of the system with a single index [137] via the mapping of the two species populations (x_1, x_2) to state s as

$$s(x_1, x_2) = (x_1 - 1)C_K + x_2 - 1, \tag{3.12}$$

where s serves as the index for our concatenated probability vector, uniquely enumerating all the states. In this representation, the non-zero elements of the sparse matrix $\hat{M}$ are $\hat{M}_{s,s} = -b_1(s) - b_2(s) - d_1(s) - d_2(s)$ along the diagonal, $\hat{M}_{s,s+1} = d_2(s+1)$ and $\hat{M}_{s+1,s} = b_2(s)$ at ± 1 off the diagonal, and $\hat{M}_{s,s+C_K} = d_1(s+C_K)$ and $\hat{M}_{s+C_K,s} = b_1(s)$ off-diagonal at $\pm C_K$. Some diagonal elements are modified to ensure the reflecting boundary at $x_i = C_K$.

Numerical results obtained from the Gillespie algorithm are accurate, assuming a sufficient number are averaged over [108]. Unfortunately even for a system size as small as $K = 20$ some of the simulations took over ten million steps before fixating. A tau-leaping implementation helps [109], but the problem remains that this fixation is a slow process and simulations of large K will be prohibitively long. As shown in the previous chapter, the distribution of fixation times is approximately exponential. Any simulations that do not finish will be from the tail end of the distribution but will have the largest contribution to the mean time, hence cannot be ignored.

Inverting the truncated transition matrix, as has been done in this chapter and the next, is a much

faster computational problem, and is hindered by insufficient RAM rather than interminable runtimes. Essentially it involves solving equation 2.13, $\hat{M}^T\vec{T} = -\vec{1}$ [78, 83]. Changing the cutoff means that the solution can be arbitrarily precise. In the left panel of figure 3.3, the direct solution from inverting the truncated transition matrix compares favourably with the Gillespie simulations.

To ensure accuracy of the mean times to 0.1% or better I choose $C_K = 5K$. This is largely excessive and even $C_K = 2K$ is sufficient for all but the smallest carrying capacities, for which it is least important to be accurate. The sparse matrix LU decomposition algorithm is implemented with the C++ library Eigen [171]. With 8GB of RAM this allows for a maximum carrying capacity around two hundred.

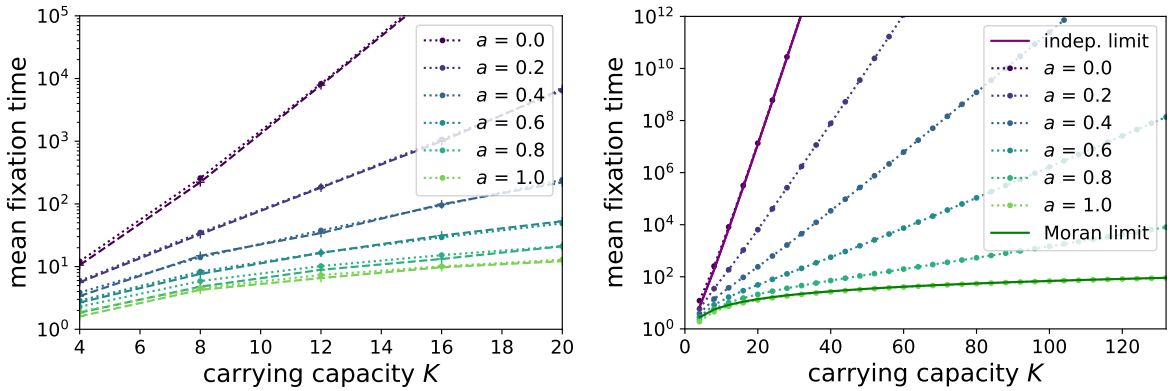

Figure 3.3: *Dependence of the fixation time on carrying capacity and niche overlap. Left:* Dotted lines come from directly solving the backwards master equation by inverting the transition matrix as per equation 3.22, after a cutoff has been applied to the matrix to make it finite. Dashed lines connecting crosses are each an average of a hundred realizations of the stochastic process, as simulated using the Gillespie algorithm with tau-leaping. The simulations and direct solution are in good agreement, as one would expect. *Right:* The same direct solution data as in the left panel are extended to larger carrying capacities. The lowest line, $a = 1$, recovers the Moran model results in solid green with the fixation time algebraically dependent on K for $K \gg 1$. For all other values of a, the fixation time is exponential in K for $K \gg 1$. At $a = 0$ the system acts as two independent stochastic logistic systems, and matches that limit as shown with the solid purple line.

3.6 Mean fixation time in the classical Moran model

Here I show the literature derivation of the mean fixation time for the Moran model [7], which will be used later as a limiting case of the Lotka-Volterra dynamics. Previous authors have already shown that this is the limit [47–49], and the fixation time for the Moran model is already known [7]. I only include it here for completeness. The Wright-Fisher model gives similar results for large K, but is less intuitable, dealing as it does with a whole generation at a time, rather than one birth and one death.

In the classical Moran model, at each time step, an individual is chosen at random to reproduce. In order to keep the population constant, another one is chosen at random to die. The probabilities that the number of individuals of species 1 increases or decreases by one in one time step are [7]:

$$b_M(n) = f(1-f) = (1-f)f = d_M(n) = \frac{n}{K}\left(1 - \frac{n}{K}\right) = \frac{1}{K^2}n(K-n), \tag{3.13}$$

where n is the number and f is the fraction of species 1 in the system (of total system size K). The

mean fixation time, $\tau(n)$, starting from some initial number n of species 1 is described by the following backward master equation [78]:

$$\tau(n) = \Delta t + d_M(n)\tau(n-1) + (1 - b_M(n) - d_M(n))\,\tau(n) + b_M(n)\tau(n+1),$$

where Δt is the time step. Substituting the values of the 'birth' and 'death' probabilities of species 1 from equation (3.13) we get

$$\tau(n+1) - 2\tau(n) + \tau(n-1) = -\frac{\Delta t}{b_M(n)} = -\Delta t \frac{K^2}{n(K-n)}.$$

At $K \gg 1$, the Kramers-Moyal expansion in $1/K$ results in

$$\frac{\partial^2 \tau}{\partial n^2} = -\Delta t\, K \left(\frac{1}{n} + \frac{1}{K-n}\right).$$

Integrating, using the boundary conditions $\tau(0) = \tau(K) = 0$, gives

$$\tau(n) = -\Delta t\, K^2 \left(\frac{n}{K} \ln\left(\frac{n}{K}\right) + \frac{K-n}{K} \ln\left(\frac{K-n}{K}\right)\right). \tag{3.14}$$

For the initial condition analogous to the coexistence point, $n = K/2$, this gives

$$\tau = \Delta t\, K^2 \ln(2).$$

Recall that the Moran model counts one time unit Δt every birth and death pair of events. The correspondence between the Moran model and the related Wright-Fisher model occurs when the Moran model has undergone a number of births and deaths equal to the (fixed) population size of Wright-Fisher, often called the generation time [34]. The time scale regarded is important. Similarly, for comparison between Moran and the coupled logistic model, one needs to match the time scales. First, note that the birth and death events can be treated as independent under the assumption that a single birth or death does not change the rates significantly, an assumption which is valid far from the axes. Then the probability of the next birth event happening around time t is $f(t)dt = b\,e^{-b\,t}dt$, and similarly $g(t)dt = d\,e^{-d\,t}dt$. Then define the probability of the birth happening by *by* time t is $F(t) = \int_0^t f(t')dt'$, and similarly $G(t) = 1 - e^{-d\,t}$. Assuming independence, a birth and a death event have happened by time t with probability $F(t)G(t)$, and the distribution of this time is given by $\partial_t[F(t)G(t)]$. The average time of a birth and death is then

$$\begin{aligned}\Delta t &= \int_0^\infty t\partial_t[FG]dt = \int_0^\infty t\partial_t[FG] = \int_0^\infty t\left(f(t) + g(t) - (b+d)e^{-(b+d)t}\right) \\ &= \frac{1}{b} + \frac{1}{d} - \frac{1}{b+d} = \frac{b^2 + bd + d^2}{b(b+d)d}.\end{aligned}$$

In principle this should be averaged over all combinations of the two species giving birth and dying, weighted by the probabilities of each pairing. It should also account for the probability of being at a particular state, as the state affects the rates. To simplify this I provide a lower bound by assuming that most of the time is spent near the initial state for the Moran limit, $(K/2, K/2)$, such that $b_i\,(K/2, K/2) =$

$d_i\,(K/2, K/2) = K/2$. This gives

$$\Delta t = \frac{3}{2}\frac{1}{b} = \frac{3}{2}\frac{1}{K/2} = \frac{3}{K} \tag{3.15}$$

and therefore

$$\tau = 3\ln(2)\,K. \tag{3.16}$$

The fixation time of the Moran model agrees well with the results of the coupled logistic model for complete niche overlap, as shown in figure 3.4.

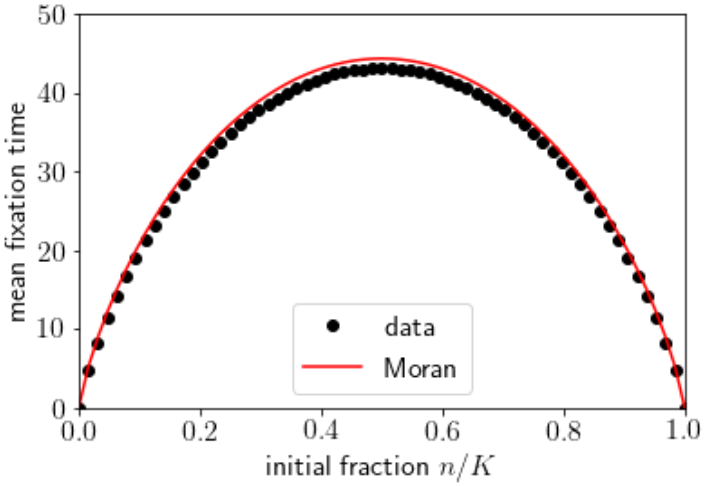

Figure 3.4: *Moran-like dynamics in the Moran limit of niche overlap in the coupled logistic model.* The coupled logistic, or Lotka-Volterra, model agrees with the Moran model in the limit of complete niche overlap, $a = 1$. Fixation time varies with initial fraction of the species in the population. The fixation time for the Moran model is in red and the coupled logistic model for $a = 1$ is in black. The population size of the Moran model is set equal to the carrying capacity $K = 64$ of the corresponding coupled logistic model.

3.7 Fixation time of the (un)coupled logistic model in the independent limit

Here I calculate the mean fixation time in the independent limit of the coupled logistic model given a distribution of extinction times for a single logistic model. Along with the Moran considerations of the previous section, this is an extreme asymptotic limit against which I will compare my data. Common knowledge in the field says that the independent limit should give exponential scaling of the fixation time with carrying capacity [88, 94–98]; this section is original research in which I estimate what the scaling should be.

The fixation occurs when either of the species goes extinct. Denoting the probability distribution of the extinction times for either of independent species as $p(t)$ and its cumulative as $F(t) = \int_{s=0}^{t} p(s)ds$, the probability that *either* of the species goes extinct in the time interval $[t, t + dt]$, is the probability of species 1 going extinct while species 2 has not, plus the probability that species 2 goes extinct while

species 1 has not, since these are the two possibilities. That is,

$$p_{min}(t)dt = \Big(p(t)\,(1-F(t)) + (1-F(t))\,p(t)\Big)dt = 2p(t)\,(1-F(t))\,dt. \tag{3.17}$$

The mean time to fixation $\langle t\rangle$ is

$$\langle t\rangle = \int_0^\infty dt\, t\, p_{min}(t). \tag{3.18}$$

As shown in figure 2.3 from the previous chapter, the probability distribution of fixation times of a single species is dominated by the exponential tail. It can be approximated as

$$p(t) = \alpha e^{-\alpha t}, \quad F(t) = 1 - e^{-\alpha t} \tag{3.19}$$

with $\frac{1}{\alpha} \simeq \frac{1}{K}e^K$ from the previous chapter [95, 113]. Finally, I obtain for the mean time to fixation

$$\langle t\rangle = \int_0^\infty dt\, t\, 2\alpha e^{-2\alpha t} = \frac{1}{2\alpha}. \tag{3.20}$$

which leads to the equation $\tau \simeq \frac{1}{2K}e^K$.

3.8 Fixation time as a function of the niche overlap

Henceforth in this chapter the results and analyses are novel.

In this section I calculate the first passage times to the extinction of one of the species and the corresponding fixation of the other, induced by demographic fluctuations, starting from an initial condition of the deterministically stable coexistence point. The master equation (3.11) has a formal solution obtained by the exponentiation of the matrix: $\vec{P}(t) = e^{\hat{M}t}\vec{P}(0)$. However, direct matrix exponentiation, as well as direct sampling of the master equation using the Gillespie algorithm [108, 109], are impractical since the fixation time grows exponentially with the system size. However, the moments of the first passage times can be calculated directly without explicitly solving the master equation [172]. The mean residence time in any state s during the system evolution is

$$\langle t(s^0)\rangle_s = \int_0^\infty dt\; P(s,t|s^0) = \int_0^\infty dt\; (e^{\hat{M}t})_{s,s^0} = -(\hat{M}^{-1})_{s,s^0}. \tag{3.21}$$

The final equality in the previous equation is obtained integration by parts and requires that all the eigenvalues of the transition matrix $\hat{M}$ are negative, a fact that is evident by its construction: since the master equation conserves probability (which is bounded by one), none of the eigenvalues can be positive; since the steady state absorbing states have been removed, there are no zero eigenvalues. Thus, the mean time to fixation starting from a state s^0 is [83]

$$\tau(s^0) = -\sum_s \langle t(s^0)\rangle_s = -\sum_s \left(\hat{M}^{-1}\right)_{s,s^0}. \tag{3.22}$$

This expression can be also derived using the backward equation formalism [83]. The matrix inversion was performed using LU decomposition algorithm implemented with the C++ library Eigen [171], which has algorithimic complexity of the calculation scaling algebraically with K. Increasing the cutoff C_K

enables calculation of the mean fixation times to an arbitrary accuracy.

The right panel of figure 3.3 shows the calculated fixation times with the initial condition at the deterministically stable coexistence fixed point as a function of the carrying capacity K for different values of the niche overlap a. In the limit of non-interacting species ($a = 0$), each species evolves according to an independent stochastic logistic model, and the probability distribution of the fixation times is a convolution of the extinction time distributions of a single species, which are dominated by a single exponential tail [80, 91, 107]. Mean extinction time of a single species can be calculated exactly as in the previous chapter, and asymptotically for $K \gg 1$ it varies as $\frac{1}{K}e^K$ [95] giving for the overall fixation time in the two species model $\tau \simeq \frac{1}{2K}e^K$ as in equation (3.20). This analytical limit is shown in figure 3.3 as a solid purple line and agrees well with the numerical results of equation (3.22). From the biological perspective, for sufficiently large K, the exponential dependence of the fixation time on K implies that the fluctuations do not destroy the stable coexistence of the two species.

In the opposite limit of complete niche overlap, $a = 1$, any fluctuations along the line of neutrally stable points are not restored, and the system performs diffusion-like motion that closely parallels the random walk of the classic Moran model [47–50, 88, 90, 123, 148]. The Moran model shows a relatively fast fixation time scaling algebraically with K [7, 47], $\tau \simeq \ln(2)K^2\Delta t$; see equation (3.16). The fixation time predicted by the Moran model is shown in figure 3.3 as a solid green line and shows excellent agreement with my exact result. The relatively short fixation time in the complete niche overlap regime implies that the population can reach fixation on biologically realistic timescales.

The exponential scaling of the fixation time with K persists for incomplete niche overlap described by the intermediate values of $0 < a < 1$. However, both the exponential and the algebraic prefactor depend on the niche overlap a. The exponential scaling is expected for systems with a deterministically stable fixed point [80, 89, 90, 101, 103], as indicated in [47, 49, 88] using Fokker-Planck approximation and in [89] using the WKB approximation. However, the Fokker-Planck and WKB approximations, while providing the qualitatively correct dominant scaling, do not correctly calculate the scaling of the polynomial prefactor and the numerical value of the exponent simultaneously [13, 80, 123], as was shown in the previous chapter. For large population sizes and timescales, effective species coexistence will be typically observed experimentally whenever the fixation time has a non-zero exponential component.

To quantitatively investigate the transition from the exponentially stable fixation times to the algebraic scaling in the complete niche overlap regime, I use the ansatz

$$\tau(a, K) = e^{h(a)}K^{g(a)}e^{f(a)K}. \tag{3.23}$$

In the Moran limit, $a = 1$, I expect $f(1) = 0$, $g(1) = 1$, and $h(1) = \ln\big(\ln(2)\big)$ as follows from equation (3.16). In the independent species limit with zero niche overlap, $a = 0$, equation (3.20) suggests $f(0) = 1$, $g(0) = -1$, and $h(0) = -\ln(2)$. The left panel of figure 3.5 shows the ansatz functions $f(a)$, $g(a)$, and $h(a)$, obtained by numerical fit (using the SciPy python package) to the fixation times as a function of K shown in figure 3.3. The numerical results agree well with the expected approximate analytical results for $a = 0$ and $a = 1$ with small discrepancies attributable to the approximate nature of the limiting values. Notably, $f(a)$, which quantifies the exponential dependence of the fixation time on the niche overlap a, smoothly decays to zero at $a = 1$: only when two species have complete niche overlap ($a = 1$) does one expect rapid fixation dominated by the algebraic dependence on K. In all other cases the mean time until fixation is exponentially long in the system size [80, 107]. Even two species that occupy *almost* the same niche ($a \lesssim 1$) effectively coexist for $K \gg 1$, with small fluctuations around the

deterministically stable fixed point.

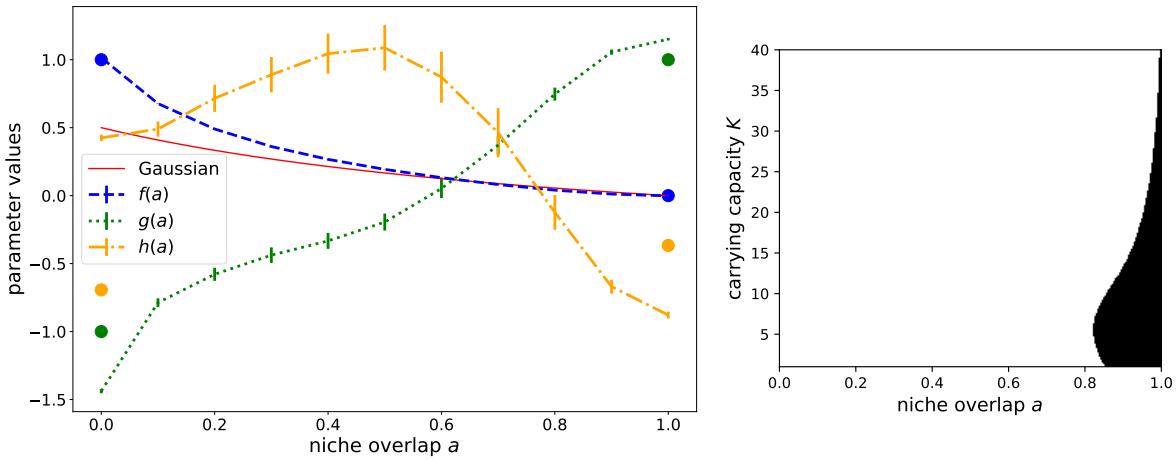

Figure 3.5: *Niche overlap controls the transition from coexistence to fixation. Left:* Blue line: $f(a)$ from the ansatz of equation (3.23) characterizes the exponential dependence of the fixation time on K; it smoothly approaches zero as the niche overlap reaches its Moran line value $a = 1$. Green line: $g(a)$ quantifies the scaling of the pre-exponential prefactor $K^{g(a)}$ with K. Yellow line: $h(a)$ is the multiplicative constant. Dashed bars represent a 95% confidence interval. For each a value, the ansatz was fit to data like those shown in figure 3.3. The dots at the extremes $a = 0$ and $a = 1$ are the expected asymptotic values from equations (3.16) and (3.20), which varies from $g(a) = -1$ for the independent processes to $g(a) = 1$ in the Moran limit. The red line comes from the Gaussian Fokker-Planck approximation described in section 3.10 below. *Right:* In part of the parameter space, fixation is always fast. The white area shows where two species are expected to effectively coexist, while the black shading identifies the regime where fixation is faster than a similarly-sized Moran model. Fixation is estimated by extrapolating the ansatz parameter fits to the a, K parameter space. See text for details.

3.9 Coexistence versus fixation in parameter space

I make the claim that when biological system sizes are large, a fixation time that scales exponentially with carrying capacity effectively implies coexistence. This is typically the case. However, some systems have only a few competing members, as in nascent cancers or plasmids in a single cell. I want to get a better sense of when the exponential scaling is relevant, especially since for those systems with almost complete niche overlap the exponential scaling is slow. To this end I compare the expected mean fixation time with that of the Moran model. The ansatz $e^{h(a)}K^{g(a)}e^{f(a)K}$ is fit to the data and then used to estimate the fixation time at a variety of parameter values. This time is compared to the fixation time of a Moran model with the same carrying capacity. In the right panel of figure 3.5 the shaded region represents those parameter combinations for which the estimated fixation is faster than the corresponding Moran model. For example, a carrying capacity of about 35 organisms is sufficient to allow for effective coexistence of two species which are not more than 99% identical in their niches. This is a small population size in most biological contexts. Even for systems with a smaller carrying capacity, unless the two species are more similar they are expected to coexist for long times before fixation.

3.10 Fokker-Planck analysis of the Lotka-Volterra model

The most common approximation to the master equation is Fokker-Planck, which assumes the state space is continuous. I attempt its use here to get an analytic estimate of the dependence of fixation time on K and a. We shall see that its utility is only marginal, though with some further approximations and an application of Kramers' theory I get my desired estimate.

The Fokker-Planck approximation to the coupled logistic system studied herein takes its traditional form [78]:

$$\begin{aligned}\frac{dP}{dt} &= -\partial_1[(b_1-d_1)P] - \partial_2[(b_2-d_2)P] + \frac{1}{2}\partial_1^2[(b_1+d_1)P] + \frac{1}{2}\partial_2^2[(b_2+d_2)P] \\ &= -\sum_i \partial_i F_i P + \sum_{i,j}\partial_i\partial_j D_{ij} P \end{aligned} \tag{3.24}$$

where F is the force vector and D is the diffusion matrix (in this case diagonal). Here, under symmetric conditions and nondimensionalization by r, $F_1 = \frac{x_1}{K}(K - x_1 - ax_2)$ and $D_{11} = \frac{x_1}{K}(K + x_1 + ax_2)$, with similar terms for species 2.

In general, equation (3.24) cannot be reduced to diffusion in a potential $U(\vec{x})$ with an equilibrium distribution function $P(\vec{x}) \sim \exp(U(\vec{x}))$. The condition of zero flux at equilibrium, $J_i = F_i P - 1/2\sum_j \partial_j D_{ij} P = 0$, would require [82]

$$\partial_i \log P = \sum_k (D^{-1})_{ik}\big(2F_k - \sum_j \partial_j D_{kj}\big) \equiv -\partial_i U,$$

However, for consistency it also requires $\partial_j\left(-\partial_i U\right) = \partial_i\left(-\partial_j U\right)$ [82]. It is easy to show that this is not upheld for the two directions unless $a_{12} = a_{21} = 0$ and the system can be decomposed into two one-dimensional logistic systems.

Instead, I use the definition of the pseudo-potential [139]

$$U(x_1, x_2) \equiv -\ln\left[P_{ss}(x_1, x_2)\right], \tag{3.25}$$

where $P_{ss}(x_1, x_2)$ is a quasi-stationary probability distribution function. I calculate $P_{ss}(x_1, x_2)$ in the approximation to the Fokker-Planck equation (3.24) linearized about the deterministic coexistence fixed point. The linearized equation is [82]

$$\partial_t P = -\sum_{i,j} A_{ij}\partial_i(x_j - x_j^*)P + \frac{1}{2}\sum_{i,j} B_{ij}\partial_i\partial_j(x_i - x_i^*)(x_j - x_j^*)P \tag{3.26}$$

where $A_{ij} = \partial_j F_i|_{\vec{x}=\vec{x}^*}$ and $B_{ij} = D_{ij}|_{\vec{x}=\vec{x}^*}$. The quasi-equilibrium solution to equation (3.26) is $P_{ss} = \frac{1}{2\pi}\frac{1}{|C|^{1/2}}\exp[-(\vec{x}-\vec{x}^*)^T C^{-1}(\vec{x}-\vec{x}^*)/2]$, a Gaussian centered on the coexistence point and with a variance given by the covariance matrix $C = B \cdot A^{-1}/2$ in the symmetric case $a_{12} = a_{21} = a$, $K_1 = K_2 = K$ [79]. In this case the diagonal term of C is $\frac{1}{1-a^2}K$ and gives the variance of a species about its mean value. The off-diagonal, which corresponds to the covariance between the two species, is $-\frac{a}{1-a^2}K$. Thus the Pearson correlation coefficient between the two species is $-a$. That is, they are maximally anti-correlated when $a = 1$, lying along the line $x_1 + x_2 = K$ - the Moran line.

For the initial condition at the coexistence fixed point and assuming that the system escapes towards fixation once it reaches one of the axial fixed points $(0, K)$ or $(K, 0)$, from equation (3.25) the well depth

is proportional to carrying capacity K, being

$$\Delta U = \frac{(1-a)}{2(1+a)}K. \tag{3.27}$$

In a Kramers' type approximation, the escape time from the pseudo-potential well scales as $\sim \exp(\Delta U)$ [107], reproducing the exponential scaling of the extinction time with K, observed numerically. Moreover, the Fokker-Planck approximation also shows that the exponential scaling disappears as niche overlap a approaches unity, in accord with the numerical results above. The correlation between the two species goes to negative one in this parameter limit, such that they are entirely anti-correlated. Whereas the well has a single lowest point at the coexistence fixed point for partial niche overlap, at $a = 1$ the potential shows a trough of constant depth going between the two axial fixed points. This is the Moran line, along which diffusion is unbiased; diffusion away from the Moran line is restored, as the system is drawn toward the bottom of the trough. Because everywhere along the Moran line is equally likely, the probability cannot be normalized, and the linearization approximation fails. This is to be expected, as it is an expansion about a fixed point, but the fixed point is replaced by the Moran line in the Moran limit of $a = 1$.

3.11 Breaking the parameter symmetries

I have addressed the symmetric case of $K_1 = K_2 \equiv K$ and $a_{12} = a_{21} \equiv a$. The result of exponential scaling of the fixation time except when the Moran line exists is true even when some symmetries are broken. However, the evidence is not as clear as in the symmetric case.

Panel A of figure 3.6 shows the dependence of the fixation time on the niche overlap a_{21} while keeping $a_{12} = 0.5$ for $K_1 = K_2 \equiv K$; using the similar ansatz, I apply the same $\tau = e^{h(a_{21})}K^{g(a_{21})}e^{f(a_{21})K}$. As the niche overlap a_{21} changes from 0 to 1, the location of the coexistence fixed point shifts from $(K/2, K/4)$ to $(K, 0)$. Accordingly, the fixation time starting from the fixed point maintains its exponential scaling with carrying capacity up until $a_{21} = 1$, where the fixed time is equal to zero, as reflected in the shape of the of $h(a_{21})$. Notably, in this asymmetric case the exponential scaling function $f(a_{21})$ is much weaker compared to the symmetric case, partially because the fixed point is located closer to an axis that in the symmetric case even at $a_{21} = 0$. I suspect the apparent non-monotonicity of the algebraic and constant terms to be the result of fitting with an insufficient number of data generated, and in any case they are of lesser import than the exponential scaling. Panel B of figure 3.6 shows the comparison of the results of the ansatz fit with the estimates of the exponential part of the fixation time using Kramers'/Fokker-Planck pseudo-potential described in the previous section that explains the observed trends of $f(a_{21})$. The Gaussian pseudo-potential shows a similar trend to the data, though quantitatively it remains incorrect.

Next let us consider breaking the symmetry such that the Moran line can still be recovered. The carrying capacity symmetry is broken, such that $K_2 = 2K_1$. The two species are still independent when $a_{12} = a_{21} = 0$, but in this case the Moran line exists when $a_{12} = 2$ and $a_{21} = 1/2$. Figure 3.6 shows the results when the symmetry is broken both in the carrying capacity and the niche overlap. It shows the change in the fixation time as a function of the niche overlap a_{21} for $K_2 = 2K_1 \equiv K$ while the niche overlaps change along the line where $a_{12} = 4a_{21}$, starting from the independent case $a_{12} = a_{21} = 0$ to $a_{12} = 2$ and $a_{21} = 1/2$ where the system reaches its corresponding Moran line. The observed behaviour

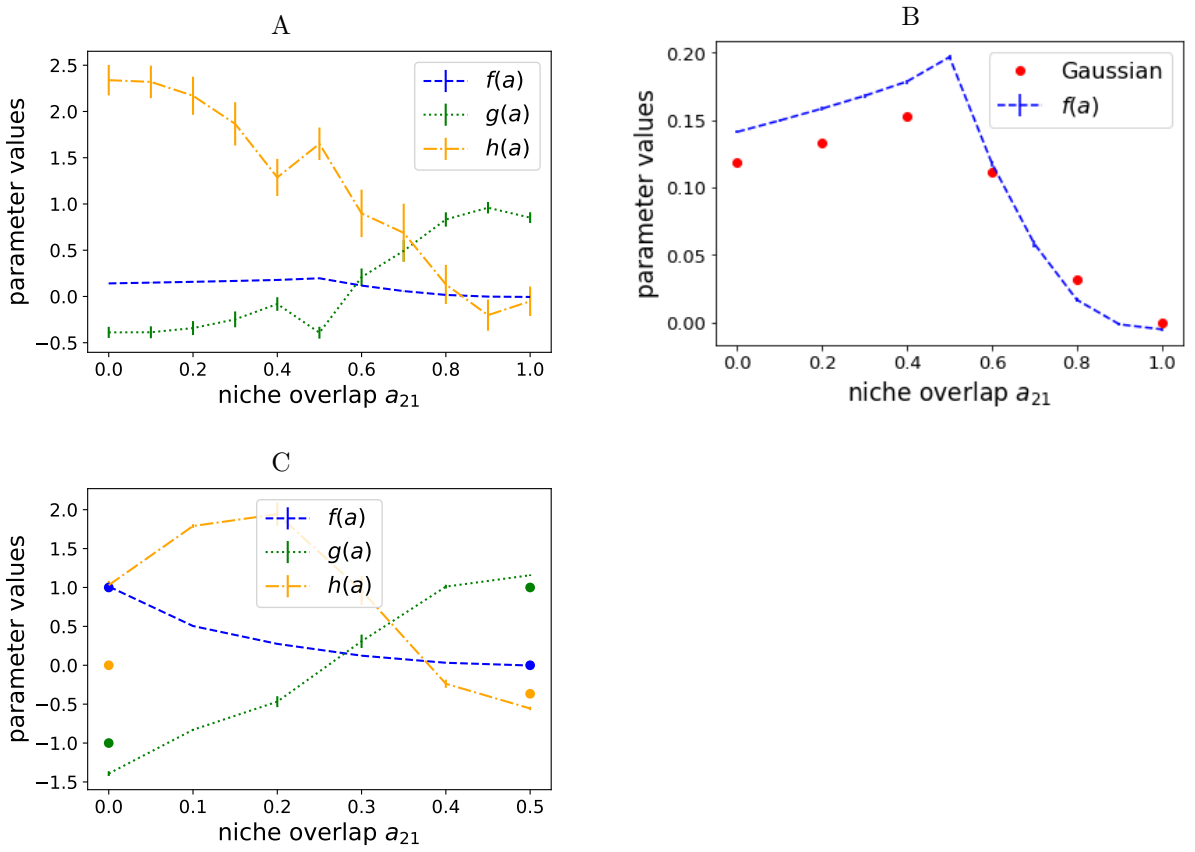

Figure 3.6: *Breaking the parameter symmetries. Panel A:* As in figure 3.5, lines come from fitting the ansatz of equation 3.23 to data generated from equation 3.22. In this case the niche overlap symmetry is broken and $a_{12} = 0.5$. The exponential dependence on carrying capacity is non-zero except at $a_{21} = 1$, at which point the "coexistence" fixed point is coincident with the fixed point on the x-axis. *Panel B:* The ansatz fit from panel A is compared with the Gaussian well depth at the same parameter values. The non-zero exponential dependence is observed in the Gaussian approximation as well. *Panel C:* The symmetry is broken in carrying capacity, such that $K_2 = 2K_1$. The ansatz is fit to K_1. The exponential dependence is non-zero except at the appearance of the Moran line at $a_{21} = 1/2$. The extreme points are the approximate asymptotic values.

is very similar to that shown in the symmetric case, with the exponential dependence transitioning smoothly to zero at the Moran line.

I uphold the conclusion that at the Moran line will fixation be fast; when the system parameters are even slightly off those niche overlap values which balance the carrying capacities and allow for the Moran line to exist, the fixation is exponential in the carrying capacity, to the point that the two species effectively coexist. I include the caveat that fixation will also be fast when the coexistence fixed point is close to one axis, as evinced with the broken niche overlap symmetry above.

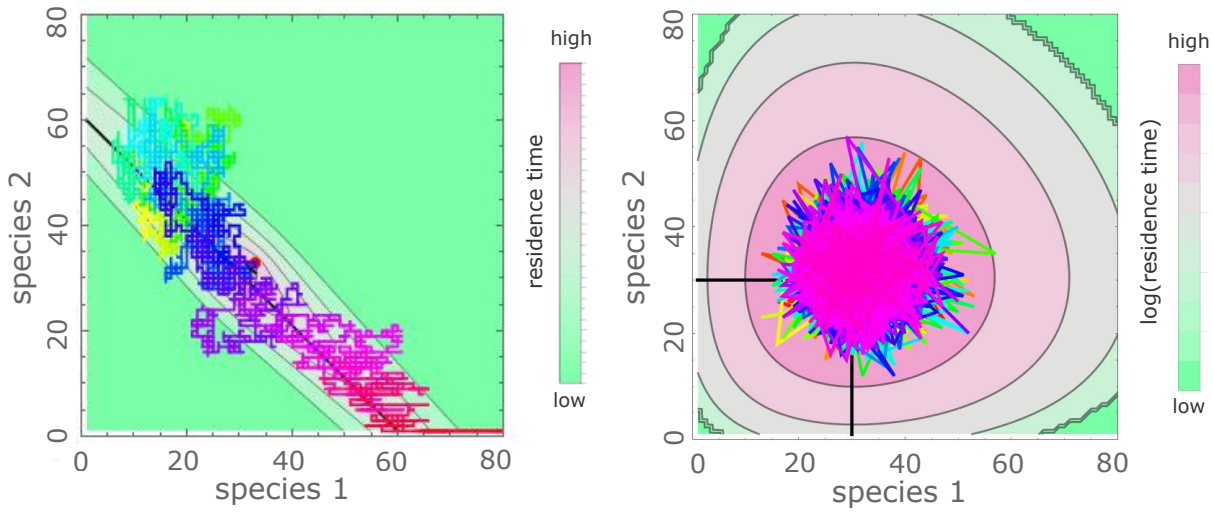

Figure 3.7: *The system samples multiple trajectories on its way to fixation.* Contour plot shows the average residency times at different population states of the system, with pink indicating longer residence time, deep green indicating rarely visited states. The colored line is a sample trajectory the system undergoes before fixation, as generated by the Gillespie algorithm; color coding corresponds to the elapsed time with orange at early times, purple at the intermediate times and red at late stages of the trajectory. The red dot shows the deterministic coexistence point, and the black lines are the most probable exit trajectories. See text for more details. *Left*: Complete niche overlap limit, $a = 1$, for $K = 64$. *Right*: Independent limit with $a = 0$ and $K = 32$.

3.12 Route to fixation

To gain deeper insight into the fixation dynamics, in this section I calculate the residency times in each state during the fixation process [172], given by equation (3.21), reproduced here:

$$\langle t(s^0)\rangle_s = \int_0^\infty dt P(s,t|s^0,0) = \hat{M}^{-1}_{s,s^0}. \tag{3.28}$$

This gives the mean total time the system resides in state s, given that it starts in state s^0. As with the fixation times, the dependence on the initial state is weak, so long as that initial state is not near an axis. Whereas I previously analyzed the fixation time scaling, the residency times themselves proffer some insight into the system. The results are shown as a contour plot in figure 3.7, where pink corresponds to the high occupancy sites and green to the rarely visited ones, for two different niche overlaps, one at and the other far from the Moran limit. The set of states lying along the steepest descent lines of the contour plot, shown as the black line, can be thought of as a "typical" trajectory [89, 114, 123, 173, 174]. However, even for two species close to complete niche overlap the system trajectory visits many states far from this line. This departure is even greater for weakly competing species, where the system covers large areas around the fixed point before the rare fluctuation that leads to fixation occurs [87]. These deviations from a "typical" trajectory are related to the inaccuracy of the WKB approximation in calculating the scaling of the pre-exponential factor [87, 95, 102, 103]; see also the previous chapter.

This occupancy landscape can be qualitatively thought of as an effective Lyapunov function/effective potential of the system dynamics [139], although the LV system does not possess a true Lyapunov function - an issue that also arises in the Fokker-Planck approximation [49, 139]. One way to deal

with this issue is the linearization in the Fokker-Planck section above (section 3.10). This allows one to easily solve the Fokker-Planck equation in any system with an attractive deterministic fixed point. More pertinently, linearizing the Fokker-Planck equation, as in equation 3.26 described above, allows one to get an estimate of the depth of the pseudo-potential: $\frac{(1-a)}{2(1+a)}K$. This provides an intuitive underpinning for the general exponential scaling in the incomplete niche overlap regime: the fixation process can be thought of as the Kramers'-type escape from a pseudo-potential well [107, 175]. The Kramers result is dominated by $\tau \simeq \exp(\text{well depth})$, corresponding to the dominant scaling $\tau \simeq \exp(f(a)K)$. As a increases and the species interact more strongly, the potential well becomes less steep, resulting in weaker exponential scaling. In the complete niche overlap limit, the pseudo-potential develops a soft direction along the Moran line that enables relatively fast escape towards fixation. This is what is seen in the residence time graph; in the Moran limit, the states along the line connecting the coexistence fixed point to the two axial fixed points are visited much more frequently than those off it. Outside of the Moran limit, it is rather the states in a cloud around the coexistence point that enjoy long residence times.

In linearizing the FP equation I also arrived at the Pearson correlation coefficient between the two species: $-a$. They are anti-correlated, and this anti-correlation becomes complete as niche overlap approaches one. In state space this corresponds to the system lying on the Moran line. Thus we expect the pseudo-potential to become less steep as a increases, eventually developing a level trough along the Moran line that enables relatively fast escape toward fixation. Though I am unaware of any direct connection, this disappearance is also mimicked in the deterministic coexistence point eigenvalue associated with the $(1, -1)$ direction, which goes to zero as niche overlap goes to one, as $-\frac{1-a}{1+a}$.

3.13 Discussion

Maintenance of species biodiversity in many biological communities is still incompletely understood. The classical idea of competitive exclusion postulates that ultimately only one species should exist in an ecological niche, excluding all others. Although the notion of an ecological niche has eluded precise definition, it is commonly related to the limiting factors that constrain or affect the population growth and death. In the simplest case, one factor corresponds to one niche, which supports one species, although a combination of factors may also serve as a niche, as discussed above. The competitive exclusion picture has encountered long-standing challenges as exemplified by the classical "paradox of the plankton" [21, 24] in which many species of plankton seem to co-habit the same niche; in many other ecosystems the biodiversity is also higher than appears to be possible from the apparent number of niches [11, 20, 21, 65, 176].

Competitive exclusion-like phenomena can appear in a number of popular mathematical models, for instance in the competition regime of the deterministic Lotka-Volterra model, whose extensive use as a toy model enables a mathematical definition of the niche overlap between competing populations [10, 59, 60, 62]. Another classical paradigm of fixation within an ecological niche is the Moran model (and the closely related Fisher-Wright, Kimura, and Hubbell models) that underlies a number of modern neutral theories of biodiversity [7, 11, 35, 47, 150, 177, 178]. Unlike the deterministic models, in the Moran model fixation does not rely on deterministic competition for space and limiting factors but arises from the stochastic demographic noise. Recently, the connection between deterministic models of the LV type and stochastic models of the Moran type has accrued renewed interest because of new focus on the stochastic dynamics of the microbiome, immune system, and cancer progression [47–49, 103, 148,

149, 179, 180].

Many of the recent studies of these systems employ various approximations, such as the Fokker-Planck approximation [47–49, 88, 90], WKB approximation [89, 123] or game theoretic [148] approach. The results of these approximations typically differ from the exact solution of the master equation, especially for small population sizes [13, 80, 101, 103, 123], as was discussed in more detail in the previous chapter. In this chapter, I have interrogated stochastic dynamics of a system of two competing species using a numerically arbitrarily accurate method based on the first passage formalism in the master equation description. The algorithmic complexity of this method scales algebraically with the population size rather than with the exponential scaling of the fixation time, (as is the case with the Gillespie algorithm [108]) enabling us to capture both the exponential behaviour and the algebraic prefactors in the fixation/extinction times for both small and large population sizes. This accuracy is needed in order to observe the transition from slow, exponentially dominated processes to the algebraically fast fixation of the Moran limit.

Stochastic fluctuations allow the system to escape from the deterministic coexistence fixed point towards fixation. If the escape time is exponential in the (typically large) system size, in practice it implies effective coexistence of the two species around their deterministic coexistence point. If the time is algebraic in K, as in degenerate niche overlap case (closely related to the classical Moran model), the system may fixate on biological timescales [7, 9]. For those biological systems with small characteristic population sizes, exponential scaling does not dominate the fixation time; power law and prefactor become more relevant. Figure 3.5 shows that a niche overlap as low as 0.8, for a carrying capacity around 6, has rapid fixation, more rapid than a corresponding Moran model. The transition between the exponential scaling of effective coexistence time to the rapid stochastic fixation in the Moran limit is governed by the niche overlap parameter, which for example can be derived in terms of the dynamics and interactions of the species and their secreted growth and death factors.

While I find that the fixation time is exponential in the system size unless the two species occupy exactly the same niche, the numerical factor in the exponential is highly sensitive to the value of the niche overlap, and smoothly decays to zero in the complete niche overlap case. These results can be understood by noticing that the escape from a deterministically stable coexistence fixed point can be likened to Kramers' escape from a pseudo-potential well [80, 88, 107, 181], where the mean transition time grows exponentially with well depth [80]. Approximating the steady state probability with a Gaussian shows that this well depth is proportional to $K(1-a)$ and disappears when $a = 1$. With complete niche overlap the system develops a "soft" marginally stable direction along the Moran line that enables algebraically fast escape towards fixation [49, 88]. Similar to the exponential term, the exponent of the algebraic prefactor is also a function of the niche overlap, and smoothly varies from -1 in the independent regime of non-overlapping niches to $+1$ in the Moran limit.

Niche overlap between two species, the similarity in how they interact with their shared environment, is of critical importance in determining whether they will coexist. For typically large biological populations, effective coexistence occurs when escape time grows exponentially with the carrying capacity, which is the case for even slightly mismatched niches. Any niche mismatch leads to species which tend to exist for long times near their respective carrying capacities; in effect, niche models are apt even for large niche overlap. Only when niche overlap is complete will fixation be relatively rapid, algebraic in K. This has important implications for understanding the long term population diversity in many systems, such as human microbiota in health and disease [27, 31, 182], industrial microbiota used in

fermented products [183], and evolutionary phylogeny inference algorithms [33, 34]. My results show that the generalized Lotka-Volterra model serves well as an extension to neutral models for problems such as maintenance of drug resistance plasmids in bacteria [136], strain survival in cancer progression [179], or the generation of coalescent or phylogenetic trees [32, 33, 35]. The theoretical results can also be tested and extended based on experiments in more controlled environments, such as the gut microbiome of a *C. elegans* [180], or in microfluidic devices [184].

Chapter 4

Invasion: Transition from One Species to Two

This chapter, along with the next one, is based on a paper written by me and my supervisor Anton Zilman, which is currently under revision for The Proceedings of the Royal Society Journal [12].

4.1 Introduction

The previous chapter regarded an ecosystem with two competing species, and asked questions about the mean time until one of the species goes extinct and the other fixates in the system. In this chapter I aim to look at the reverse problem; starting with a stable system with one species, what is the probability and timescale that a second one will enter and establish itself, given some overlap between the niches of the extant and immigrating species. First I would like to motivate the problem and discuss where a new species entering a system might come from.

Invasion, in one form or another, is a relevant factor in a variety of biological contexts. When a new allele arises in a population of genes it acts as an invader, and if it is successful it contributes to the genetic diversity of the population This is the situation considered by Kimura and Crow as they analyzed the probability of a single mutant or immigrant allele to fixate [8, 9, 150]. Invasion is also of relevance in biodiversity. The biodiversity of an island increases as immigrants from a neighbouring mainland enter (and decreases as species go locally extinct); the idea of these forces balancing was one of the historic contributions of MacArthur and Wilson [51, 185]. The biodiversity of an ecosystem is also maintained by invaders generated by speciation, as per Hubbell's neutral theory, which predicts the abundance distribution of species [11]. Bearing these historical precedents in mind, I do not distinguish from where a new strain or species might enter in my modelling below; mutation, speciation, and immigration are all viable. What is important to my research is that a distinct second species is attempting to invade an already occupied system. Whether the invader is under selection [70] or the system is neutral [8, 11], the literature regards cases where the system is constrained to the Moran line, to constant population size. What has *not* been done is to look at an invasion attempt into an established niche when the invader has partial niche overlap with the established species.

By using the two species Lotka-Volterra model from the previous chapter I can study invasion in the neutral case where the system is allowed to fluctuate off the Moran line, or even when the two species

should happily coexist in the deterministic limit, *i.e.* with partial niche overlap and a single stable coexistence fixed point. I do this by continuing to use the truncated transition matrix inverse to solve the backward master equation for arbitrary accuracy. Furthermore, the literature typically argues that invasion attempts are sufficiently rare that when an invader arrives it will either successfully invade or die off before another member of the same strain invades. Indeed, this is one of my assumptions when using the Lotka-Volterra model below. But this need not be the case, depending on the immigration rate (see, for example, [186]); in chapter 5 I analyze the Moran model with an immigration term, which allows for repeated concurrent invaders of the same species. In either case I do not worry about effects like clonal interference or multiple mutations (as they do in [187]), since the mutations are either rare or equivalent in my models. Anyway, immigration is more appropriate than mutation for the introduction of invaders, since having the same mutation recurring independently is unlikely, unless there is a common mutation pathway or if we categorize all equivalent mutants into one category of invader.

In this chapter I shall investigate how the success probability and mean times scale with niche overlap, carrying capacity, and immigration rate, and in so doing I shall uncover critical combinations of these parameters as they affect the scaling of the mean times and the shape of the steady state population probability distribution. Having increased niche overlap leads to lesser chance of invasion and greater times before the attempt resolves. In the Moran model with immigration, the steady state distribution changes from unimodal to bimodal around when the inverse immigration rate of a strain is equal to the expected population of that strain in the system.

There are a few steps needed to get to these conclusions. Within the generalized Lotka-Volterra model there is some ambiguity in the definition of a successful invasion, which I will discuss in the next section before providing a definition. And since there is a chance of success or failure, I shall also find the mean times conditioned on the outcome of that attempt. In the previous chapter because of the initial conditions each species was equally likely to go extinct first. In this chapter's case, it is possible (and indeed true) that an invasion attempt that is ultimately successful will take a long time (though still short when compared to the fixation times of the previous chapter), whereas one that is transient and ultimately unsuccessful will fail quickly. These are the conditional mean times, and their scaling with carrying capacity will be analyzed, since exponential scaling implies that the event effectively does not happen. Neutral theories of the maintenance of biodiversity argue that no species truly establishes itself, and biodiversity is maintained by transient species in the system. Calculation of the steady state number of species requires the time that these transient species exist in the system. My results hold both for a species in an ecosystem (hence its relevance to conservation biology, where biodiversity is a marker of ecosystem robustness [17, 73, 188, 189]) and a gene in a population (hence its use in calculating heterozygosity, which confers resilience to environmental changes [190–193]). There are also more practical applications, for example the susceptibility of a microbiome ecosystem like the gut or lungs to invasion, say from salmonella or pneumococcus [30, 31, 194–198].

4.2 Defining invasion in the 2D Lotka-Volterra model

As before, I employ the symmetric generalized LV model with niche overlap a and carrying capacity K. I study the case where the system starts with $K-1$ individuals of the established species and 1 invader. This initial condition corresponds to a birth of a mutant. An initial condition of K established organisms and the 1 invader gives similar results. The species' dynamics are described by the birth and

death rates defined by equations (3.10) from the previous chapter, which I reproduce here:

$$b_i/x_i = r_i$$
$$d_i/x_i = r_i \frac{x_i + a_{ij}x_j}{K_i}.$$

As before, the times I write are expressed in units of $1/r$, such that the rate constant r does not explicitly show up in the results.

An invasion is unsuccessful if the invading species dies out before establishing itself in the system. There are many ways to define what it means for a species to be established, and I will outline one such definition below. Deterministically the system would grow to asymptotically approach the coexistence fixed point; deterministically, all invasion attempts are successful, and stochasticity is required for non-trivial invasion probabilities. In a stochastic system, the populations could very easily fluctuate *near* the fixed point without touching that exact point. This would overestimate the time to establishment, or even misrepresent a successful invasion as unsuccessful if the system gets near the fixed point without reaching it but then goes extinct. Indeed, there is even a chance the established species dies out before the system reaches the coexistence fixed point, which would be counted as an unsuccessful invasion. For these reasons a successful invasion should not be defined as the system arriving at the coexistence point. The same arguments hold for a defined region near the fixed point (for instance, within three birth or death events, or within a circle of radius ε): the region might by chance be avoided for a time even after the invader is more populous than the original species, which could even go extinct before the invader. Inspired by the observation that in the symmetric case, the coexistence fixed point has the same population of each species, I consider the invasion successful if the invader grows to be half of the total population without dying out first. So long as the invader population matches that of the established species, regardless what random fluctuations may have made that population to be, the invasion is a success. These considerations of the definition of invasion are similar to those of Parsons [105], who regards a single species problem, but nowhere else in the literature have I seen invasion treated in this way; typically (especially in the genetics literature) when an author says invasion they mean fixation. Thus all the results of this chapter are novel (although the techniques employed are not).

Along with the probability of a successful invasion attempt (which I denote $\mathcal{P}$), I am interested in the timescales involved. As such, I will consider conditional mean times, conditioned on either success or failure of the invasion attempt. The mean time to a successful invasion is written as τ_s, and the mean time of a failed invasion attempt as τ_f. More generally, invasion probability and the successful and failed times starting from an arbitrary state s^0 are denoted as $\mathcal{P}^{s^0}$, $\tau_s^{s^0}$ and $\tau_f^{s^0}$, respectively.

Similar to equation (3.22) in a previous chapter, the invasion probability can be obtained from [78, 83]

$$\mathcal{P}^{s^0} = -\sum_s \hat{M}^{-1}_{s,s^0}\alpha_s \tag{4.1}$$

and the times from

$$\Phi^{s^0} = -\sum_s \hat{M}^{-1}_{s,s^0}\mathcal{P}^s, \tag{4.2}$$

where α_s is the transition rate from a state s directly to extinction or invasion of the invader and $\Phi^{s^0} = \tau^{s^0}\mathcal{P}^{s^0}$ is a product of the invasion or extinction time and probability. Similar equations describe τ_f [78, 83]. As in the previous chapter, I truncate the transition matrix and invert it in order to solve

these equations.

4.3 Invasion probability and times into the Lotka-Volterra model

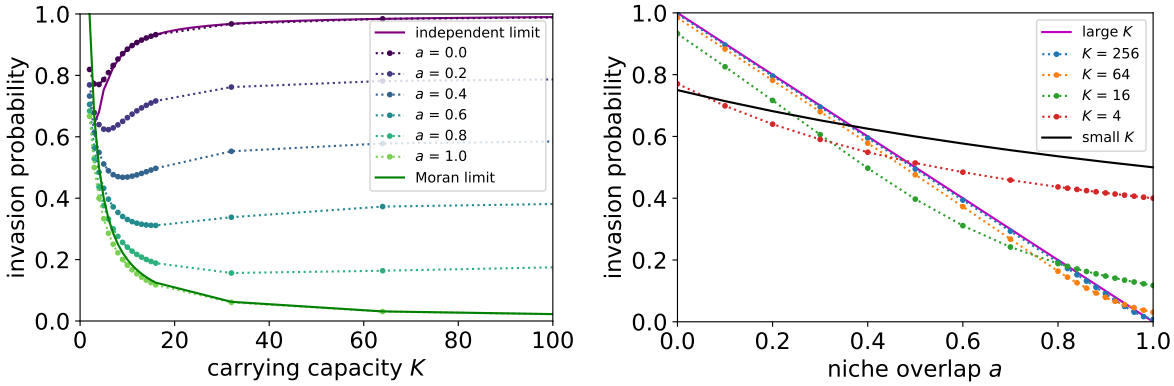

Figure 4.1: *Probability of a successful invasion attempt into a two-dimensional Lotka-Volterra system. Left:* Numerical results, from $a = 0$ at the top to $a = 1$ at the bottom. The purple solid line is the expected analytical solution in the independent limit. The green solid line is the prediction of the Moran model in the complete niche overlap case. Data come from equation 4.1 and are connected with dotted lines to guide the eye. *Right:* The red data show the results for carrying capacity $K = 4$, and suggest the solid black line $\frac{b_{mut}}{b_{mut}+d_{mut}}$ is an appropriate small carrying capacity limit. Successive lines are at larger system size, and approach the solid magenta line of $1 - d_{mut}/b_{mut} \approx 1 - a$.

Figure 4.1 shows the calculated invasion probabilities as a function of the carrying capacity K and of the niche overlap a between the invader and the established species. In the complete niche overlap limit, $a = 1$, the dependence of the invasion probability on the carrying capacity K closely follows the results of the classical Moran model, $\mathcal{P}^{s^0} = 2/K$ [7], shown in the blue dotted line in the left panel, and tends to zero as K increases. In the other limit, $a = 0$, the problem is well approximated by the one-species stochastic logistic model starting with one individual and evolving to either 0 or K individuals; the exact result in this limit is shown in black dotted line, referred to as the independent limit [78]. In the independent limit, $a = 0$, the invasion probability asymptotically approaches 1 for large K, reflecting the fact that the system is deterministically drawn towards the deterministic stable fixed point with equal numbers of both species. As K gets large, fluctuations are minimal and the system becomes more deterministic. Interestingly, the invasion probability is a non-monotonic function of K and exhibits a minimum at an intermediate/low carrying capacity, which might be relevant for some biological systems, such as in early cancer development [179] or plasmid exchange in bacteria [136].

For the intermediate values of the niche overlap, $0 < a < 1$, the invasion probability is observed to be a monotonically decreasing function of a, as shown in the right panel of figure 4.1. For large K, the outcome of the invasion is typically determined after only a few steps: since the system is drawn deterministically to the mixed fixed point, the invasion is almost certain once the invader has reproduced several times. At early times, the invader birth and death rates (3.10) are roughly constant, and the invasion failure can be approximated by the extinction probability of a birth-death process with constant death d_{mut} and birth b_{mut} rates. The invasion probability is then $\mathcal{P} = 1 - d_{mut}/b_{mut} \approx 1 - a$. This heuristic estimate is in excellent agreement with the numerical predictions, shown in the right panel of figure 4.1

as a purple dashed and the blue lines respectively. Similarly, for small K either invasion or extinction typically occurs after only a small number of steps. The invasion probability in this limit is dominated by the probability that the lone mutant reproduces before it dies, namely $\frac{b_{mut}}{b_{mut}+d_{mut}} = \frac{K}{K(1+a)+1-a}$, as shown in black dotted line in the right panel of figure 4.1.

The upper panels of figure 4.2 show the dependence of the mean time to successful invasion, τ_s, on K and a. Increasing K can have potentially contradictory effects on the invasion time, as it increases the number of births before a successful invasion on the one hand, while increasing the steepness of the potential landscape and therefore the bias towards invasion on the other. Nevertheless, the invasion time is a monotonically increasing function of K for all values of a. In the complete niche overlap limit $a = 1$ the invasion time scales linearly with the carrying capacity K, as expected from the predictions of the Moran model, $\tau_s = \Delta t K^2(K-1)\ln\left(\frac{K}{K-1}\right)$ with $\Delta t \simeq 1/K$, as explained above. The quantitative discrepancy arises from the breakdown of the $\Delta t \simeq 1/K$ approximation off of the Moran line. For all values $0 \leq a < 1$ the invasion time scales sub-linearly with the carrying capacity, indicating that successful invasions occur relatively quickly, even when close to complete niche overlap, where the invading mutant strongly competes against the stable species. In the $a = 0$ limit of non-interacting species, the invading mutant follows the dynamics of a single logistic system with the carrying capacity K, resulting in the invasion time that grows approximately logarithmically with the system size, as shown in the upper left panel of figure 4.2 as a purple line. This result is well-known in the literature, often stated without reference [95, 105]. It is easy to see: by writing $\tau_s = \int dt = \int_{x_o}^{x_f} dx \frac{1}{\dot{x}}$ for initial state $x_0 = 1$ and final state $x_f = (1-\epsilon)K$ with small ϵ and large K we get

$$\begin{aligned}\tau_s &= \frac{1}{r}\int_{x_o}^{x_f} dx \frac{K}{x(K-x)} = \frac{1}{r}\int_{x_o}^{x_f} dx \left(\frac{1}{x} - \frac{1}{K-x}\right) = \frac{1}{r}\ln\left[\frac{x}{K-x}\right]|_{x_o}^{x_f} = \frac{1}{r}\ln\left[\frac{x_f(K-x_o)}{x_o(K-x_f)}\right] \\ &\approx \frac{1}{r}\ln\left[\frac{(1-\epsilon)K}{\epsilon}\right] \approx \frac{1}{r}\left(\ln[K] - \ln[\epsilon]\right) \end{aligned} \tag{4.3}$$

and so expect the invasion time to grow logarithmically with carrying capacity.

Unlike the mean times conditioned on success, the failed invasion time, shown in the lower left panel of figure 4.2, is non-monotonic in K. The analytical approximations of the Moran model and the of two independent 1D stochastic logistic systems recover the qualitative dependence of the failed invasion time on K at high and low niche overlap, respectively. All failed invasion times are fast, with the greatest scaling being that of the Moran limit. For $a < 1$ these failed invasion attempts appear to approach a constant timescale at large K.

The dependence of the time of an attempted invasion (both for successful and failed ones) on the niche overlap a is different for small and large K, as shown in the right panels of figure 4.2. For small K both τ_s and τ_f are monotonically decreasing functions of a, with the Moran limit having the shortest conditional times. In this regime, the extinction or fixation already occurs after just a few steps, and its timescale is determined by the slowest steps, namely the mutant birth and death. Thus $\tau \approx \frac{1}{b_{mut}+d_{mut}} = \frac{K}{K+1+a(K-1)}$, as shown in the figure as the solid cyan line. By contrast, at large K, the invasion time is a non-monotonic function of the niche overlap, increasing at small a and decreasing at large a. This behavior stems from the conflicting effect of the increase in niche overlap: on the one hand, increasing a brings the fixed point closer to the initial condition of one invader, suggesting a shorter timescale; on the other hand, it also makes the two species more similar, increasing the competition that hinders the invasion.

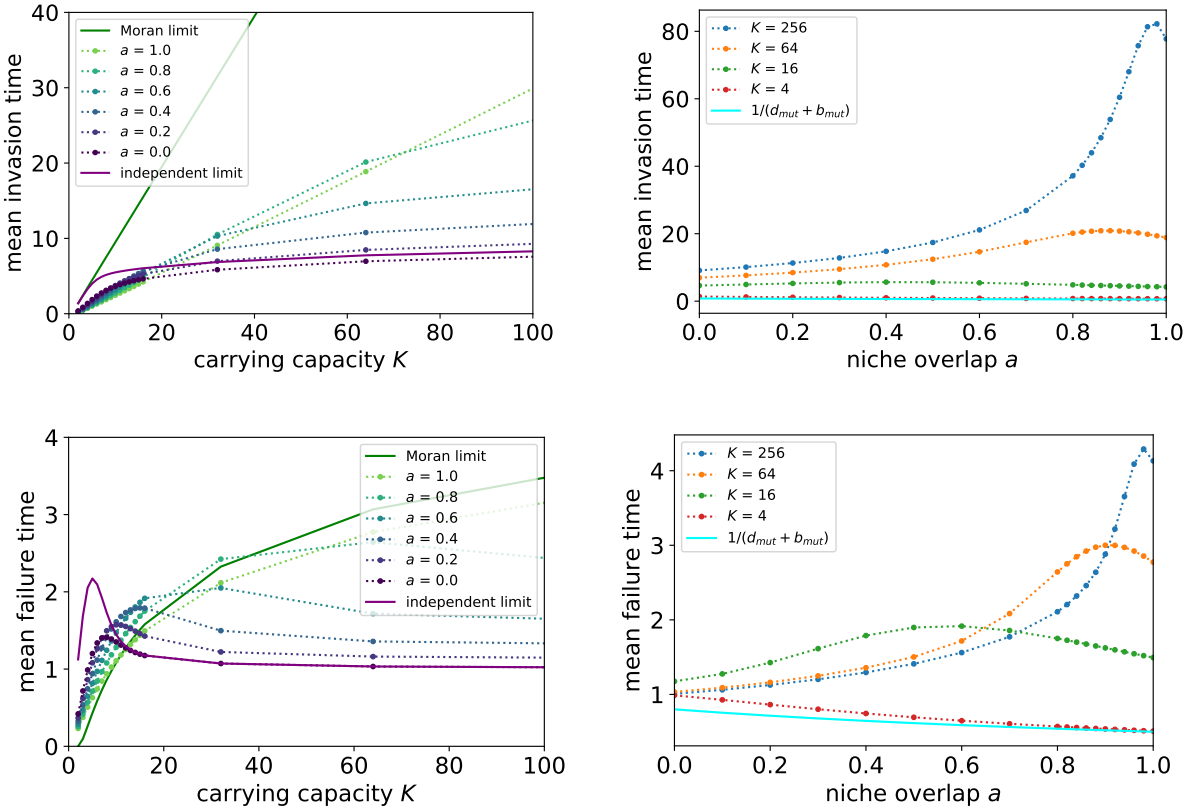

Figure 4.2: *Mean time of a successful or failed invasion attempt. Upper Left:* Dotted lines connect the numerical results of invasion times conditioned on success, from $a = 0$ at the bottom being mostly fastest to $a = 1$ being slowest. The solid green line shows for comparison the predictions of the Moran model in the complete niche overlap limit, $a = 1$; see text. The solid purple line correspond to the solution of an independent stochastic logistic species, $a = 0$, and overestimates the time at small K but fares better as K increases. *Upper Right:* The red line shows the results of successful invasion time for carrying capacity $K = 4$, and successive lines are at larger system size, up to $K = 256$. The cyan line is $1/(b_{mut} + d_{mut})$ and matches with small K. *Lower Panels:* Same as upper panels, but for the mean time conditioned on a failed invasion attempt.

4.4 Discussion

Unlike the fixation times of the previous chapter, invasions into the system do not show exponential scaling in any limit. Indeed, all scaling with K is sublinear except in the complete niche overlap limit for successful invasion times. The timescale of a successful invasion varies between linear and logarithmic scaling in the system size. The mean time of an unsuccessful invasion is even faster than logarithmic, and for large K it becomes independent of K. Curiously, these failed invasion attempts are non-monotonic, at intermediate carrying capacity and niche overlap values. As for the probabilities, the likelihood of a failed invasion attempt grows linearly with niche overlap, for sufficiently large K. For complete niche overlap the invasion probability goes asymptotically to zero, but it is low even for partially mismatched niches.

High niche overlap makes invasion difficult due to strong competition between the species. In this regime, the times of the failed invasions become important because they set the timescales for transient species diversity. If the influx of invaders is slower than the mean time of their failed invasion attempts,

most of the time the system will contain only one settled species, with rare "blips" corresponding to the appearance and quick extinction of the invader. On the other hand, if individual invaders arrive faster than the typical times of extinction of the previous invasion attempt, the new system will exhibit transient coexistence between the settled species and multiple invader strains, determined by the balance of the mean failure time and the rate of invasion [11, 21, 187, 199, 200]. Recent research from the Gore lab shows that these transient species can have lasting effects on the distribution of extant species [198]. Full discussion of diversity in this regime is beyond of the scope of the present work. The weaker dependence of the invasion times on the population size and the niche overlap, as compared to the escape times of a stably coexisting system to fixation, imply that the transient coexistence is expected to be much less sensitive to the niche overlap and the population size than the steady state coexistence. Curiously, both niche overlap and the population size can have contradictory effects on the invasion times (as discussed in the previous section) resulting in a non-monotonic dependence of the times of both successful and failed invasions on these parameters.

For species with low niche overlap, the probability of invasion is likely, and for large K decreases monotonically as $1 - a$ with the increase in niche overlap, independent of the population size K. The mean time of successful invasion is relatively fast in all regimes, and scales linearly or sublinearly with the system size K and is typically increasing with the niche overlap a.

The fixation times of two coexisting species, discussed in the previous chapter, determine the timescales over which the stability of the mixed populations can be destroyed by stochastic fluctuations. Similarly, the times of successful and failed invasions set the timescales of the expected transient coexistence in the case of an influx of invaders, arising from mutation, speciation, or immigration [11, 187, 200]. Our results provide a timescale to which the rate of immigration or mutation can be compared. If the influx of invaders is slower than the mean time of their failed invasion attempts, each attempt is independent and has the invasion probability we have calculated. In the extreme case of this, that is, if the time between invaders is even longer than the fixation times calculated in the previous chapter, then serial monocultures are expected. If the rate in is greater than the mean failure time, the system will diversify. The balance between mutation or immigration coming into the system and these invaders failing to establish themselves determines how diverse a system will be. With different strains of invaders arising faster than the time it takes to suppress the previous invasion attempt, the new strains interact with one another in ways beyond the scope of this thesis, leading to greater biodiversity.

Chapter 5

Maintenance: A Balance of Extinction and Invasion

5.1 Introduction

In the previous chapter I argued that the biodiversity of a system depends on a comparison of the timescales of transient invasion attempts and immigration, mutation, or speciation. The number of invader progeny fluctuates and ultimately it either dies out or occupies half of the total population, as per my definition of a successful invasion. If new species enter the system faster than they go extinct, the number of extant coexisting species should increase to some steady state. Conversely, if extinction is much more rapid than speciation, a monoculture of one single species is expected in the system. Whether the monocultural system consists of the same species over multiple invasion attempts or whether it experiences sweeps, changing from monocultures of one species to the next, depends on the probability of a successful invasion [21, 187, 201]. In order to extend the results of the previous chapter to the circumstance of repeated concurrent invaders in the Moran limit I analyze the Moran model with an immigration term. I previously calculated numeric invasion probabilities and times, but in the Moran model with immigration I look for analytic solutions. I will be able to find the expected population of one species on which I focus (called the focal species), how the model parameters qualitatively change how the focal population is distributed, and the characteristic timescales of the system.

The application is in neutral theories like that of Hubbell [11] and Kimura [8, 70] Without immigration, the Moran model is the basis for Kimura's neutral model [8, 70, 202, 203], as well as coalescent theory [34, 35, 204]. With immigration, it is akin to the Hubbell model [11, 205], although in the Hubbell model each immigrant is from an entirely new species, arising from speciation rather than immigration from a metapopulation. Hubbell's work reinvigorated the debate between niche and neutral mechanisms of biodiversity maintenance. Early numerical solution of the Hubbell model was done by Bell [67]. Hubbell composed his theory to describe species abundance curves, rather than my interests of the population probability distribution or lifetime of a single species in a community. By an abundance curve I mean a Preston plot, a plot of the number of species that belong in bins of exponentially increasing population size [11]. This contrasts with the stationary probability distribution of the population (or abundance) of a single species.

With regard to a single species abundance, models with selection and without the chance of repeat

immigrants have been popular [34, 75, 110, 115, 116, 165, 206, 207]. With immigrants repeatedly from the focal species, pioneering work was done by Crow and Kimura [8, 71], who had to assume both continuous time (as do I) and continuous population densities (which I do not), arriving at numerical results for the distribution. The Moran model with immigration was analyzed by McKane *et al.* [73] to find the probability distribution exactly and the time evolution approximately. The difference between my work and that of McKane *et al.* is that I find the critical value of parameters at which the distribution changes from aggregating at extinction and fixation to being moderately distributed. These qualitatively different regimes correspond to there being monocultures or biodiversity in a system. I also find the first passage times analytically and link the Moran model with immigration to the results of a single invader as studied in the previous chapter.

One experimental motivation for my research is recent work from the Gore lab [180], measuring the gut microbiome of bacteria-consuming *C. elegans* grown in a 50:50 environment of two strains of fluorescence-labeled but otherwise identical *E. coli*. After an initial colonization period, each nematode has a stable number of bacteria in their gut, presumably from a balance of immigration, birth, and death/emigration. The researchers find the population distribution depending on the comparison of two experimental timescales, those of establishment and fixation time conditioned on a successful invasion. In this chapter I calculate the stationary probability distribution of a single species [73], analyzing the critical parameter choices that change its qualitative form, as is observed in the nematode gut [180]. But first I must review the classic Moran model and some quantities that can be calculated from it.

5.2 Known Moran model results

In the classic Moran model, each iteration or time step involves a birth and a death event. Each organism is equally likely to be chosen (for either birth or death), hence a species is chosen according to its frequency, $f = n/K$, where K is the total population and n is the number of organisms of that species. (In the literature the total population is usually represented by N, but as it gives the system size and is analogous to the Lotka-Volterra carrying capacity in the Moran limit I maintain the use of K.) We focus on one species of population n, which will be referred to as the focal species. Note that $K - n$ represents the remaining population of the system, and need not all be the same species, so long as they are not the focal species [81]. The focal species increases in the population if one of its members gives birth (with probability f) while a member of a different species dies (with probability $1 - f$); that is, in time step Δt the probability of focal species increase is $b(n) = f(1 - f)$. Similarly, decrease in the focal species comes from a birth from outside the focal group and a death from within, such that the probability of decrease is $d(n) = (1 - f)f$. By commutativity of multiplication, increase and decrease of the focal species are equally likely, with

$$b(n) = d(n) = n(K - n)/K^2. \tag{5.1}$$

Each time step, the chance that nothing happens is $1 - (b(n) + d(n)) = f^2 + (1 - f)^2$.

Note that, unlike in previous chapters where I used b and d as rates, here these are not rates, rather they are the probability of an increase or decrease of the focal species in one time step. I use the same notation not to be confusing but to hint at an approximation I employ in the following sections. Taking Δt to be infinitesimal, $b(n)\Delta t$ and $d(n)\Delta t$ serve as probabilities of birth and death of the focal species

during this small time interval. This creates a continuous time analogue to the Moran model, with b and d serving as rates. The timescale is now in units of Δt, which is only relevant if one were to compare with other models, which I do not (but see chapter 3). With this approximation I can employ the formulae explored in chapter 2 for quantities like quasi-stationary probability distribution and mean time to extinction.

For reference, I include the mean and variance of a focal population as a function of time [7, 9, 73], so that I may later compare with the immigration case. If the system starts with n_0 individuals of the focal species, then on average there should be n_0 individuals in the next time step as well. Therefore the mean population as a function of time is $\langle n \rangle(t) = n_0$. Since the extremes of $n = 0$ and $n = K$ are absorbing, the ultimate fate of the system is in one of these two states, despite the mean being constant. The variance starts at zero for this delta function initial condition. After k time steps the variance is

$$V_k = n_0(K - n_0)\big(1 - (1 - 2/K^2)^k\big). \tag{5.2}$$

For finite K the variance goes to $K^2 f_0(1 - f_0) = n_0(K - n_0)$ at long times. This is easy to intuit: there is probability f_0 that the system ended in $n = K$, and probability $(1 - f_0)$ of ending at $n = 0$, since at long times the system has fixated at one end or the other. Notice that as $K \to \infty$ the variance, a measure of the fluctuations, goes to zero, and the system becomes deterministic, as any change of $\pm 1/K$ in the frequency of the focal species becomes negligibly small.

The mean and variance characterize the distribution of outcomes that could occur when running an ensemble of identical trials of the same system. The average over the ensemble is denoted $\langle \cdot \rangle$. Any individual trajectory, any individual realization, will take its own course, independent of any others, and after fluctuations will ultimately end up with either the focal species dying (extinction) or all others dying (fixation). Both of these cases are absorbing states, so once the system reaches either it will never change. Since a species is equally likely to increase or decrease each time step, the model is akin to an unbiased random walk [82], and therefore the probability of extinction occurring before fixation is just

$$E(n) = 1 - n/K = 1 - f. \tag{5.3}$$

The first passage time, however, does not match a random walk, as there is a probability of no change in a time step, and this probability varies with f.

The unconditioned first passage time can be found using the techniques outlined in chapter 2. The (mean) unconditioned first passage time $\tau(n)$ is the time the system takes, starting from n organisms of the focal species, to reach either fixation *or* extinction. I focus on the one species, with one or more other species distinct from this focal species also being present in the system; this first passage time is not the time for one of the non-focal species to go extinct, but only registers when the focal species goes extinct or fixates. If the focal species goes extinct there may still be many different non-focal species in the system, or there may be a monoculture of one. The first passage time can be calculated by regarding how the mean from one starting position n relates to the mean starting from neighbouring positions.

$$\tau(n) = \Delta t + d(n)\tau(n-1) + (1 - b(n) - d(n))\,\tau(n) + b(n)\tau(n+1) \tag{5.4}$$

Substituting in the values of the increase and decrease rates and rearranging this gives

$$\tau(n+1) - 2\tau(n) + \tau(n-1) = -\frac{\Delta t}{b(n)} = -\Delta t \frac{K^2}{n(K-n)}.$$

Similar to the Fokker-Planck approximation, I approximate the LHS of the above with a double derivative (ie. $1 \ll K$) to get $\frac{\partial^2 \tau}{\partial n^2} = -\Delta t\, K \left(\frac{1}{n} + \frac{1}{K-n}\right)$. Double integrate and use the bounds $\tau(0) = 0 = \tau(K)$ gives

$$\tau(n) = -\Delta t\, K^2 \left(\frac{n}{K} \ln\left(\frac{n}{K}\right) + \frac{K-n}{K} \ln\left(\frac{K-n}{K}\right)\right). \tag{5.5}$$

Note that it was not necessary to use the large K approximation, there is an exact solution [7],

$$\tau(n) = \Delta t\, K \left(\sum_{j=1}^{n} \frac{K-n}{K-j} + \sum_{j=n+1}^{K} \frac{n}{j}\right) \tag{5.6}$$

though it is less clear how this scales with K and f. The exact and approximate solutions match when K is large.

5.3 Population distribution of a Moran model with immigration

Just as with the classic Moran model, the model with immigration focuses on one species of n organisms, called the focal species, with the remaining $K - n$ organisms being of a different strain (or strains). I focus on one species among potentially many, with the fractional abundance of the focal species being $f = n/K$. The remaining $1-f$ fraction of the population is composed of one or more species different from the focal species. The system is treated as a rapidly evolving population, with immigrants coming from a static metapopulation of larger size and diversity. As with the Moran population, the metapopulation contains the focal species and other species, with new parameters m, M and g being analogous to n, K and f. That is, an immigrant into the Moran population is a member of the focal species with probability g, and of another species with probability $1 - g$. The immigrant is not necessarily a member of the focal species; in most biological systems there are many species, so no species, such as focal species, is likely to have $g > 0.5$. The metapopulation contains $m = g\,M$ members of the focal species out of M total organisms. In principle g should be a random number drawn from the probability distribution associated with an evolving metapopulation, but for $M \gg K$ one can treat the metapopulation as stationary. In practice, I am assuming that the metapopulation changes much slower than the Moran population [73]. In the context of the Gore experiment [180], the system of interest is the nematode gut, and the metapopulation is the environment in which the nematode lives (and in which it uptakes bacteria to its gut). The consumption of one bacterium will influence the gut microbiome while having a negligible effect on the external environment. In a more general setting, the system of interest is a small island receiving immigrants from a larger mainland; the arrival of one immigrant on the island is impactful even when the loss of that same emigrant is negligible to the mainland.

Each step of the Moran model with immigration involves one birth and one death. As before, the focal species dies with probability f. Immigration is incorporated by having a fraction ν of the birth events be replaced by immigration events. The classic Moran model has the focal species increasing in population with probability $f(1-f)$; this is now modified to occur only a fraction $(1-\nu)$ of the time,

and there is also a contribution $\nu g(1-f)$ that increases the focal population when an immigrant enters (a fraction ν of the cases) of the focal species (a fraction g of the cases) when a death of a non-focal species occurs (a fraction $1-f$ of the cases). As before, I take the time interval Δt of each step to be infinitesimal, such that b and d are rates, which are:

transition	function	value
$n \to n+1$	$b(n)$	$f(1-f)(1-\nu) + \nu g(1-f)$
$n \to n-1$	$d(n)$	$(1-f)f(1-\nu) + \nu(1-g)f$
$n \to n$	$1-b(n)-d(n)$	$\left(f^2+(1-f)^2\right)(1-\nu) + \nu\,(1-f-g)$

Note that the rates of increase and decrease of the focal species are no longer the same as each other (as they are in the classic Moran model); there is a bias in the system, toward having a population of gK. Setting the immigration rate ν to zero recovers the classic Moran model. Immigration depends on the ease of access to the system from the metapopulation, analogous to the distance between an island and the mainland [10], but is typically less frequent than birth, so I take it to be a small parameter.

If a new mutant or immigrant species is unlikely to enter again (ie. if $g \simeq 0$) then the model corresponds to the Moran model with selection [34, 75, 110, 115, 116, 165, 206, 207], which I will not explicitly treat, though it is included in the general treatment below. Since there is immigration from the static metacommunity, the system will never truly fixate, as there will always be immigrants of the 'extinct' species to be reintroduced to the population. Rather, the system will settle on a stationary distribution of P_n, the probability of having n organisms of the focal species. The process is described by the master equation $\frac{d\,P_n(t)}{dt} = P_{n-1}(t)b(n-1) + P_{n+1}(t)d(n+1) - \big(b(n)+d(n)\big)P_n(t)$, the steady state solution of which is [78]

$$\widetilde{P}_n = \frac{q_n}{\sum_{i=0}^{K} q_i} \tag{5.7}$$

where

$$q_i = \frac{b(i-1)\cdots b(1)}{d(i)d(i-1)\cdots d(1)}$$

recalling that $\frac{b(i)}{d(i)} = \frac{i(K-i)(1-\nu)+\nu K g(K-i)}{i(K-i)(1-\nu)+\nu K(1-g)i}$. The unnormalized steady-state probability q_n can be written compactly as

$$q_n = \frac{K^2\Gamma(K)\Gamma\left(n+\frac{gK\nu}{1-\nu}\right)\Gamma\left(K-n+1+\frac{(1-g)K\nu}{1-\nu}\right)}{\big(n(K-n)(1-\nu)+(1-g)nK\nu\big)\Gamma(n)\Gamma(K-n+1)\Gamma\left(1+\frac{gK\nu}{1-\nu}\right)\Gamma\left(K+\frac{(1-g)K\nu}{1-\nu}\right)} \tag{5.8}$$

and the sum of these is the normalization

$$\sum q_i = \frac{1}{g\nu}\frac{\Gamma[1-\frac{K(1-g\nu)}{1-\nu}]\Gamma[K+1-\frac{K}{1-\nu}]}{\Gamma[K+1-\frac{K(1-g\nu)}{1-\nu}]\Gamma[1-\frac{K}{1-\nu}]}, \tag{5.9}$$

which follows formally from the definition of the hypergeometric function ${}_2F_1$. See also [73].

Figure 5.1 shows a visualization of the steady-state probability distribution for different immigration rates. When immigration is frequent the distribution is drawn near the middle, peaked at $g\,K$, which is the most common population to occur. This high likelihood of having a moderate population (far from $n=0$ and $n=K$) is contrasted with the case when immigration is rare. Instead of a unimodal distribution with the focal species existing at some moderate value, the species is most likely to be locally extinct, unless immigration is most often from the focal species ($g > 0.5$), in which case the species is

most likely to be found as the dominant, fixated species in the system. These qualitatively different outcomes suggest some critical parameter combination that divides them, which is discussed below.

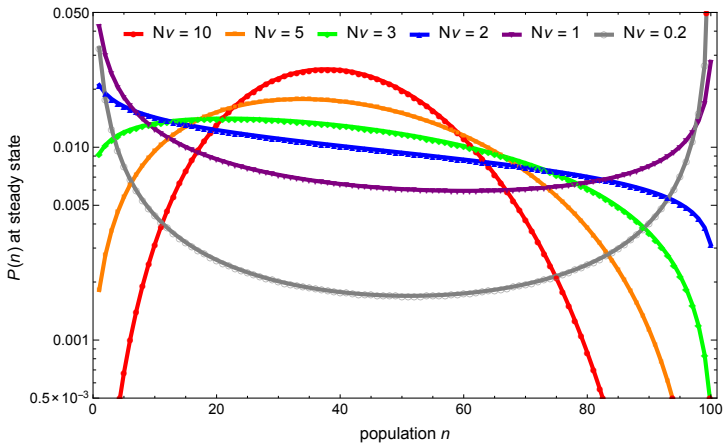

Figure 5.1: *PDF of stationary Moran process with immigration.* Metapopulation focal fraction is $g = 0.4$, local system size $K = 100$, immigration rate ν is given by the colour. Notice that the curvature of the distribution inverts around $\nu = 2/K$. For high immigration rate the distribution should be centered near the metapopulation fraction $g\,K$ whereas for low immigration the system spends most of its time fixated at either 0 or K.

While the time dependent population probability distribution is difficult to calculate before it attains the steady state [73], the mean and variance of the distribution are more tractable at all times. If the mean μ at some time step k has $\mu_k = n_k$ individuals, then after one time step $\mu_{k+1} = n_k - d(n_k) + b(n_k) = n_k + \nu(g - f_k)$ individuals. That is, $\mu_{k+1} - \mu_k = \nu(g - \mu_k/K)$. This is solved by

$$\mu_k = \langle n \rangle(k) = gK\left(1 - (1 - n_0)(1 - \nu/K)^k\right). \tag{5.10}$$

At long times the mean fraction f approaches g, the fraction of the focal species in the metapopulation. Finding the variance involves solving a difficult difference equation; to get the an approximation of the variance, I consider the continuous time analogue to the model by taking Δt to be infinitesimal, as described previously. First, the above difference equation of the mean is written as a differential equation $\partial_t \mu(t) = \langle b(n) - d(n) \rangle = \nu\,(g - \mu(t)/K)$, which has solution $\mu(t) = gK + (\mu_0 - gK)e^{-\nu t/K}$, and the timescale is set by K/ν. The dynamical equation for the second moment is

$$\begin{aligned} \partial_t \langle n^2 \rangle &= 2\langle nb(n) - nd(n) \rangle + \langle b(n) + d(n) \rangle \\ &= 2\nu\left(g\mu - \langle n^2 \rangle / K\right) + 2(1 - \nu)\left(K\mu - \langle n^2 \rangle\right)/K^2 + \nu(\mu + gK - 2\mu g)/K \end{aligned} \tag{5.11}$$

which is an inhomogeneous linear differential equation. Recalling that $\sigma^2(t) = \langle n^2 \rangle(t) - \mu^2(t)$ I solve the above equation and write the variance as

$$\sigma^2(t) = \sigma^2(\infty) + A \exp\left\{ -\frac{\nu}{K} t \right\} - B \exp\left\{ -2\frac{\nu}{K} t \right\} + C \exp\left\{ -\frac{2}{K}\left(\nu + \frac{(1 - \nu)}{K}\right) t \right\} \tag{5.12}$$

where $A = \left(1 + g\nu - g(1 - \nu)/K\right)K^2 \frac{\mu_0 - gK}{K\nu + 2(1-\nu)}$, $B = (gK - \mu_0)^2$, and C is an integration constant; $C = \sigma^2(0) - \sigma^2(\infty) + (gK - \mu_0)^2 + (gK - \mu_0)(2 - \nu)(1 - 2g)/\left(K\nu + 2(1 - \nu)\right)$ if the initial variance is

$\sigma^2(0)$.

$$\sigma^2(\infty) = g(1-g)K^2\frac{1}{1+\nu(K-1)} \tag{5.13}$$

is the long time, steady state variance of the system. The variance also has a timescale set by K/ν, after which the steady state variance is approached. The steady state variance is plotted in the left panel of figure 5.2.

Notice that for $g = 0$ or $g = 1$ the long term variance $\sigma^2(\infty)$ asymptotically tends to zero. This contrasts with the results of the Moran model without immigration, which has a nonzero variance. Without immigration there is a nonzero chance of ending up with the focal species fixated or extinct, with fixation ultimate probability equal to initial fractional abundance. Having a supply of immigrants destabilizes one of these absorbing states; for instance for $g = 0$ the ultimate fate is to have none of the focal species remaining. This is true even if the initial population fraction was entirely of the focal species. If immigration is rare the system may temporarily fixate with the focal species, but with the repeated invasion attempts eventually a non-focal species will fixate, after which the system cannot recover the focal species. Ultimately there is only one fate, hence no variance.

For $g \notin \{0, 1\}$ I would first like to consider the low immigration case when the time $1/\nu$ between immigration events is longer than the timescale of the classic Moran model, which scales proportional to K. In this case we recover similar results to the no immigration case of the Moran model. Instead of $f_0(1-f_0)K^2$ from the Moran model we get $\sigma^2(\infty) \approx g(1-g)K^2$, with the metapopulation focal species abundance g acting analogously to the initial abundance f_0. This is easy to intuit. Because the immigration events are rare, each time an immigrant arrives it does so into a system that has already fixated into a monoculture, either of the focal species or without the focal species. A fraction g of the events the immigrant is of the focal species; this is akin to having multiple independent iterations of a classic Moran model, hence the appearance of g as the initial abundance analogue.

In the other extreme, immigration happens much more rapidly than the fixation time of the classic Moran model. When $K\nu \gg 1$ the system is still evolving when a new immigrant is introduced, which acts to keep the probability distribution near g and away from fixation. In this limit the long term variance tends to $\sigma^2(\infty) \approx g(1-g)K/\nu$. For a fixed system size K, increasing the immigration rate decreases the variance, as the system is drawn more toward the metapopulation abundance and away from the extremes of focal species fixation or extinction.

To the best of my knowledge, these observations on the variance of a Moran model with immigration are novel. The variance limits, and indeed figure 5.1, suggest that there are at least two parameter space regimes of the Moran model with immigration. At low immigration rate the system undergoes a series of monocultures punctuated by the occasional immigrant [187]. It spends most of its time resting in the fixated state, rarely seeing a new immigrant, which upon arrival quickly either dies out or takes over in a new fixation. When immigration is frequent the system follows the metapopulation and is maintained at moderate population in the system. Deviations away from the metapopulation abundance are suppressed and the probability of having n focal organisms gathers near the mean value gK. These regimes will be investigated further in the following paragraphs.

Like the mean and variance, another way to characterize the distribution is the extremum (minimum or maximum), which for large immigration rate corresponds to the mode of the system. The extremum is the highest or lowest point of a function and occurs at the n for which $\partial_n \widetilde{P}_n = 0$. For ease of analysis note that, using equation 5.7, $\partial_n \widetilde{P}_n = \partial_n \left(q_n / \sum_i q_i\right) = \partial_n q_n = q_n \partial_n \ln(q_n)$ and therefore I can instead

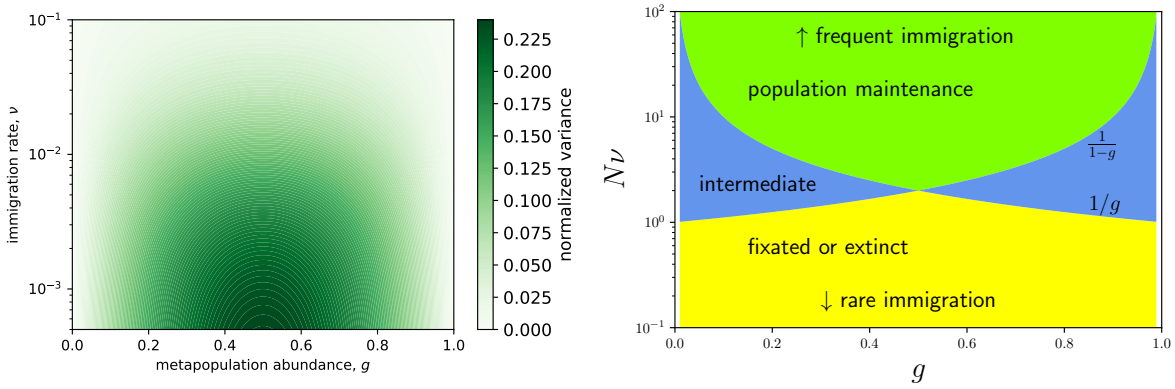

Figure 5.2: *Mapping the parameter space of the Moran model with immigration. Left:* The heat map shows the steady state variance $\sigma^2(\infty)$ of a focal species' population probability distribution in the Moran model with immigration, normalized by K^2. System size is $K = 100$. As immigration probability ν is increased the variance decreases monotonically. Variance is optimal in metapopulation focal species fractional abundance g for $g = 0.5$, as at this fraction there is the greatest likelihood of an immigrant not matching the most populous species in the system. *Right:* Parameter space is divided into the qualitatively different regimes of the system based on the comparison of $K\nu$ with $1/g$ and $1/(1-g)$, with system size K, immigration rate ν, and focal species metapopulation abundance g. When immigration is frequent (green region) the focal species is likely to be maintained at a moderate population by new immigrants. When immigration is rare (yellow region) the steady state of the system is either an absence or monoculture of the focal species. There is an intermediate regime (blue region) for which the focal species is present but not fixated.

calculate the n that gives $\partial_n \ln(q_n) = 0$. Starting from $\ln(q_n)$, I employ the Stirling approximation $\ln[x!] = x\ln[x] - x + O(1/x)$, set $\partial_n \ln[q_n] = 0$, and collect all the logarithmic terms to the left-hand side to get

$$\ln\left[\frac{(1-f)(f-\gamma+\epsilon g)}{(f-\gamma)(1-f+\epsilon(1-g))}\right] = \gamma\frac{1-2f-\epsilon g}{f\,(1-f-\epsilon g)} \tag{5.14}$$

where $\gamma = 1/K$ and $\epsilon = \nu/(1-\nu)$, and recalling that $f = n/K$. The parameters γ and ϵ are typically small, so I perform an expansion in them. For this expansion the lowest order in these parameters is $O(\gamma)$, followed by $O(\epsilon\gamma)$. The left-hand side has an infinite series in ϵ starting at $O(\epsilon^1)$, before picking up $O(\epsilon\gamma)$ terms. Keeping only the $O(\epsilon^1)$ terms from the left and $O(\gamma^1)$ terms from the right gives

$$f^* = \frac{1 - g\epsilon/\gamma}{2 - \epsilon/\gamma}. \tag{5.15}$$

This analysis agrees with the observation that there are multiple regimes in parameter space. When immigration is large, $\epsilon/\gamma \approx K\nu \gg 1$, and the maximum or mode of the distribution, the extremum, matches with the mean. The bulk of the probability is centred near gK. But in the opposite limit, when the probability is concentrated at zero and one, the minimal value is half way between these two.

The question remains, how does the distribution switch between these two qualitatively different regimes as ν changes. First, note that there is in fact an intermediate regime, as shown by the blue line $K\nu = 2$ in figure 5.1. The probability need not only be concentrated near both extremes or near gK: for moderate values of immigration there is the possibility that the curvature near one edge of the domain is positive while it is negative near the other. To this end, I calculate whether the ratio of $\widetilde{P}_0/\widetilde{P}_1$ is greater than one for g (assuming $g < 0.5$) and for the symmetric case $g \leftrightarrow 1-g$ (rather than

also considering $\widetilde{P}_K/\widetilde{P}_{K-1}$ as a function of g). There are three regimes, with two critical parameter combinations dividing them. At the lower division,

$$\frac{\widetilde{P}_0}{\widetilde{P}_1} - 1 = \frac{q_0}{q_1} - 1 = \frac{K - \nu K^2 g - \nu K g - 1 + \nu}{\nu K^2 g} \approx \frac{K - \nu K^2 g}{\nu K^2 g} < 0 \tag{5.16}$$

which implies the probability distribution is concave down when $K\nu > 1/g$. By symmetry the other bound is at $1/(1-g)$, below which the distribution is concave down. It turns out these same bounds can be found by requiring $0 < f^* \approx \frac{1-gK\nu}{2-K\nu} < 1$, since only when the extremum f^* is inside the domain can the distribution have a consistent curvature; when the extremum is outside the domain the distribution is monotonic (between 0 and K) and therefore in the intermediate regime. The regimes are shown in the right panel of figure 5.2.

To recapitulate, when the immigration rate is low, specifically $K\nu < \min\big(1/g, 1/(1-g)\big)$, the Moran model with immigration will have its focal species either fixated or extinct most of the time. In the case of frequent immigration, with $K\nu > \max\big(1/g, 1/(1-g)\big)$, the focal species is maintained at moderate abundance in the system, spending most of its time near the average value gK, with a fraction of the focal species equal to the faction in the metacommunity from which the system receives its immigrants. Qualitatively, these regimes correspond to the system spending most of its time as a monoculture or as having multiple species present, respectively. And there is a third, intermediate regime for $K\nu$ between $1/g$ and $1/(1-g)$ for which the system is often fixated to one extreme but not the other (of $f = 0, 1$), with occasional fluctuations bringing the system away from this extreme. If the metapopulation is equally likely as not to provide an immigrant of the focal species ($g = 0.5$) then there are only the two qualitative regimes of low and high immigration rate.

Regarding the results of the Gore lab [180] one observes two qualitatively different regimes. In those experiments, $g = 0.5$ and $K = 35,000$ for wild type worms or $4,700$ for the immune-compromised strain. They vary the external bacterial concentration, of which ν should be a monotonically increasing function (ranging from $0.1/K \lesssim \nu \lesssim 100/K$). At low bacterial concentration (and therefore low ν), the system has a bimodal population probability distribution dominated by peaks at extinction and fixation. At high bacterial concentration the distribution is more peaked toward the middle. They use a numerical model to match their observations. My research predicts that the immune-compromised worms should require a greater external bacterial concentration before the bimodal to unimodal transition is observed when compared to the wild type. The evidence from the data is not obvious.

I had previously written that $K\nu \gg 1$ is the condition of frequent immigration. One also needs to make the comparison between $K\nu$ and $1/g$ to predict, for the focal species, whether it is expected to be locally extinct most of the time (for $K\nu < 1/g$) or maintained at the fractional abundance g (for $K\nu > 1/g$). Of course, how the focal species' metapopulation abundance compares to $K\nu$ is not indicative of how the rest of the (non-focal) species will fare. The metapopulation is expected to contain many species, thus when any one of them is the focal species it is likely that the associated g is small. For each species i that $K\nu > 1/g_i$ we expect it to exist in the system, and so the number of species with g_i's greater than $1/(K\nu)$ gives a estimate of the expected number of species extant in the system when immigration is frequent. To this extent, the distribution of g_i's in the metapopulation prescribes the biodiversity of the local system.

5.4 First passage probability and times of a Moran model with immigration

Figure 5.1 gave the probability distribution of the species of interest at steady state, but does not allow us to infer anything about the timescales or dynamics of the system. We can guess that if immigration is common the system will fluctuate about its mean, and if immigrants are rare the system will be in a fixated state punctuated by occasional invasion attempts. Starting from the focal species at an intermediate abundance, I want to find the probability of that species locally fixating before going extinct, and the timescales of these conditions, recognizing that both local fixation and extinction are temporary states, since there is always another immigrant on the way. By local I mean in the system, rather than in the metapopulation, which does not evolve. As is standard practice [78, 83], we take $b(0) = d(K) = 0$ for the focal species. This allows us to find the mean time the system first reaches focal species fixation or extinction, recognizing that this will only be a temporary state. Unlike in the coupled logistic model considered earlier, in this model this mean first passage time is affected by the continual influx of immigrants, and depends on immigration rate ν and focal fraction g.

The technique I employ follows that laid out in the chapter 2, which itself follows Nisbet and Gurney [78]. Define the temporary extinction probability E_i as the probability that the focal species goes extinct in this modified system with absorbing states at $n = 0$ and $n = K$, *i.e.* the system reaches the former before the latter, given that it starts at $n = i$. Then $E_i = \frac{b(i)}{b(i)+d(i)}E_{i+1} + \frac{d(i)}{b(i)+d(i)}E_{i-1}$. Further define $S_i = \frac{d(i)\cdots d(1)}{b(i)\cdots b(1)}$. Then

$$E_i = \frac{\sum_{j=i}^{K-1} S_j}{1 + \sum_{j=1}^{K-1} S_j}. \tag{5.17}$$

See figure 5.3 for the graphical representation of the results. As with the stationary distribution, the extinction probabilities can be written explicitly in terms of K, ν, and g, but graphical interpretation is easier than understanding such a complicated expression. See the appendix.

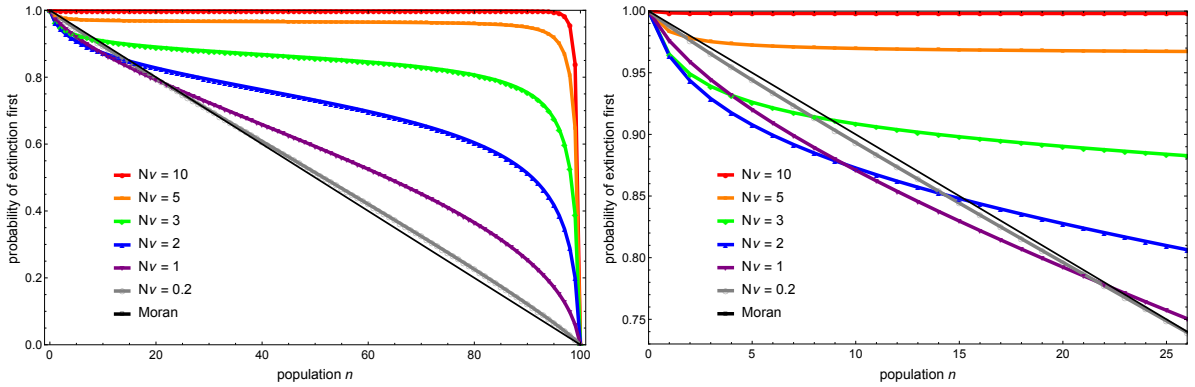

Figure 5.3: *Probability of the focal species reaching temporary extinction before fixation, as a function of initial population. Left:* Metapopulation focal fraction is $g = 0.4$, local system size $K = 100$, immigration rate ν is given by the colour. Lines are included to guide the eye. The black line is the regular Moran result without immigration. Generally when the immigrant is unlikely to be from the focal species ($g < 0.5$) immigration increases the likelihood of the focal species going extinct before fixating. *Right:* Same as the left panel but focused on the small n, to show that immigration acts to lower the probability of extinction as compared to the Moran model for some f less than g, even though $g < 0.5$ and more often than not the immigrant is not from the focal species.

When immigrants of the focal species are uncommon ($g < 0.5$) figure 5.3 shows that the temporary extinction probability E_i is generally increased compared to the Moran model without immigration. Even though there are occasional immigrants of the focal species, they generally do not help prevent their species from reaching extinction before fixation. If the species gets close to fixation the immigration hinders its chances, since most of the time the immigrant will be of another species, and in this model an immigrant acts to fill a vacancy in the system caused by a death, a vacancy that otherwise would be filled by a birth event in the classic Moran model. A populous focal species will still be the most likely to die in a given time step, just as it is most likely to reproduce - unless the reproduction is substituted by immigration, as it is a fraction ν of the steps. For this reason the probability of fixation is decreased (hence extinction probability increased) for $g < 0.5$. The exception, as highlighted in the right panel of figure 5.3, is observed when the focal species is rare. In this case the occasional focal species immigrant acts to buoy the population, giving it a greater chance to fixate before extinction. What constitutes sufficiently rare as to benefit from this effect depends on the immigration rate and on g. Unlike with the steady state results, the different trends for the extremes of $K\nu$ compared to $1/g$ and $1/(1-g)$ are less pronounced; there is no qualitative change at the critical parameter ratio. One observation is that immigration acts to reduce dependence of the temporary extinction probability on initial conditions. In all parameter combinations (with $g \neq 0, 1$) the probability is more level, more horizontal, as compared to the Moran model (in black). At large immigration rate, for instance the red line in figure 5.3, g has a significant effect on the probability, almost guaranteeing that temporary extinction is certain for $g < 0.5$, and temporary fixation for $g > 0.5$. More generally, regarding whether the next fate of a species will be extinction or fixation in a system, immigration from a metapopulation acts in a nontrivial way: assuming $g < 0.5$ it tends to increase the chance of a species reaching extinction first, except when that species is already close to going extinct.

Unconditioned first passage time

Similar to the extinction probabilities, we can write the unconditioned mean first passage time to either temporary fixation or extinction of the focal species [78]:

$$\tau[i] = \sum_{k=1}^{K-1} q_k + \sum_{j=1}^{i-1} S_j \sum_{k=j+1}^{K-1} q_k. \tag{5.18}$$

At $n = 0$ the focal species has temporarily gone extinct and at $n = K$ it has fixated; for both of these cases we get $\tau[n] = 0$ since the system has already attained one of these extremes. The closed analytical expression is cumbersome and shown in the appendix; the results are graphically summarized in the left panel of figure 5.4. Immigration acts to stabilize the system, drawing the focal fraction towards g and hence away from the extremes, at which temporary fixation or extinction occurs. Certainly the system will still reach $n = 0$ or $n = K$ eventually, but with immigration the time is increased when compared to the classic Moran model. What is more, immigration skews this unconditioned first passage time to be longer for initial focal fractions away from g. Figure 5.4 shows an example with $g = 0.4$. At small n the focal species is more likely to go extinct before it fixates, thus the largest contribution to the unconditioned time is from the mean time conditioned on extinction. Immigration may help delay the inevitable, but the effect is not great, as the majority immigrants do not increase the focal species population. At large n, however, fixation is the main contributor to the unconditioned time. Most of

the immigrants act in opposition to fixation of the focal species, greatly increasing the time to either fixation or extinction.

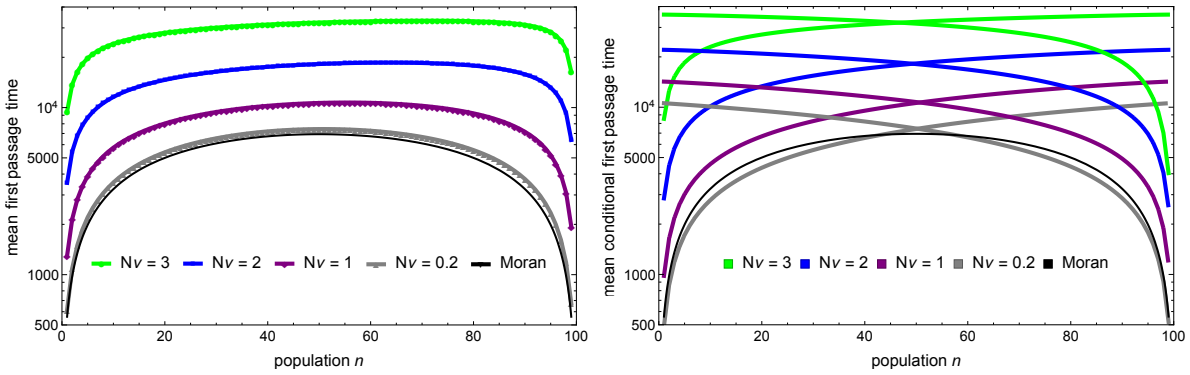

Figure 5.4: *Mean first passage times depending on initial population. Left:* Unconditioned mean time to first reaching either fixation or extinction, from a given starting population of the focal species. Focal immigration fraction is $g = 0.4$, system size is $K = 100$, and immigration rate ν is coloured as in figure 5.3. The black line shows regular Moran results without immigration. Immigration acts to increase the first passage time, and the effects are greatest away from gK. *Right:* Same as the left panel but for conditioned first passage times. Times conditioned on first reaching fixation decrease from left to right, and those conditioned on extinction first increase from left to right. Note that the curves follow their corresponding unconditioned times from the left panel when the occurrence is probable but are much longer when improbable.

Conditioned first passage times

In interpreting the unconditioned mean time I made reference to the times conditioned on local focal fixation or extinction. With the clock stopping when the focal population first reaches 0 or K individuals, I calculate the conditional times, respectively to extinction and to fixation. The extinction probability is given by equation 5.17. Equation 4.2 gives the general equation for solving the conditional time, but it can be written more clearly, following the notation of the fixation probability and unconditioned time, as

$$\phi_n = \phi_1 + \sum_{j=1}^{n-1} \left(\phi_1 - \sum_{i=1}^{j} q_i E_i \right) S_j. \tag{5.19}$$

Here $\phi_i \equiv E_i \theta_i$ (not a dot product, just multiplication of elements), where θ_i is the conditional extinction time [83]. The boundary conditions are both zero, since $E_K = 0$ as does θ_0 [78]. These boundary conditions allow me to rearrange the previous equation to get

$$\phi_1 = \frac{\sum_{j=1}^{K-1} \sum_{i=1}^{j} q_i E_i}{1 + \sum_{j=1}^{K-1} S_j}. \tag{5.20}$$

Equation 5.20 substituted into equation 5.19 allows us to solve for ϕ_n, and therefore the conditional time θ_n. One arrives at the graph shown in the right panel of figure 5.4. The conditional times mostly match the unconditioned time, except near the rare events that do not much contribute to the average. For instance, a low focal species population close to zero is more likely to go extinct and will only rarely fixate first. Naturally, the rare fixation takes much longer than the common extinction, the latter of which tends to dominate the unconditioned time.

5.5 Discussion

The previous chapter modelled a single invading immigrant into a Lotka-Volterra system, an event which was assumed to happen infrequently enough that it would resolve before other invaders arrived. Within the Moran model with immigration, analogous to the $a = 1$ limit of the Lotka-Volterra model, I have explicitly considered the cases of high and low immigration rate. When immigration is sufficiently high, such that $K\nu > \max\big(1/g, 1/(1-g)\big)$, the focal species is maintained at steady state most often at a fractional abundance equal to that in the metapopulation from which the immigrants arrive. For low immigration rate, specifically $K\nu < \min\big(1/g, 1/(1-g)\big)$, the focal species spends the bulk of its time either temporarily extinct or else fixated in the local system (not the metapopulation). One way to characterize biodiversity is by the number of different species that reside in a system [11, 20, 21]. An estimate of the expected number of species in a system, at least when immigration is frequent, is given by the number of g_i's greater than $1/(K\nu)$, where g_i is the fractional abundance of species i in the static large metapopulation that provides immigrants to the system.

For incomplete niche overlap where species can effectively coexist (as studied in chapter 3), the number of species in a system, as well as their abundances, depends on how their K_i's are distributed. This can be connected back to theories of the apportionment of resources common to niche theories of biodiversity [36, 65, 66]. Calculating the abundance curve of systems will less than complete niche overlap is outside of the scope of this thesis. I can, however, make qualitative arguments on how a lesser niche overlap would affect Hubbell's abundance curve, given that the Hubbell model is similar to the Moran model with immigration. Those species in disparate niches will exist at their local carrying capacity modified by an averaged niche overlap with the community, and will be effectively unsuppressed by their neighbours, thus there should be more species at higher abundance, higher mean population. Only those species that have a naturally low carrying capacity and those that have high niche overlap with others in the system will be found at low abundance or in a transient state. Based on my results, an observed species abundance curve that shows more species at high abundance but lesser at low abundance when compared to the prediction of Hubbell is a signature of a non-neutral ecosystem influenced by niche differences.

Chapter 6

Discussion

6.1 Limitations and caveats

Although some of the assumptions underlying the theories outlined in this thesis might not hold in many real systems, they serve as a minimal working model. Comparison of experimental data against my theoretical predictions illuminates the way in which that particular system differs from a simple model and the assumptions underlying it. These deviations are informative as they indicate what properties of that system differentiate it from the simple model and characterize its behaviour. While there is a broad range of experiments to which my results would apply, there are also a number of ways they could fall short.

For the bulk of this thesis I have assumed the species interactions are symmetric (except section 3.11), with true neutrality as the limiting case of complete niche overlap. The symmetry implies no species has an explicit fitness advantage. Selection due to differing fitnesses tends to lead to greater fixation probabilities and faster fixation times than the unselective case. It is hard to believe that two species that occupy even partially overlapping niches would not have a fitness difference between them such that one of them is favoured (but see [68, 77]). This dissonance is especially potent if two species evolved in different systems and are optimized for different conditions before one of them immigrates to the environment of the other. I have largely been silent on where new strains might arise from. On the molecular level, mutation is most likely to come from single nucleotide polymorphisms, which has three common outcomes: most often, the mutation is deleterious and selected against; often the mutation is synonymous and therefore neutral; occasionally the mutation is beneficial. There is a large body of work on mutation selection [71, 93, 187, 191, 202, 208, 209]. Synonymous mutations should obey the Moran limit of my results [70], but to have symmetric partial niche overlap the mutant must use a resource less effectively than the wild type strain while simultaneously not decreasing the mutant's basal growth rate. Intuitively this should require at least two mutations; one to decrease the usage efficacy and a second to improve a different resource usage to compensate. The idea is not so far-fetched, however, since most enzymes have some activity on a variety of substrates (typically optimized for one compound) [210, 211], it is not inconceivable that a mutation should decrease the catalytic activity of an enzyme on one substrate while simultaneously improving it for another.

One aspect of this thesis is that most of the parameters, like reproductive ratio r, carrying capacity K, and niche overlap a, are phenomenological. Often these parameters can be connected to real physical

quantities [10, 212], as I demonstrated in chapter 2 with the example of two bacterial strains producing antibacterial toxins. Niche overlap, for example, was an amalgam of the basal birth and death rates, the toxin production and degradation rates, and the effect of toxin on the death rate. Deriving the phenomenological parameters from physical and biological quantities is case dependent and is outside the scope of this thesis. Phenomenological parameters see wide use in the literature; nevertheless an astute reader should be wary whenever they are presented.

At times I have suggested that those organisms not from the focal species could be all from some second species or from a variety of non-focal species. Lumping all non-focal species together is justified under the assumptions of the Moran and Hubbell models, that in some way each species affects the others as strongly as itself. Neutral theory apologists have made such arguments [68, 77]. For incomplete niche overlap I imply that those non-focal species all occupy the same niche as each other and have the same overlap with the focal species. My results are more readily applied to those systems wherein only two species might coexist.

Another major assumption is that species are well-mixed, such that each organism has a chance of interacting with every other organism in the system. The well-mixed assumption is more valid for some systems than others. It seems to work well with mobile organisms like animals or tree seeds as considered in [11], or mobile bacteria in a fluid like in [149, 213–215]. There are situations for which it is clearly not applicable, where spatial arrangement matters, as reflected in the mathematical models [17, 192, 216–219]. One of the motivating questions for this thesis is the paradox of the plankton, why there are so many species of plankton that seem to coexist in a seemingly small niche with little variety of resources [24]. One resolution of this paradox is that spatial effects act to stabilize the competing populations, and that otherwise they would collapse to only a few species coexisting [26]. Briefly, the idea is that in different patches a given species might go extinct, while elsewhere it is flourishing, and migration between the patches is what supports the global continued existence of each species.

One caveat of my research is that I have regarded demographic fluctuations while ignoring environmental noise. In reality both sources of stochasticity should contribute, to varying degrees. Typically, environmental fluctuations are of larger magnitude and therefore lead to larger variances and faster first passage times [80]. However, this depends on the particular experimental or biological setup. It is also worth noting that an experimentalist can act to minimize environmental noise, but demographic stochasticity is inherent to any system of finite population and therefore cannot be removed.

There are many other simplifications I have employed to make my research questions tractable. For instance, I have assumed that reproduction is (or can at least be effectively treated as being) asexual. As such I can make no comment on how demographic stochasticity and interspecies competition should affect heterozygosity. I have also not considered any life stages or structured populations. Genotypically an organism has died when it can no longer reproduce, yet this aged organism still can compete for resources. There are many ways that my research could be made more realistic or otherwise extended. I discuss some such examples in the Next steps section below. The results of this thesis come from very simple models, which can nevertheless capture qualitative behaviours in extinction rates and coexistence phase diagrams.

6.2 Experimental tests and applications of the theory

The research presented in previous chapters was theoretical in nature. I will now present some experiments from the literature that have relevance to the theoretical work I have done. I will also propose other sets of experiments that would test my results. My research predicts how long a species is expected to survive before going extinct, which is an important consideration when performing experiments on a species.

It is possible, for instance, to experimentally corroborate some of the claims made in chapter 2. As previously discussed, measuring the average dynamics of a population increasing and decreasing is insufficient on its own to predict its eventual stochastic demise. Instead, each of the birth and death rates must be measured. For example, in a bacterial species the birth rate can be inferred by the uptake and usage of radioisotope-doped nucleotides in nucleic acid synthesis [142]. The death rate can also be measured using radioisotopes [132], and both birth and death can be tracked by following one or a few cells [220–224]. These two rates, and their dependence on neighbour density [121, 125–128], constitute all that are required to make predictions in an experiment where the environment is tightly controlled. The quasi-steady state population probability distribution could be measured by having multiple parallel replicates or by having just the one population but repeatedly measuring the population to collect statistics on the distribution. The experimentalist would have to wait for the system to relax back to its quasi-steady state between measurements, but some preliminary work suggests that this is a fast process, on the order of a generation [13]. At sufficiently low carrying capacity it would be possible to verify the dependence of the extinction time on δ and q.

The extinction times I predict are long, and not just those that scale exponentially with the carrying capacity. Even the relatively fast results of the Moran model, which scale linearly with K, will be longer than is experimentally viable for typical biological populations and timescales. The fastest reproducing model organism is the *E. coli* bacterium, which reproduces every twenty minutes in ideal conditions [124, 143]. A carrying capacity as low as 10^3 would show fixation in the Moran limit in a week, but the complete extinction of the population (as described in chapter 2) would take longer than life has existed on the Earth. For example, the famous long running experiments by Lenski [143] would take something like 10^{10^8} years for one of their vials to have all the bacteria die out due to demographic fluctuations. The typical carrying capacity for bacteria gives a density of $10^6 - 10^8$ bacteria per millilitre. Larger organisms tend to have lower densities (lower K) but also slower birth rates (lower r), such that it is not obvious whether these species will have longer or shorter lifespans. Nevertheless some results have been corroborated experimentally, specifically those propounded by Kimura [71, 225].

Regarding small populations, figure 3.5 (from chapter 3) suggests that the exponential term is less relevant than the algebraic term when it comes to the fixation time of two competing species as compared to a similarly sized Moran-like system. One experimental system that lends itself to small populations, albeit not populations of organisms, is that of plasmids within a cell [136]. Plasmids are small loops of DNA that typically code for a few/handful genes, often one of which confers some antibiotic resistance[124, 127, 226]. Their reproduction can be thought of as asexual, since only one plasmid copy is required as a template to make a new copy. Plasmid copy numbers, the average number of copies of a plasmid per cell, tend to be low, ranging from 10^1 to 10^3. The copy number can be thought of as the carrying capacity of that plasmid in the cell, and is maintained primarily by a negative regulatory circuit, whereby an antisense RNA expressed by the plasmid acts to inhibit the replication of new plasmids. The bacterial chromosome is typically thousands or a million times longer than that of a plasmid,

and one expects a similarly disparate timescale for their replication. The bacterium divides when it has copied its whole chromosome, so a thousand or a million plasmid 'generations' may have occurred before division. A low copy number plasmid might have a carrying capacity of $K = 10$ to 20, which would suggest a mean extinction time of $e^K/K \sim 2$ thousand to 20 million replications, which could feasibly occur before the bacterium divides once. Furthermore, different types of plasmids can have the same or similar maintenance mechanisms, such that they compete, as mediated by their shared inhibitor antisense RNAs [226]. Then the relevant comparison would not be chapter 2's extinction of a single species but the competition of chapters 3 and 4. The niche in this case is defined by the replication inhibitor, and niche overlap relates how much the antisense RNA of each plasmid type inhibits the replication of the other; if there is a shared inhibitor, the plasmids are in the Moran limit, and we expect fixation to be rapid, much faster than the cell division time scale.

Similar to plasmids, the number of mitochondria in a cell is small and tends to be controlled within a cell [227–229]. Of interest to researchers is how the integrity of mitochondrial DNA is maintained [229]. Sometimes a mitochondrion will have large deletions in its DNA. There are conflicting selection forces in this system: the mutant mitochondria reproduce faster than the wildtype but hinder the viability of the cell, hence the cell's reproduction. But when one mutant arises in a population, what is the chance it will fixate, and will fixation occur before the cell reproduces? The analyses of chapter 4 are relevant to such a problem.

The most promising work on small populations of organisms has been with microfluidic devices [220, 222, 224]. Often these researchers ask different questions to those that I address in this thesis, and are not interested in species persistence and extinction in general. Nevertheless, with their setups they are well positioned to study the dynamics of a small population. Some labs can even observe a single individual cell over the span of generations; if they can maintain a population of one, surely they can maintain a few. With lab space provided by Josh Milstein at the University of Toronto, and inspired by similar designs [220, 222, 224], some undergraduate students and I attempted to build a microfluidic device that would constrain a bacterial population to a population on the order of tens or a few hundred. The challenge was to design a device that allowed for the population to receive a constant small influx of nutrients in a confined space (hence a small carrying capacity) without flushing them out of the system too quickly. The flow rate could not be too slow, however, as it was the mechanism by which the bacteria would be well mixed. Otherwise the bacteria would be spatially arranged and death (in this case, being flowed out of the system) would not be random but depend on proximity to the main channel. It later turned out that this was indeed the case, which was problematic both in that it would not allow for competition of species (instead simply favouring the one farthest from the mouth of the chamber) and it would not allow for extinction of a single species (as the death rate dropped to negligible magnitude for bacteria in far back positions). Nevertheless the bacteria grew and were maintained. Further investigation of this system, both in experimental refinement and theoretical modelling, is warranted.

One manifestation of the theories I have analyzed in this thesis was done by the Gore lab, growing bacteria in the guts of nematodes [180]. These *C. elegans* worms are grown in an environment filled with red- and green-tagged *E. coli* bacteria that are otherwise identical. The bacteria invade the nematode guts by infrequently surviving the eating process and then slowly reproducing to colonize the system. As the bacteria have the same reproductive rate and chance of entering the gut unscathed this is an experimental realization of the Moran model with immigration from chapter 5 with $g = 0.5$. The researchers

use a version of the two-dimensional Lotka-Volterra model in the Moran limit to numerically simulate their data, compared to the more analytically tractable model of the Moran model with immigration that I propose. The data are sparse but both theories appear to fit nicely. The gut microbiome work of Gore and others [180, 195] suggests that the theories in this thesis could be applicable to microbiota more generally, be they in the gut or other areas [27, 29, 30, 154, 183, 194, 230].

Coalescent theory is a model that predicts the time in the past when two variants of a gene most recently shared a common ancestor [32, 34, 35, 93]. In its simplest form it treats all mutants as equally viable, interacting with other variants as strongly as they do with themselves [68, 231] - it is a neutral model. In this way it is like a Moran model, or a symmetric Lotka-Volterra model with complete niche overlap. The time it predicts since the last common ancestor is approximately exponentially distributed, with a mean proportional to the system size [35]. An inclusion of incomplete niche overlap, such as has been investigated in chapter 2, would only act to increase the estimated times. Niche overlap less than one would be most appropriate for very dissimilar variants that now serve different but equally vital purposes in the organism. The longer timescale of incomplete niche overlap of course would not change the historical record. Rather, coalescent theory is used to make inferences about historical population genetic parameters, like mutation rate and population size. For those genes to which incomplete niche overlap applies, the longer timescales that result from $a < 1$ must be balanced by shortened timescales from a smaller population size or greater mutation rate in order for the observed records to match. Conversely, if we know the historic population size and mutation rate, we could infer the niche overlap between disparate gene variants. Phylogenetic reconstruction is related to coalescent theory, and would be similarly affected by incomplete niche overlap [231].

6.3 Conclusions

This thesis treats extinction of a one dimensional logistic system in chapter 2, fixation of a coupled logistic system in chapter 3, invasion into a coupled logistic system in chapter 4, and species maintenance in a Moran model with immigration in chapter 5. The coupled logistic system of chapters 3 and 4, which typically has a deterministic fixed point, acts like a neutral model in the Moran limit, and I have characterized the transition to this limit. Chapter 5 looks at dynamics and steady state distributions of a single species in the Moran model with immigration. The results, in short, are:

- higher commensurate birth and death rates (*i.e.* higher δ, lower q) lead to faster extinction;
- the WKB approximation is usually fine to recover the dominant (exponential) scaling of the MTE but miscalculates the algebraic prefactor; the Fokker-Planck equation fails on both accounts, though it does model the probability distribution near the fixed point;
- two species will effectively coexist unless they have exactly the same niche;
- similarly, greater niche overlap leads to longer invasion times, and lesser likelihood of success of an invasion attempt;
- in a Moran model with repeated immigration a focal species will be most likely to have a moderate population size if $K\nu > \max\big(1/g, 1/(1-g)\big)$, where K is the system size, ν is the immigration rate, and g is the fractional abundance of the focal species in the nearby reservoir population;

- with incomplete niche overlap the abundance curve of a system should match the distribution of carrying capacities modified by niche overlaps;
- with complete niche overlap (neutrality) the abundance curve of an island system will match the mainland abundance curve for those species with $g_i > 1/K\nu$, with the remaining species contributing to low abundance transients.

More detailed discussions and conclusions specifically related to these topics can be found in their respective chapters; below I shall summarize them and extend them beyond the topics of their chapters and to the broader questions discussed in this thesis.

How long will a single species with only intraspecies interactions persist before going extinct? As was already known in the literature, the simplest model of a deterministically stable species, namely the logistic model, gives a mean extinction time whose scale is dominated by an exponential dependence on the system size. What was *not* known was the particulars of how the extinction time depends on the other parameters of the model. Along with carrying capacity K and mean reproductive rate r these parameters are the basal death rate δ (as opposed to the difference of basal birth and death rate, r) and a parameter q which scales the intraspecies interactions from reducing the birth rate to increasing the death rate. I have demonstrated that, after the carrying capacity, the most impactful parameter on the quasi-steady state distribution and extinction time is the death rate. I find that increasing the death rate while maintaining the reproductive rate (and consequently also increasing the birth rate) tends to broaden the probability distribution and decreases the extinction time. Moving the effect of interspecies interactions from birth to death by decreasing q has a similar but lesser effect. Biologically speaking, those species with larger birth and death rates tend to have greater stochastic fluctuations in their populations and are therefore less stable, being more probable to go extinct sooner. This is true both for basal birth and death rates and when intraspecies interactions tend to cause death (rather than simply slowing birth). I conclude that the incorporation of noise to a deterministic model is ambiguous and the δ and q parameterization of birth and death rates that do not affect the deterministic limit nevertheless have a significant effect on stochastic quantities like the mean time to extinction. Furthermore, I used this exemplar system to investigate which mathematical techniques are effective to model stochastic extinction. If a researcher wants to model noise in their system but is only concerned with near equilibrium dynamics, the Fokker-Planck and WKB approximations appear acceptable. WKB also captures the dominant exponential scaling of extinction time with system size. When investigating far-from-equilibrium quantities like the rare fluctuations that lead to extinction in a deterministically stable system these approximation miss out on subtleties like the algebraic prefactor of the scaling. The failure of the Fokker-Planck equation was known [101, 117]; not so for WKB. These approximations remain appealing for getting an idea of the qualitative far-from-equilibrium behaviour but if the goal is to be precise there are better alternatives. For instance, the approximation employed throughout most of this thesis, namely introducing a cutoff to the transition matrix and then inverting it to solve the master equation directly, is both accurate and fast.

It has been long known in the literature that extinction from the stochastic logistic model is dominated by an exponential scaling with carrying capacity [80, 91, 96, 102], and so too is the fixation time of two independent logistic systems. Coupling two logistic systems gives the Lotka-Volterra model, for which it has been recently noted that when intra- and interspecies interactions are equal the stochastic Lotka-Volterra model exhibits fixation dynamics similar to the Moran model [47–50]. Some of these papers even investigated partial niche overlap, and find the system still exhibits the long coexistence of a logistic

model [48–50], as is expected for a deterministically stable fixed point [107]. So then how long will a species exist with intraspecies interactions and some lesser but non-zero interspecies interactions? That is, how long will two species coexist given some partial niche overlap? I conducted a systematic study of the mean time to extinction's scaling with carrying capacity to find out how the LV model transitions from the independent to the Moran limit. I find that the MTE transitions from slow exponential scaling to the relatively fast extinction of algebraic scaling as found in the Moran limit via the continuous decrease of the exponential prefactor to zero as a function of increasing niche overlap. Only with the neutrality of complete niche overlap does the exponential dependence disappear. For large carrying capacity, I interpret this to mean that two species will effectively coexist if their niches have even a slight mismatch, a slight departure from neutrality.

Hubbell's model, being neutral, has equal intra- and interspecies interactions. There have been many pages written either decrying the unintuitive supposition that two disparate species might be equivalent [19, 200, 231], and many others defending the theory, arguing there must be a way in which species are effectively neutral [68, 77]. My research shows that there is no room for compromise between neutral and niche theories of two species coexisting. Even though neutral theory appears as a limit of niche theory, there is no such thing as being 'close' to neutral, as even partial niche mismatch leads to qualitatively different dynamics. I include the caveat that for low carrying capacity there are partial niche overlaps for which the system fixates faster than the corresponding Moran model, with this window of partial niches going to zero as carrying capacity increases. Barring this caveat, unless the species are truly neutral they will coexist, and their respective carrying capacities should regulate their abundance as per niche apportionment theory [36, 65, 66], rather than the random fluctuations of a neutral model. It remains possible that collections of species are neutral with respect to each other but together exist in a different niche from other such collections, with the outcome that neutral theory is applicable within such a niche niche.

I have also investigated the stability of an ecosystem with respect to invasion into the stochastic Lotka-Volterra model. For an ecosystem with a species already established, I have shown that the probability of failure of an invasion attempt of a new species in the large carrying capacity limit is directly proportional to the niche overlap between the established and invading species. The timescale of a successful invasion attempt is never exponential in the system size, being linear at most, in the Moran limit of complete niche overlap, and follows the deterministic trend of logarithmic scaling when the invader has independent resource needs from the established species. I find that unsuccessful invasion attempts are even faster to resolve. The implication is that one could test the applicability of the Hubbell model by measuring invasion success probability or timescale. If invasion (as defined in chapter 4) is more common than Hubbell predicts then it suggests that the neutral model is not a good model of the biological system being measured. Similarly, if invasion attempts, whether successful or not, resolve themselves more rapidly than the neutral model predicts then the system is better characterized by a theory of niches.

The Hubbell model assumes that each invader is from a new species [11], but was inspired by the island model of MacArthur and Wilson [51], which supposes that a small island gets repeated invasions from a larger repository of species on the mainland. This was the motivation for considering the Moran model with immigration in chapter 5, which allows for the calculation of the probability distribution of a species in a neutral system, and how this distribution depends on the immigration rate. The research is similar to that of McKane [114], but I offer a more biological analysis of the results; I also worked out

the probability and times for a species to first reach extinction before fixation. I find that the probability distribution has three characteristic qualitative shapes, with the probability either concentrated at the extremes of extinction and fixation, somewhere near the middle, or mostly near the middle but with sizable density at one of the extremes. The three shapes occur in different regimes of parameter space, bounded by how $K\nu$ compares with $1/g$ and $1/(1-g)$. Each mainland species will have its own abundance g, and the distribution of g's, specifically the number of species with g's greater than $1/(K\nu)$, suggests the number of species we expect to see with population around Kg in the island system. Those with lesser g's will likely have low or zero population in the system.

Competitive exclusion within a niche and the observation that the ocean surface has very few resources compared to its abundance of species was one initial motivation for my research: the paradox of the plankton. Ultimately, I cannot conclude whether neutral or niche theories are more appropriate for explaining the maintenance of biodiversity in general. One or the other will be more appropriate on a case by case basis. I situate my research among those theories which accommodate both niche and neutral theories [43, 75, 76, 90, 232]. Neutral theory is more parsimonious [43]; above I have suggested some bounds or checks to what it should predict. Namely, my results predict that invasion is easier with incomplete niche overlap, so compared to neutral theory there will be more species with large abundance. However, those small populations due to transients are lessened because times for both successful and failed invasion attempts are shorter, so I expect there will be fewer species at small abundance. Invasions into a neutral model should be rare and slow, and an island abundance distribution should follow the mainland abundance distribution. Others have suggested different tests that call neutral theory into question [23, 68, 122, 200, 231, 233]. Conversely, niche theories are hard to disprove, as they suffer from an overabundance of parameters. What I can say is that coexisting species need not be in entirely disparate niches; they can effectively coexist even with large, albeit incomplete, niche overlaps.

The bulk of this thesis deals with a two species Lotka-Volterra model and implies that two species with partial niche overlap will effectively coexist, or that one of the two species can quickly invade a system in which the other is established. If interactions between two species do not destabilize either species, then likely any three species effects will be even lesser. Thus a modified niche theory composed of many pair-wise interacting species can be imagined, with the extinction of a given species related to its own carrying capacity and the greatest niche overlap it has among the other species.

6.4 Next steps for the research

I will now indulge in some speculation. In this section I present some straightforward extensions of my research. Also included are some more extensive next steps. As with all my research, there is the next step of applying my results to specific real biological systems, finding a way to estimate the phenomenological parameters based on measurable evidence, and then making predictions. See the experimental tests section of this chapter for more details, but two promising systems are microfluidic devices [221] and small microbiomes like the gut of nematodes [180].

The stochastically relevant parameters of chapter 2 were those that did not show up in the deterministic analogue of the system which nevertheless affect the stochastic dynamics. They have a natural

extension to powers greater than quadratic:

$$b(n) = r\,n + c(n) \qquad (6.1)$$
$$d(n) = r\,n^2/K + c(n)$$

with an arbitrary $c(n)$. It is unclear how c affects the stochastic measurable quantities like the MTE. Writing c as a polynomial, I predict the higher orders will have a lesser and lesser effect, since the linear parameter δ is already has greater effect than the quadratic parameter q. Furthermore, I investigated the deterministic equation $\dot{x} = r\,x(1 - x/K)$. I speculate that any concave down system will behave similarly, as is the case with logistic difference equations [234]. Assaf and Meerson [103] included the Allee effect and found that the MTE still scales exponentially with carrying capacity; I predict there is an effective carrying capacity given by the distance between the stable and unstable fixed points, which could be generalizable to systems with multiple minima.

A natural extension of my work would be to include selection, explicit fitness advantages, to the system, for instance by increasing one r to increase the birth rate while simultaneously increasing K to keep the same death rate. I have not done so already because selection has been treated many times in many ways [21, 43, 47, 110, 115, 178, 187, 191, 202, 208, 235]. Selection actually tends to simplify the system as the higher fitness species rapidly fixates, quickly reducing the dimensionality of the problem. Nevertheless there are some advantages to how I treat stochastic systems that would aid the analysis of systems with selection. In the independent limit any fitness advantage should be irrelevant, so there will at least be a transition between coexistence in the independent limit and rapid fixation otherwise. What is more, many models with selection, like that of Kimura, must make the assumption that the effect of selection is weak, typically much less than $1/K$ [9, 71, 236]. Inverting the transition matrix, as I do in chapter 3, is arbitrarily precise, and so does not suffer from any requirement of such an assumption. It can treat the range of selection, from weak to strong. Not only does this give access to regimes not normally considered, it provides a way to verify the small selection results that rely on approximation. The way in which selection acts is to cause selective sweeps. In the literature there is a debate about selective sweeps [237], specifically whether it is more common for a new fit mutant to quickly fixate in a population, or whether it is more often the case that a mutant trait in a population is neutral until the environment changes, after which it is more fit and fixates. The distinction between these hard and soft selective sweeps requires more careful treatment, with fewer assumptions; the method employed in chapter 3 of this thesis would be an ideal tool to use, given its arbitrary accuracy. Selection can also be incorporated into the invasion dynamics of chapter 4.

In chapters 3 and 4 I considered the two species stochastic generalized Lotka-Volterra model in the regime in which it had a stable fixed point or a line of marginal stability along which the stochastic trajectories diffused. With a different choice of parameters it gives the predator-prey system, which has a fixed point of marginal stability, about which deterministic orbits cycle. Gottesman and Meerson [87] analyzed the predator-prey system using a clever rotating reference frame and the WKB approximation. Arbitrarily correct data obtained via the matrix inverse (rather than the approximate results of WKB) would allow for a complete analysis of the scaling of the MTE with system size. One could look also at the effect of initial conditions on the MTE, whether the MTE is cyclic starting at different points along an orbit.

The techniques applied in this thesis, specifically the use of a truncated transition matrix being

inverted to solve for the first passage times exactly, can easily be applied to other low species number systems. The calculation for each point in parameter space is not lengthy; the main constraint is RAM, rather than computational time, and so a larger memory computer could deal with problems with larger carrying capacities or more species. For example, in chapter 3 I considered a two dimensional generalized Lotka-Volterra system to explore competition between two species. The Lotka-Volterra system has been generalized to any dimension, any number of species, with a number of three species systems being of interest. With three species the Lotka-Volterra model can show limit cycles, which (along with fixed points) is another way of allowing for deterministic coexistence of species [39, 146]. This contradicts the intuition that the number of resources constrains the number of species that can exist in a system. Future investigations will probe whether the MTE from a stable limit cycle also scales exponentially with the system size, and how the system size should be characterized given that there is no asymptotic population size. This could serve as a way to distinguish between systems with a fixed point and those with an extended attractor. One example of a three species limit cycle system is called the rock-paper-scissors system, and occurs in biology in lizards and bacteria [238–240]. Extension to three dimensions also allows for the possibility of observing a chaotic system [234]. It is an open question how best to distinguish between chaotic systems and non-chaotic systems with stochastic fluctuations [20], but the scaling of the MTE may serve such a purpose.

Another three species model that has enjoyed widespread usage is the SIR model of disease outbreak [101, 241, 242]. It counts the number of susceptible (S), infected (I), and recovered (R) individuals with regards to the disease. There are many variations of this model, but the simplest has a stable spiral node deterministic fixed point. Application of the WKB approximation shows a route to extinction that spiraled in the opposite direction [96]. In chapter 2 I showed that WKB does not recover the correct prefactor for the extinction time, and in chapter 3 I showed that the idea of a route to extinction is questionable. Thus the SIR model is ripe for further analysis. Specifically, the next step is to calculate the residence times for the model, and from these times construct a probable route to extinction, to compare to the WKB route.

The final next step I will outline is the coupling of the ecology of this thesis with evolution. In chapter 3 I regarded how the scaling of the extinction time changes as niche overlap increases from independence ($a = 0$) to complete niche overlap ($a = 1$), at which point the MTE is that of the Moran model. Despite the biological significance of this limit, in parameter space it is only one point, of measure zero, and seems unlikely to arise randomly. Perhaps there is a biological reason for convergence toward this point, that could be shown with a simple model. If a mutant strain arises from a single population, it is likely to have a very similar niche to the wildtype, hence a large niche overlap. And from there, what would the forces of evolution dictate? One could simulate the evolution of the niche overlap (for instance following the work of MacArthur [65]) in an individual based model with a given resource distribution. The question is whether having selection optimize the fitness of the individuals would cause the niches to converge to better match the resource distribution, supporting neutral models, or diverge to minimize niche overlap and competition, supporting niche theory. Do fitness considerations act to make the already-unlikely Moran limit entirely untenable, or is this limit actually a natural consequence of evolution? Coupling ecology with evolution is a large field of research [10, 17, 20, 21, 36, 47–49, 58, 76, 111, 131, 143, 149, 177, 178, 187, 237, 243–245], and there is more work to be done with stochasticity, especially demographic stochasticity.

Bibliography

[1] Thomas Malthus. An essay on the principle of population. *St. Paul's church-yard, London*, pages 1–126, 1798.

[2] Alfred J Lotka. Analytical note on certain rhythmic relations in organic systems. *Proceedings of the National Academy of Sciences*, 6(7):410–415, 1920.

[3] Vito Volterra. Fluctuations in the abundance of a species considered mathematically. *Nature*, 118(2972):558–560, 1926.

[4] Pierre-Francois Verhulst. Notice sur la loi que la population suit dans son accroissement. *Corresp. Math. Phys.*, 10:113–126, 1838.

[5] Sewall Wright. Evolution in Mendelian populations. *Genetics*, 16(2):97, 1931.

[6] R.A. Fisher. *The genetical theory of natural selection*. Clare, Oxford, 1930.

[7] Patrick Moran. *The statistical processes of evolutionary theory*. Clarendon Press, Oxford, 1962.

[8] James Crow and Motoo Kimura. Some genetic problems in natural populations. In *Proc. Third Berkeley Symp. Math. Stat. Probab. Vol. 4 Contrib. to Biol. Probl. Heal.*, number 580, pages 1–22, 1956.

[9] Motoo Kimura. Diffusion models in population genetics. *J. Appl. Probab.*, 1(2):177–232, 1964.

[10] Robert MacArthur and Richard Levins. The limiting similarity, convergence, and divergence of coexisting species. *Am. Nat.*, 101(921):377–385, 1967.

[11] S.P. Hubbell. *The Unified Theory of Biodiversity and Biogeography*. Princeton University Press, 2001.

[12] MattheW A Badali and Anton Zilman. Effects of niche overlap on co-existence, fixation and invasion in a population of two interacting species (under revision). *Journal of the Royal Society: Interfaces*.

[13] MattheW A Badali, Jeremy Rothschild, and Anton Zilman. Intraspecies interactions in birth or in death rates. *(in Prep.)*.

[14] Serguei Saavedra, Rudolf P Rohr, Vasilis Dakos, and Jordi Bascompte. Estimating the tolerance of species to the effects of global environmental change. *Nat. Commun.*, 4:2350, Aug 2013.

[15] Mark L Shaffer. Minimum population sizes for species conservation. *BioScience*, 31(2):131–134, 1981.

[16] S Pimm, H L Jones, and J Diamond. On the risk of extinction. *Am. Nat.*, 132(6):757–785, 1988.

[17] Garry Peterson, Craig R. Allen, and C. S. Holling. Ecological resilience, diodiversity, and scale. *Ecosystems*, 1(1):6–18, 1997.

[18] Alan McKane, David Alonso, and Ricard V. Sole. Mean-field stochastic theory for species-rich assembled communities. *Phys. Rev. E - Stat. Physics, Plasmas, Fluids, Relat. Interdiscip. Top.*, 62(6 B):8466–8484, 2000.

[19] Michael Kalyuzhny, Efrat Seri, Rachel Chocron, Curtis H Flather, Ronen Kadmon, and Nadav M Shnerb. Niche versus neutrality: a dynamical analysis. *The American Naturalist*, 184(4):439–446, 2014.

[20] R May. Unanswered questions in ecology. *Philos. Trans. R. Soc. Lond. B. Biol. Sci.*, 354(1392):1951–9, 1999.

[21] Peter Chesson. Mechanisms of maintenance of species diversity. *Annu. Rev. Ecol. Syst*, 31(May):343–66, 2000.

[22] Elizabeth Pennisi. What determines species diversity? *Science (80-.).*, 309:90, 2005.

[23] Colleen K Kelly, Michael G Bowler, Oliver Pybus, and Paul H Harvey. Phylogeny, niches, and relative abundance in natural communities. *Ecology*, 89(4):962–970, 2008.

[24] G.E. Hutchinson. The Paradox of the plankton. *The American Naturalist*, 95(882):137–145, 1961.

[25] Georgii Frantsevitch Gause. Experimental analysis of vito volterra's mathematical theory of the struggle for existence. *Science*, 79(2036):16–17, 1934.

[26] Shovonlal Roy and J. Chattopadhyay. Towards a resolution of 'the paradox of the plankton': A brief overview of the proposed mechanisms. *Ecol. Complex.*, 4(1-2):26–33, 2007.

[27] Bryan Coburn, Pauline W Wang, Julio Diaz Caballero, Shawn T Clark, Vijaya Brahma, Sylva Donaldson, Yu Zhang, Anu Surendra, Yunchen Gong, D Elizabeth Tullis, Yvonne C W Yau, Valerie J Waters, David M Hwang, and David S Guttman. Lung microbiota across age and disease stage in cystic fibrosis. *Sci. Rep.*, 5:10241, 2015.

[28] T. Korem, D. Zeevi, J. Suez, A. Weinberger, T. Avnit-Sagi, M. Pompan-Lotan, E. Matot, G. Jona, A. Harmelin, N. Cohen, A. Sirota-Madi, C. A. Thaiss, M. Pevsner-Fischer, R. Sorek, R. Xavier, E. Elinav, and E. Segal. Growth dynamics of gut microbiota in health and disease inferred from single metagenomic samples. *Science (80-.).*, 349(6252):1101–1106, 2015.

[29] Chaysavanh Manichanh, Jens Reeder, Prudence Gibert, Encarna Varela, Marta Llopis, Maria Antolin, Roderic Guigo, Rob Knight, and Francisco Guarner. Reshaping the gut microbiome with bacterial transplantation and antibiotic intake. *Genome Res.*, 20(10):1411–1419, 2010.

[30] Casey M Theriot, Mark J Koenigsknecht, Paul E Carlson Jr, Gabrielle E Hatton, Adam M Nelson, Bo Li, Gary B Huffnagle, Jun Li, and Vincent B Young. Antibiotic-induced shifts in the mouse gut microbiome and metabolome increase susceptibility to Clostridium difficile infection. *Nature communications*, 2014.

[31] James M Kinross, Ara W Darzi, and Jeremy K Nicholson. Gut microbiome-host interactions in health and disease. *Genome Med.*, 3(3):14, 2011.

[32] Jeffrey Rogers and Richard A Gibbs. Comparative primate genomics: emerging patterns of genome content and dynamics. *Nat. Rev. Genet.*, 15(5):347–59, 2014.

[33] Sean H. Rice. *Evolutionary theory: mathematical and conceptual foundations*. Sinauer Associates, Sunderland, Mass., 2004.

[34] Richard A Blythe and Alan J Mckane. Stochastic models of evolution in genetics, ecology and linguistics. *J. Stat. Mech. Theory Exp.*, 2007(07):P07018, 2007.

[35] J Kingman. The coalescent. *Stoch. Process. their Appl.*, 13(3):235–248, 1982.

[36] Matthew A Leibold. The niche concept revisited: mechanistic models and community context. *Ecology*, 76(5):1371–1382, 1995.

[37] Joseph Grinnell. The niche-relationships of the california thrasher. *Auk*, 34(4):427–433, 1917.

[38] Robert D Holt, James P Grover, and David Tilman. Simple rules for interspecific dominance in systems with exploitative and apparent competition. *Am. Nat.*, 144(5):741–771, 1994.

[39] Robert A Armstrong and Richard McGehee. Coexistence of species competing for shared resources. *Theor. Popul. Biol.*, 9:317–328, 1976.

[40] Richard McGehee and Robert A. Armstrong. Some mathematical problems concerning the ecological principle of competitive exclusion. *J. Differ. Equ.*, 23(1):30–52, 1977.

[41] Robert A. Armstrong and Richard McGehee. Competitive exclusion. *Am. Nat.*, 115(2):151–170, 1980.

[42] Charles S Elton. The nature and origin of soil-polygons in spitsbergen. *Quarterly Journal of the Geological Society*, 83(1-5):163–NP, 1927.

[43] M A Leibold and Mark A McPeek. Coexistance of the niche and neutral perspectives in community ecology. *Ecology*, 87(6):1399–1410, 2006.

[44] David Tilman. *Resource competition and community structure*. Number 17. Princeton university press, 1982.

[45] Bart Haegeman and Michel Loreau. A mathematical synthesis of niche and neutral theories in community ecology. *J. Theor. Biol.*, 269(1):150–165, 2011.

[46] Alfred J Lokta. Analytical note on certain rhythmic relations in organic systems. *Proc. Natl. Acad. Sci. U. S. A.*, 6(7):410–415, 1920.

[47] Yen T Lin, Hyejin Kim, and Charles R. Doering. Features of fast living: on the weak selection for longevity in degenerate birth-death processes. *J. Stat. Phys.*, 148(4):646–662, 2012.

[48] George W.A. Constable and Alan J. McKane. Models of genetic drift as limiting forms of the Lotka-Volterra competition model. *Phys. Rev. Lett.*, 114(3):1–5, 2015.

[49] Thiparat Chotibut and David R. Nelson. Evolutionary dynamics with fluctuating population sizes and strong mutualism. *Phys. Rev. E - Stat. Nonlinear, Soft Matter Phys.*, 92(2), 2015.

[50] Glenn Young and Andrew Belmonte. Explicit probability of fixation formula for mutual competitors in a stochastic population model under competitive trade-offs. *arXiv preprint arXiv:1809.06917*, pages 1–24, 2018.

[51] R. H. MacArthur and E. O. Wilson. *The theory of island biogeography*. Princeton University Press, Princeton, New Jersey, 1 edition, 1967.

[52] Robert MacArthur. Species packing and competitive equilibrium for many species. *Theor. Popul. Biol.*, 11, 1970.

[53] Peter H. Klopfer and Robert MacArthur. On the causes of tropical species diversity: niche overlap. *Univ. Chicago Press Am. Soc. Nat.*, 95(883):223–226, 1961.

[54] E.R. Pianka. The structure of lizard communities. *Annual review of ecology and systematics*, 4(1):53–74, 1973.

[55] E. R. Pianka. Niche overlap and diffuse competition. *Proc. Natl. Acad. Sci.*, 71(5):2141–2145, 1974.

[56] P.A. Abrams. Density-independent mortality and interspecific competition: a test of Pianka's niche overlap hypothesis. *Am. Nat.*, 111(979):539–552, 1977.

[57] Stuart H. Hurlbert. The measurement of niche overlap and some relatives. *Ecology*, 59(1):67–77, 1978.

[58] Joseph H Connell. Diversity and the coevolution of competitors, or the ghost of competition past. *Oikos*, pages 131–138, 1980.

[59] Peter Abrams. Some comments on measuring niche overlap. *Ecology*, 61(1):44–49, 1980.

[60] Thomas W. Schoener. Some comments on Connell's and my reviews of field experiments on interspecific competition. *Am. Nat.*, 125(5):730–740, 1985.

[61] P. Chesson. MacArthur's resource model. *Theor. Popul. Biol.*, 37:26–38, 1990.

[62] Peter Chesson and Jessica J Kuang. The interaction between predation and competition. *Nature*, 456(7219):235–238, 2008.

[63] Claudia Neuhauser and Stephen W . Pacala. An explicitly spatial version of the Lotka-Volterra model with interspecific competition. *Ann. Appl. Probab.*, 9(4):1226–1259, 1999.

[64] J Theodore Cox, Mathieu Merle, and Edwin Perkins. Coexistence in a two-dimensional Lotka-Volterra model. *Electron. J. Probab.*, 15:1190–1266, 2010.

[65] R. H. MacArthur. On the relative abundance of bird species. *Proc. Natl. Acad. Sci. U. S. A.*, 43(3):293–295, 1957.

[66] G. Sugihara, L.-F. Bersier, T. R. E. Southwood, S. L. Pimm, and R. M. May. Predicted correspondence between species abundances and dendrograms of niche similarities. *Proc. Natl. Acad. Sci.*, 100(9):5246–5251, 2003.

[67] G Bell. Neutral Macroecology. *Ecology*, 293(5539):2413–2418, 2001.

[68] James Rosindell, Stephen P. Hubbell, and Rampal S. Etienne. The unified neutral theory of biodiversity and biogeography at age ten. *Trends Ecol. Evol.*, 26(7):340–348, 2011.

[69] Egbert G Leigh Jr. Neutral theory: a historical perspective. *Journal of evolutionary biology*, 20(6):2075–2091, 2007.

[70] Motoo Kimura. Stochastic processes and distribution of gene frequencies under natural selection. *Cold Spring Harb. Symp. Quant. Biol.*, 20:33–53, 1955.

[71] Motoo Kimura. *The neutral theory of molecular evolution*. Cambridge University Press, 1983.

[72] Ronald A Fisher, A Steven Corbet, and Carrington B Williams. The relation between the number of species and the number of individuals in a random sample of an animal population. *The Journal of Animal Ecology*, pages 42–58, 1943.

[73] Alan McKane, David Alonso, and Ricard V. Sole. Analytic solution of Hubbell's model of local community dynamics. *Evolution*, 65:10, 2004.

[74] Sandro Azaele, Simone Pigolotti, Jayanth R Banavar, and Amos Maritan. Dynamical evolution of ecosystems. *Nature*, 444(7121):926, 2006.

[75] S. Pigolotti, R. Benzi, P. Perlekar, M. H. Jensen, F. Toschi, and D. R. Nelson. Growth, competition and cooperation in spatial population genetics. *Theor. Popul. Biol.*, 84(1):72–86, 2013.

[76] David A. Kessler and Nadav M. Shnerb. Generalized model of island biodiversity. *Phys. Rev. E - Stat. Nonlinear, Soft Matter Phys.*, 91(4), 2015.

[77] Stephen P Hubbell. Neutral theory and the evolution of ecological equivalence. *Ecology*, 87(6):1387–1398, 2006.

[78] R.M. Nisbet and W.S.C. Gurney. *Modelling fluctuating populations*. John Wiley & Sons, Toronto, 1982.

[79] N.G. Van Kampen. *Stochastic processes in physics and chemistry*. North Holland, North-Holland, Amsterdam, 1992.

[80] Otso Ovaskainen and Baruch Meerson. Stochastic models of population extinction. *Trends Ecol. Evol.*, 25(11):643–52, 2010.

[81] Andrew J. Black and Alan J. McKane. Stochastic formulation of ecological models and their applications. *Trends Ecol. Evol.*, 27(6):337–345, 2012.

[82] C.W. Gardiner. *Handbook of stochastic methods*. Springer, New York, 3 edition, 2004.

[83] Srividya Iyer-Biswas and Anton Zilman. First passage processes in cellular biology. *Adv. Chem. Phys.*, 160(261), 2016.

[84] Alex Kamenev, Baruch Meerson, and Boris Shklovskii. How colored environmental noise affects population extinction. *Phys. Rev. Lett.*, 101(26):268103, dec 2008.

[85] Thiparat Chotibut, David R. Nelson, and Sauro Succi. Striated populations in disordered environments with advection. *Phys. A Stat. Mech. its Appl.*, 465:500–514, 2017.

[86] Michael Assaf and Baruch Meerson. Spectral theory of metastability and extinction in birth-death systems. *Phys. Rev. Lett.*, 97(20):1–4, 2006.

[87] Omer Gottesman and Baruch Meerson. Multiple extinction routes in stochastic population models. *Phys. Rev. E*, 85(2):021140, feb 2012.

[88] Alexander Dobrinevski and Erwin Frey. Extinction in neutrally stable stochastic Lotka-Volterra models. *Phys. Rev. E - Stat. Nonlinear, Soft Matter Phys.*, 85(5):1–14, 2012.

[89] Alan Gabel, Baruch Meerson, and S. Redner. Survival of the scarcer. *Phys. Rev. E*, 87(1):010101, 2013.

[90] C. K. Fisher and P. Mehta. The transition between the niche and neutral regimes in ecology. *Proc. Natl. Acad. Sci.*, 111(36):13111–13116, 2014.

[91] R H Norden. On the distribution of the time to extinction in the stochastic logistic population model. *Adv. Appl. Probab.*, 14(4):687–708, 1982.

[92] I Nåsell. Extinction and quasi-stationarity in the Verhulst logistic model. *J. Theor. Biol.*, 211(1):11–27, Jul 2001.

[93] I. M. Rouzine, A. Rodrigo, and J. M. Coffin. Transition between stochastic evolution and deterministic evolution in the presence of selection: general theory and application to virology. *Microbiol. Mol. Biol. Rev.*, 65(1):151–185, 2001.

[94] Egbert Giles Leigh. The average lifetime of a population in a varying environment. *J. Theor. Biol.*, 90(2):213–239, 1981.

[95] Russell Lande. Risks of population extinction from demographic and environmental stochasticity and random catastrophes. *Am. Nat.*, 142(6):911–927, 1993.

[96] Alex Kamenev and Baruch Meerson. Extinction of an infectious disease: a large fluctuation in a non-equilibrium system. *Phys. Rev. E*, pages 1–4, 2008.

[97] Jonas Cremer, Tobias Reichenbach, and Erwin Frey. The edge of neutral evolution in social dilemmas. *New J. Phys.*, 11, 2009.

[98] Xiaoquan Yu and Xiang-Yi Li. Application of WKB and Fokker-Planck methods in analyzing demographic stochasticity. *Bulletin of mathematical biology*, pages 1–19, 2017.

[99] Patrick Foley. Predicting extinction times from environmental stochasticity and carrying capacity. *Conservation Biology*, 8(1):124–137, 1994.

[100] Linda J S Allen and Edward J. Allen. A comparison of three different stochastic population models with regard to persistence time. *Theor. Popul. Biol.*, 64(4):439–449, 2003.

[101] Charles R Doering, Khachik V Sargsyan, and Leonard M Sander. Extinction times for birth-death processes: exact results, continuum asymptotics, and the failure of the Fokker-Planck approximation. *Multiscale Model. Simul.*, 3(2):283–299, 2005.

[102] Michael Assaf, Baruch Meerson, and Pavel V Sasorov. Large fluctuations in stochastic population dynamics: momentum-space calculations. *J. Stat. Mech. Theory Exp.*, 2010(07):P07018, jul 2010.

[103] Michael Assaf and Baruch Meerson. Wkb theory of large deviations in stochastic populations. *Journal of Physics A: Mathematical and Theoretical*, 50(26):263001, 2017.

[104] J Cremer, T Reichenbach, and E Frey. Neutral evolution can maintain cooperation in social dilemmas. *Imprint*, 2009.

[105] Todd L. Parsons. Invasion probabilities, hitting times, and some fluctuation theory for the stochastic logistic process. *J. Math. Biol.*, 77(4):1193–1231, 2018.

[106] Yen Ting Lin, Hyejin Kim, and Charles R. Doering. Demographic stochasticity and evolution of dispersion I. Spatially homogeneous environments. *J. Math. Biol.*, 70(3):647–678, 2015.

[107] P Hänggi, P Talkner, and M Borovec. Reaction rate theory - 50 years after Kramers. *Rev. Mod. Phys.*, 62(2):251–341, 1990.

[108] Daniel T Gillespie. Exact stochastic simulation of coupled chemical reactions. *J. Phys. Chem.*, 81(25):2340–2361, 1977.

[109] Yang Cao, Daniel T Gillespie, and Linda R Petzold. Efficient step size selection for the tau-leaping simulation method. *J. Chem. Phys.*, 124(4):044109, jan 2006.

[110] Todd L. Parsons and Christopher Quince. Fixation in haploid populations exhibiting density dependence II: The quasi-neutral case. *Theor. Popul. Biol.*, 72(4):468–479, 2007.

[111] Todd L. Parsons, Christopher Quince, and Joshua B. Plotkin. Some consequences of demographic stochasticity in population genetics. *Genetics*, 185(4):1345–1354, 2010.

[112] Jonathan Dushoff. Carrying capacity and demographic stochasticity: Scaling behavior of the stochastic logistic model. *Theor. Popul. Biol.*, 57(1):59–65, 2000.

[113] Amaury Lambert. The branching process with logistic growth. *Ann. Appl. Probab.*, 15(2):1506–1535, may 2005.

[114] Alan J. McKane and Martin B. Tarlie. Optimal paths and the calculation of state selection probabilities. *Phys. Rev. E - Stat. Physics, Plasmas, Fluids, Relat. Interdiscip. Top.*, 69(4):10, 2004.

[115] Amaury Lambert. Probability of fixation under weak selection: A branching process unifying approach. *Theor. Popul. Biol.*, 69(4):419–441, 2006.

[116] Fabio A.C.C. Chalub and Max O. Souza. Fixation in large populations: a continuous view of a discrete problem. *J. Math. Biol.*, 72(1-2):283–330, 2016.

[117] J. Grasman and D. Ludwig. The accuracy of the diffusion approximation to the expected time to extinction for some discrete stochastic processes. *J. Appl. Probab.*, 20(2):305–321, 1983.

[118] T J Newman, Jean-Baptiste Ferdy, and C Quince. Extinction times and moment closure in the stochastic logistic process. *Theor. Popul. Biol.*, 65(2):115–26, mar 2004.

[119] Edward J Allen, Linda J S Allen, and Henri Schurz. A comparison of persistence-time estimation for discrete and continuous stochastic population models that include demographic and environmental variability. *Math. Biosci.*, 196(1):14–38, Jul 2005.

[120] Michael Assaf, Alex Kamenev, and Baruch Meerson. Population extinction risk in the aftermath of a catastrophic event. *Phys. Rev. E*, 79(1):011127, jan 2009.

[121] David Greenhalgh. An epidemic model with a density-dependent death rate. *Math. Med. Biol.*, 7(1):1–26, 1990.

[122] Peter B. Adler, Stephen P. Ellner, and Jonathan M. Levine. Coexistence of perennial plants: An embarrassment of niches. *Ecol. Lett.*, 13(8):1019–1029, 2010.

[123] David A. Kessler and Nadav M. Shnerb. Extinction rates for fluctuation-induced metastabilities: a real-space WKB approach. *J. Stat. Phys.*, 127(5):861–886, 2007.

[124] Michael T Madigan and John Martinko. *Brock Biology of Microorganisms*. Prentice Hall, Upper Saddle River, NJ, 11th edition, 2006.

[125] Carey D. Nadell, Joao B. Xavier, Simon A. Levin, and Kevin R. Foster. The evolution of quorum sensing in bacterial biofilms. *PLoS Biol.*, 6(1):0171–0179, 2008.

[126] Marin Vulic and Roberto Kolter. Evolutionary cheating in Escherichia coli stationary phase cultures. *Genetics*, 158(2):519–526, 2001.

[127] Laurence Van Melderen and Manuel Saavedra De Bast. Bacterial toxin-antitoxin systems: more than selfish entities? *PLoS Genet.*, 5(3), 2009.

[128] Daniel J Rankin, Leighton A Turner, Jack A Heinemann, and Sam P Brown. The coevolution of toxin and antitoxin genes drives the dynamics of bacterial addiction complexes and intragenomic conflict. *Proc. Biol. Sci.*, 279(1743):3706–15, 2012.

[129] Marc Mangel and Donald Ludwig. Probability of extinction in a stochastic competition. *SIAM J. Appl. Math.*, 33(2):256–266, 1977.

[130] H. Roozen. Equilibrium and extinction in stochastic population dynamics. *Bull. Math. Biol.*, 49(6):671–696, 1987.

[131] Arne Traulsen, Jens Christian Claussen, and Christoph Hauert. Coevolutionary dynamics in large, but finite populations. *Phys. Rev. E*, 74(1):011901, jul 2006.

[132] Pierre Servais, Gilles Billen, and Jose Vives Rego. Rate of bacterial mortality in aquatic environments. *Appl. Environ. Microbiol.*, 49(6):1448–1454, 1985.

[133] Golan Bel, Brian Munsky, and Ilya Nemenman. The simplicity of completion time distributions for common complex biochemical processes. *Phys. Biol.*, 7(1):016003, 2010.

[134] Gian Marco Palamara, Gustav W Delius, Matthew J Smith, and Owen L Petchey. Predation effects on mean time to extinction under demographic stochasticity. *Journal of theoretical biology*, 334:61–70, 2013.

[135] Tobias Reichenbach, Mauro Mobilia, and Erwin Frey. Coexistence versus extinction in the stochastic cyclic Lotka-Volterra model. *Phys. Rev. E*, 74(5):051907, nov 2006.

[136] Robert Gooding-Townsend, Steven Ten Holder, and Brian Ingalls. Displacement of bacterial plasmids by engineered unilateral incompatibility. *IEEE Life Sci. Lett*, 1:19–21, 2015.

[137] Brian Munsky and Mustafa Khammash. The finite state projection algorithm for the solution of the chemical master equation. *J. Chem. Phys.*, 124(4), 2006.

[138] Johan Grasman. The expected extinction time of a population within a system of interacting biological populations. *Bull. Math. Biol.*, 58(3):555–568, 1996.

[139] J. X. Zhou, M. D. S. Aliyu, E. Aurell, and S. Huang. Quasi-potential landscape in complex multi-stable systems. *J. R. Soc. Interface*, 9(77):3539–3553, 2012.

[140] H. Yan, L. Zhao, L. Hu, X. Wang, E. Wang, and J. Wang. Nonequilibrium landscape theory of neural networks. *Proc. Natl. Acad. Sci.*, 110(45):E4185–E4194, 2013.

[141] Paul J Channell and Clint Scovel. Symplectic integration of hamiltonian systems. *Nonlinearity*, 3(2):231, 1990.

[142] David Kirchman, Hugh Ducklow, and Ralph Mitchell. Estimates of bacterial growth from changes in uptake rates and biomass . Estimates of Bacterial Growth from Changes in Uptake Rates and Biomass. *Appl. Environ. Microbiol.*, 44(6):1296–1307, 1982.

[143] Richard E. Lenski, Michael R. Rose, Suzanne C. Simpson, and Scott C. Tadler. Long-term experimental evolution in Escherichia coli. I. adaptation and divergence during 2,000 generations. *Am. Nat.*, 138(6):1315, 1991.

[144] Garrett Hardin. The competitive exclusion principle. *Science (80-.).*, 131(1960):1292–1297, 1960.

[145] Michael W Palmer. Variation in species richness: Towards a unification of hypotheses. *Folia Geobot. Phytotaxon.*, 29(4):511–530, 1994.

[146] S Smale. On the differential equations of species in competition. *J. Math. Biol.*, 3:5–7, 1976.

[147] Immanuel M Bomze. Lotka-Volterra equation and replicator dynamics: a two-dimensional classification. *Biol. Cybern.*, 211:201–211, 1983.

[148] Tibor Antal and Istvan Scheuring. Fixation of strategies for an evolutionary game in finite populations. *Bull. Math. Biol.*, 68(8):1923–1944, 2006.

[149] Anna Posfai, Thibaud Taillefumier, and Ned S. Wingreen. Metabolic trade-offs promote diversity in a model ecosystem. *Phys. Rev. Lett.*, 118(2):028103, 2017.

[150] Motoo Kimura et al. Evolutionary rate at the molecular level. *Nature*, 217(5129):624–626, 1968.

[151] Emily R. Stirk, Grant Lythe, Hugo A. van den Berg, and Carmen Molina-Paris. Stochastic competitive exclusion in the maintenance of the naive T cell repertoire. *J. Theor. Biol.*, 265(3):396–410, 2010.

[152] José A. Capitán, Sara Cuenda, and David Alonso. Stochastic competitive exclusion leads to a cascade of species extinctions. *J. Theor. Biol.*, 419(1980):137–151, 2017.

[153] David A Kessler, Robert H Austin, and Herbert Levine. Resistance to chemotherapy: Patient variability and cellular heterogeneity. *Cancer Res.*, 74(17):4663–4670, 2014.

[154] Charles K. Fisher, Thierry Mora, and Aleksandra M. Walczak. Habitat fluctuations drive species covariation in the human microbiota. *arXiv preprint arXiv:1510.00198*, pages 1–18, 2015.

[155] Ted J Case and RG Casten. Global stability and multiple domains of attraction in ecological systems. *Am. Nat.*, 113(5):705–714, 1979.

[156] C O Jacob. Cytokines and anti-cytokines. *Curr. Opin. Immunol.*, 2(2):249–257, 1989.

[157] Rachael A Maplestone, Martin J Stone, and Dudley H Williams. The evolutionary role of secondary metabolites–a review. *Gene*, 115(1-2):151–7, 1992.

[158] Ping Shen and Simon Fillatreau. Antibody-independent functions of b cells: a focus on cytokines. *Nature reviews Immunology*, 15(7):441, 2015.

[159] Thomas A. Wynn. Type 2 cytokines: mechanisms and therapeutic strategies. *Nat. Rev. Immunol.*, 15:271–282, 2015.

[160] Tannishtha Reya, Sean J Morrison, Michael F Clarke, and Irving L Weissman. Stem Cells, Cancer, and Cancer Stem Cells. *Nature*, 414:105–111, 2001.

[161] Michael Wink. Evolution of secondary metabolites from an ecological and molecular phylogenetic perspective. *Phytochemistry*, 64(1):3–19, 2003.

[162] A. Belle, A. Tanay, L. Bitincka, R. Shamir, and E. K. O'Shea. Quantification of protein half-lives in the budding yeast proteome. *Proc. Natl. Acad. Sci.*, 103(35):13004–13009, 2006.

[163] E O Powell. Growth rate and generation time of bacteria, with special reference to continuous culture. *J. Gen. Microbiol.*, 15(3):492–511, 1956.

[164] Simon A. Levin. Community equilibria and stability, and an extension of the competitive exclusion principle. *Am. Nat.*, 104(939):413–423, 1970.

[165] Peter Czuppon and Arne Traulsen. Fixation probabilities in populations under demographic fluctuations. *Journal of mathematical biology*, 77(4):1233–1277, 2018.

[166] Ron Larson. *Elementary linear algebra*. Nelson Education, 2016.

[167] Baruch Meerson and Pavel V. Sasorov. Noise-driven unlimited population growth. *Phys. Rev. E - Stat. Nonlinear, Soft Matter Phys.*, 78(6):2–5, 2008.

[168] Vlad Elgart and Alex Kamenev. Rare event statistics in reaction-diffusion systems. *Phys. Rev. E - Stat. Nonlinear, Soft Matter Phys.*, 70(4 1):1–12, 2004.

[169] Matthew Parker and Alex Kamenev. Extinction in the Lotka-Volterra model. *Phys. Rev. E*, 80(2):021129, 2009.

[170] Youfang Cao, Anna Terebus, and Jie Liang. State space truncation with quantified errors for accurate solutions to discrete chemical master equation. *Bull. Math. Biol.*, 78(4):617–661, 2016.

[171] Gaël Guennebaud, Benoît Jacob, et al. Eigen v3. http://eigen.tuxfamily.org, 2010.

[172] Charles M Grinstead and Laurie J Snell. *Introduction to Probability*. American Mathematical Society, Providence, RI, 2nd edition, 2003.

[173] BJ Matkowsky, Z Schuss, C Knessl, C Tier, and M Mangel. Asymptotic solution of the Kramers-Moyal equation and first-passage times for Markov jump processes. *Phys. Rev. A*, 29(6):3359, 1984.

[174] Gareth Baxter, Alan J. McKane, and Martin B. Tarlie. Quantifying stochastic outcomes. *Phys. Rev. E - Stat. Nonlinear, Soft Matter Phys.*, 71(1), 2005.

[175] Nils Berglund. Kramers' law: Validity, derivations and generalisations. *arXiv preprint arXiv:1106.5799*, 2011.

[176] A Shmida and S Ellner. Coexistence of plant-species with similar niches. *Vegetatio*, 58(1):29–55, 1984.

[177] Peter Abrams. The theory of limiting similarity. *Annu. Rev. Ecol. Syst.*, 14(1):359–376, 1983.

[178] Margaret M. Mayfield and Jonathan M. Levine. Opposing effects of competitive exclusion on the phylogenetic structure of communities. *Ecol. Lett.*, 13(9):1085–1093, 2010.

[179] Peter Ashcroft, Franziska Michor, and Tobias Galla. Stochastic tunneling and metastable states during the somatic evolution of cancer. *Genetics*, 199(4):1213–1228, 2015.

[180] Nicole M. Vega and Jeff Gore. Stochastic assembly produces heterogeneous communities in the Caenorhabditis elegans intestine. *PLoS Biol.*, 15(3):1–20, 2017.

[181] W Bez and P Talkner. A new variational method to calculate escape rates in bistable systems. *Phys. Lett. A*, 82(7):313–316, 1981.

[182] Jr Palmer, K. Kazmerzak, M. C. Hansen, and P. E. Kolenbrander. Mutualism versus independence: Strategies of mixed-species oral biofilms in vitro using saliva as the sole nutrient source. *Infect. Immun.*, 69(9):5794–5804, 2001.

[183] Benjamin E. Wolfe, Julie E. Button, Marcela Santarelli, and Rachel J. Dutton. Cheese rind communities provide tractable systems for in situ and in vitro studies of microbial diversity. *Cell*, 158(2):422–433, 2014.

[184] Paul J Hung, Philip J Lee, Poorya Sabounchi, Nima Aghdam, Robert Lin, and Luke P Lee. A novel high aspect ratio microfluidic design to provide a stable and uniform microenvironment for cell growth in a high throughput mammalian cell culture array. *Lab Chip*, 5(1):44–8, 2005.

[185] Robert H MacArthur and Edward O Wilson. An equilibrium theory of insular zoogeography. *Evolution*, 17(4):373–387, 1963.

[186] Sidhartha Goyal, Sanggu Kim, Irvin SY Chen, and Tom Chou. Mechanisms of blood homeostasis: lineage tracking and a neutral model of cell populations in rhesus macaques. *BMC Biol.*, 13(1):85, 2015.

[187] Michael M. Desai and Daniel S. Fisher. Beneficial mutation-selection balance and the effect of linkage on positive selection. *Genetics*, 176(3):1759–1798, 2007.

[188] Jessica L. Green, Alan Hastings, Peter Arzberger, Francisco J. Ayala, Kathryn L. Cottingham, Kim Cuddington, Frank Davis, Jennifer a. Dunne, Marie-Josée Fortin, Leah Gerber, and Michael Neubert. Complexity in ecology and conservation: mathematical, statistical, and computational challenges. *Bioscience*, 55(6):501–510, 2005.

[189] David Bickford, David J. Lohman, Navjot S. Sodhi, Peter K L Ng, Rudolf Meier, Kevin Winker, Krista K. Ingram, and Indraneil Das. Cryptic species as a window on diversity and conservation. *Trends Ecol. Evol.*, 22(3):148–155, 2007.

[190] Motoo Kimura. Theoretical foundation of population genetics at the molecular level. *Theoretical population biology*, 208:174–208, 1971.

[191] Tadeusz J. Kawecki and Dieter Ebert. Conceptual issues in local adaptation. *Ecol. Lett.*, 7(12):1225–1241, 2004.

[192] K. S. Korolev and David R. Nelson. Competition and cooperation in one-dimensional stepping-stone models. *Phys. Rev. Lett.*, 107(8):1–5, 2011.

[193] Pleuni S Pennings, Sergey Kryazhimskiy, and John Wakeley. Loss and recovery of genetic diversity in adapting populations of HIV. *PLoS Genet.*, 10(1):e1004000, jan 2014.

[194] Jeremy E Koenig, Aymé Spor, Nicholas Scalfone, Ashwana D Fricker, Jesse Stombaugh, Rob Knight, Largus T Angenent, and Ruth E Ley. Succession of microbial consortia in the developing infant gut microbiome. *Proc. Natl. Acad. Sci. U. S. A.*, 108 Suppl:4578–4585, 2011.

[195] Guus Roeselers, Erika K. Mittge, W. Zac Stephens, David M. Parichy, Colleen M. Cavanaugh, Karen Guillemin, and John F. Rawls. Evidence for a core gut microbiota in the zebrafish. *ISME J.*, 5(10):1595–1608, 2011.

[196] Charles K. Fisher and Pankaj Mehta. Identifying keystone species in the human gut microbiome from metagenomic timeseries using sparse linear regression. *PLoS One*, 9(7):1–10, 2014.

[197] Jukka Corander, Christophe Fraser, Michael U. Gutmann, Brian Arnold, William P. Hanage, Stephen D. Bentley, Marc Lipsitch, and Nicholas J. Croucher. Frequency-dependent selection in vaccine-associated pneumococcal population dynamics. *Nat. Ecol. Evol.*, 1(12):1950–1960, 2017.

[198] Daniel R Amor, Christoph Ratzke, and Jeff Gore. Transient invaders can induce shifts between alternative stable states of microbial communities. *BioRxiv*, page 659052, 2019.

[199] Paula C Dias. Sources and sinks in population biology. *Trends Ecol. Evol.*, 11(8):326–330, 1996.

[200] Ian T. Carroll and Roger M. Nisbet. Departures from neutrality induced by niche and relative fitness differences. *Theor. Ecol.*, 8(4):449–465, 2015.

[201] Peter L. Chesson and Nancy Huntly. The roles of harsh and fluctuating conditions in the dynamics of ecological communities. *Am. Nat.*, 150(5):519–553, 1997.

[202] Z Patwa and L M Wahl. The fixation probability of beneficial mutations. *J. R. Soc. Interface*, 5(28):1279–89, nov 2008.

[203] Bahram Houchmandzadeh and Marcel Vallade. Alternative to the diffusion equation in population genetics. *Phys. Rev. E - Stat. Nonlinear, Soft Matter Phys.*, 82(5):1–8, 2010.

[204] Alison M Etheridge, Robert C Griffiths, and Jesse E Taylor. A coalescent dual process in a Moran model with genic selection, and the lambda coalescent limit. *Theor. Popul. Biol.*, 78(2):77–92, Sep 2010.

[205] Graham Bell. The distribution of abundance in neutral communities. *Am. Nat.*, 155(5):606–617, 2000.

[206] Christine Taylor, Drew Fudenberg, Akira Sasaki, and Martin a Nowak. Evolutionary game dynamics in finite populations. *Bull. Math. Biol.*, 66(6):1621–44, nov 2004.

[207] Jens Claussen and Arne Traulsen. Non-Gaussian fluctuations arising from finite populations: Exact results for the evolutionary Moran process. *Phys. Rev. E*, 71(2):025101, feb 2005.

[208] H Allen Orr. The genetic theory of adaptation: a brief history. *Nat. Rev. Genet.*, 6(2):119–27, feb 2005.

[209] Michael M. Desai, Daniel S. Fisher, and Andrew W. Murray. The speed of evolution and maintenance of variation in asexual populations. *Curr. Biol.*, 17(5):385–394, 2007.

[210] Nana-Maria Grüning, Hans Lehrach, and Markus Ralser. Regulatory crosstalk of the metabolic network. *Trends in biochemical sciences*, 35(4):220–227, 2010.

[211] Mordechai Liscovitch. Crosstalk among multiple signal-activated phospholipases. *Trends in biochemical sciences*, 17(10):393–399, 1992.

[212] John Caperon. Population growth in micro-organisms limited by food. *Ecology*, 48(5):715–722, 1967.

[213] Jeff Gore, Hyun Youk, and Alexander van Oudenaarden. Snowdrift game dynamics and facultative cheating in yeast. *Nature*, 459(7244):253–6, may 2009.

[214] Erwin Frey. Evolutionary game theory: Theoretical concepts and applications to microbial communities. *Phys. A Stat. Mech. its Appl.*, 389(20):4265–4298, 2010.

[215] Clare I. Abreu, Jonathan Friedman, Vilhelm L. Andersen Woltz, and Jeff Gore. Mortality causes universal changes in microbial community composition. *Nat. Commun.*, 10(1), 2019.

[216] R. Durrett and S. A. Levin. Stochastic spatial models: a user's guide to ecological applications. *Philos. Trans. R. Soc. B Biol. Sci.*, 343(1305):329–350, Feb 1994.

[217] David Tilman. *Spatial ecology.* Princeton University Press, Princeton, New Jersey, 1997.

[218] D. T. Haydon, N. C. Stenseth, M. S. Boyce, and P. E. Greenwood. Phase coupling and synchrony in the spatiotemporal dynamics of muskrat and mink populations across Canada. *Proc. Natl. Acad. Sci.*, 98(23):13149–13154, 2001.

[219] Bahram Houchmandzadeh, Eric Wieschaus, and Stanislas Leibler. Establishment of developmental precision and proportions in the early Drosophila embryo. *Nature*, 415(6873):798–802, 2002.

[220] Aaron R. Wheeler, William R. Throndset, Rebecca J. Whelan, Andrew M. Leach, Richard N. Zare, Yish Hann Liao, Kevin Farrell, Ian D. Manger, and Antoine Daridon. Microfluidic device for single-cell analysis. *Anal. Chem.*, 75(14):3581–3586, 2003.

[221] Alex Groisman, Caroline Lobo, HoJung Cho, J Kyle Campbell, Yann S Dufour, Ann M Stevens, and Andre Levchenko. A microfluidic chemostat for experiments with bacterial and yeast cells. *Nature methods*, 2(9):685, 2005.

[222] Ping Wang, Lydia Robert, James Pelletier, Wei Lien Dang, Francois Taddei, Andrew Wright, and Suckjoon Jun. Robust growth of Escherichia coli. *Curr. Biol.*, 20(12):1099–1103, 2010.

[223] S. S. Lee, I. A. Vizcarra, D. H. E. W. Huberts, L. P. Lee, and M. Heinemann. Whole lifespan microscopic observation of budding yeast aging through a microfluidic dissection platform. *Proc. Natl. Acad. Sci.*, 109(13):4916–4920, 2012.

[224] Alexander Grunberger, Wolfgang Wiechert, and Dietrich Kohlheyer. Single-cell microfluidics : opportunity for bioprocess development. *Curr. Opin. Biotechnol.*, 29:15–23, 2014.

[225] Motoo Kimura. A simple method for estimating evolutionary rates of base substitutions through comparitive studies of nucleotide sequences. *J. Mol. Evol.*, 16:111–120, 1980.

[226] Gloria del Solar, Rafael Giraldo, Maria Jesus Ruiz-Echevarria, Manuel Espinosa, and Ramon Diaz-Orejas. Replication and control of circular bacterial plasmids. *Microbiol. Mol. Biol. Rev.*, 62(2):434–464, 1998.

[227] GS Michaels, WW Hauswirth, and PJ Laipis. Mitochondrial dna copy number in bovine oocytes and somatic cells. *Developmental biology*, 94(1):246–251, 1982.

[228] Robert C Shuster, Andrew J Rubenstein, and Douglas C Wallace. Mitochondrial dna in anucleate human blood cells. *Biochemical and biophysical research communications*, 155(3):1360–1365, 1988.

[229] Jan-Willem Taanman. The mitochondrial genome: structure, transcription, translation and replication. *Biochimica et Biophysica Acta (BBA)-Bioenergetics*, 1410(2):103–123, 1999.

[230] Manoshi S. Datta, Elzbieta Sliwerska, Jeff Gore, Martin F. Polz, and Otto X. Cordero. Microbial interactions lead to rapid micro-scale successions on model marine particles. *Nat. Commun.*, 7(May):1–7, 2016.

[231] Robert E Ricklefs. The neutral theory of biodiversity: do the numbers add up. *Ecology*, 87(6):1424–1431, 2006.

[232] I. D. Ofiteru, M. Lunn, T. P. Curtis, G. F. Wells, C. S. Criddle, C. A. Francis, and W. T. Sloan. Combined niche and neutral effects in a microbial wastewater treatment community. *Proc. Natl. Acad. Sci.*, 107(35):15345–15350, 2010.

[233] Brian McGill and Cathy Collins. A unified theory for macroecology based on spatial patterns of abundance. *Evol. Ecol. Res.*, 5(4):469–492, 2003.

[234] Steven H Strogatz. *Nonlinear dynamics and chaos*. Perseus Books, Reading, Massachusetts, 1994.

[235] George W. A. Constable, Tim Rogers, Alan J. McKane, and Corina E. Tarnita. Demographic noise can reverse the direction of deterministic selection. *Proceedings of the National Academy of Sciences*, 2016.

[236] Motoo Kimura and Tomoko Ohta. The average number of generations until fixation of a mutant gene in a finite population. *Genetics*, 61(692):763–771, 1969.

[237] Jeffrey D Jensen. On the unfounded enthusiasm for soft selective sweeps, 2014.

[238] Benjamin Kerr, Margaret a Riley, Marcus W Feldman, and Brendan J M Bohannan. Local dispersal promotes biodiversity in a real-life game of rock-paper-scissors. *Nature*, 418(6894):171–4, Jul 2002.

[239] Benjamin C Kirkup and Margaret a Riley. Antibiotic-mediated antagonism leads to a bacterial game of rock-paper-scissors in vivo. *Nature*, 428(6981):412–4, mar 2004.

[240] Maximilian Berr, Tobias Reichenbach, Martin Schottenloher, and Erwin Frey. Zero-one survival behavior of cyclically competing species. *Phys. Rev. Lett.*, 102(4):048102, Jan 2009.

[241] Saikrishna Gadhamsetty, Joost B. Beltman, and Rob J. de Boer. What do mathematical models tell us about killing rates during HIV-1 infection? *Immunol. Lett.*, 168(1):1–6, 2015.

[242] Marta Luksza and Michael Lässig. A predictive fitness model for influenza. *Nature*, 507(7490):57–61, 2014.

[243] T W Shoener. Resource partitioning in ecological communities. *Science (80-.).*, 185:27–39, 1974.

[244] Joao B Xavier and Kevin R Foster. Cooperation and conflict in microbial biofilms. *Proceedings of the National Academy of Sciences*, 104(3):876–881, 2007.

[245] Mario Castro, Grant Lythe, Carmen Molina-París, and Ruy M. Ribeiro. Mathematics in modern immunology. *Interface Focus*, 6(2):14, 2016.

Chapter 7

Appendix

Approximations to the one species logistic system

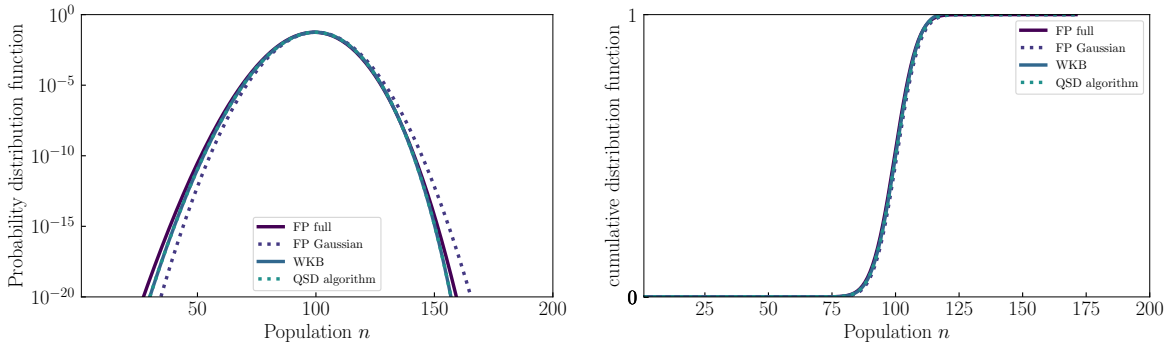

Figure 7.1: *Approximation techniques for calculating the QSD.* Carrying capacity $K = 100$, $\delta = 0.4$ and $q = 0.7$. *Left:* The quasi-stationary probability distribution function is calculated using the QSD algorithm, and approximated with the Fokker-Planck equation, Fokker-Planck Gaussian approximation, and WKB method. *Right:* The corresponding cumulative distribution function.

The probability density function given by the quasi-stationary distribution is not itself a probability, rather integrating over some region of its domain gives the probability of the population being in that region [78]. For this reason it is often more instructive to consider the cumulative distribution function, $cdf(n) = \int_0^n dx\, pdf(x)$, which gives a true probability, the probability of the system being at that population or less [78]. However, in this case it is not useful for distinguishing the different approximation techniques. The cumulative distribution function changes most rapidly at the peak of the QSD, but this peak is exactly where all the methods tend to agree, so any differences between them will be lost in the low and high cumulative populations, near probabilities zero and one respectively.

This combination of four figures, similar to the right panel of figure 2.6, shows some of the approximation methods discussed in chapter 2 applied to the mean time to extinction (MTE) of a single species logistic model as defined by the rates in equations 2.2 and 2.3. The regular Fokker-Planck approximation involves numerical integration and shows convergence issues except at low K and so it is only occasionally plotted; based on the low K results for which it converges it is a reasonable approximation at high δ, for all values of the competition mechanism parameter q. The Gaussian approximation to the

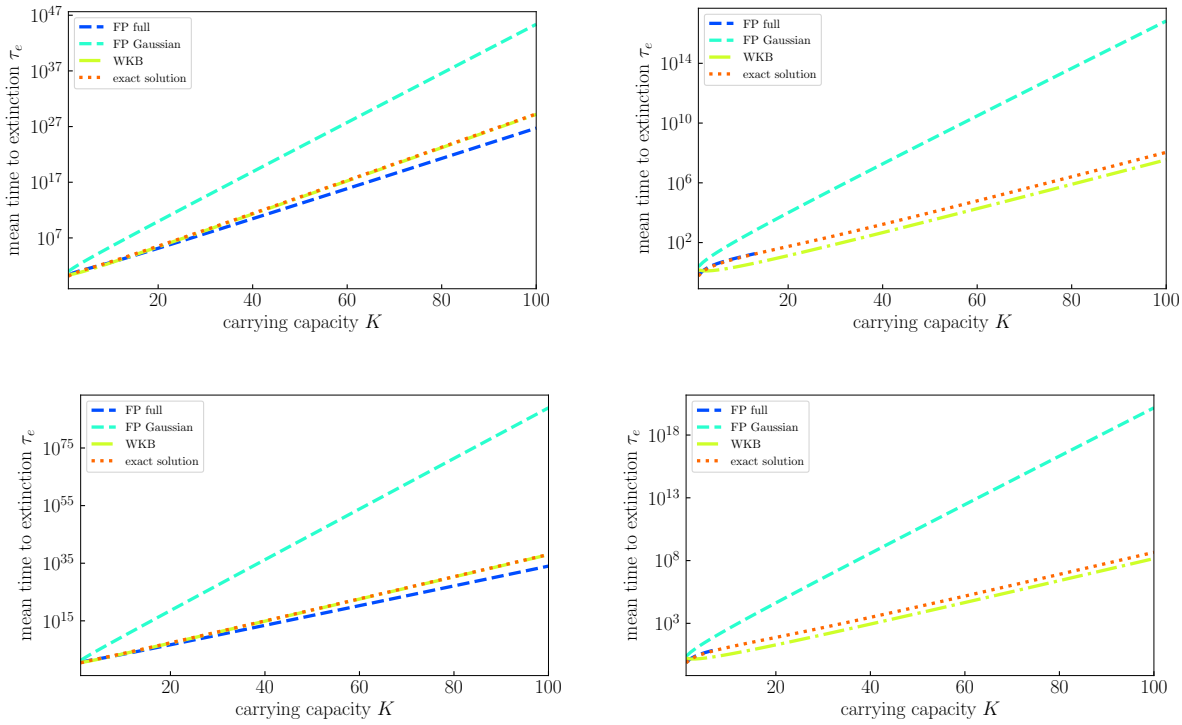

Figure 7.2: *Approximations of the MTE in various regimes of parameter space.* The approximations employed generally are parallel to the exact solution on this log-linear plot, implying that they capture the same exponential dependence on carrying capacity, but unless they are coincident get the prefactor incorrect. *Upper Left:* $q = 0.2$, $\delta = 0.4$. *Upper Right:* $q = 0.2$, $\delta = 4.0$. *Lower Left:* $q = 0.7$, $\delta = 0.4$. *Lower Right:* $q = 0.7$, $\delta = 4.0$.

Fokker-Planck equation always performs poorly. The WKB method works well when δ is small, but is off by a significant factor for large δ. The success of an approximation technique does not seem to depend on the mechanism of competition as parameterized by q, as shown in the following pair of graphs.

Exact and approximate mean extinction time for a single stochastic logistic model

A one dimensional logistic process has birth rate $b(n) = r\,n$ and death rate $d(n) = r\,n\frac{n}{K}$. The mean extinction time $\tau[n_0]$ depends on the initial state n_0. The mean extinction times for different initial state n_0 obey the usual backward recursion relation [78]

$$\tau[n_0] = \frac{1}{b(n_0) + d(n_0)} + \frac{b(n_0)}{b(n_0) + d(n_0)}\tau[n_0 + 1] + \frac{d(n_0)}{b(n_0) + d(n_0)}\tau[n_0 - 1]. \tag{7.1}$$

Some rearrangement and defining of terms allows the writing of the difference relation

$$\tau[n_0 + 1] - \tau[n_0] = \left(\tau[1] - \sum_{i=1}^{n_0} q_i\right) S_{n_0}, \tag{7.2}$$

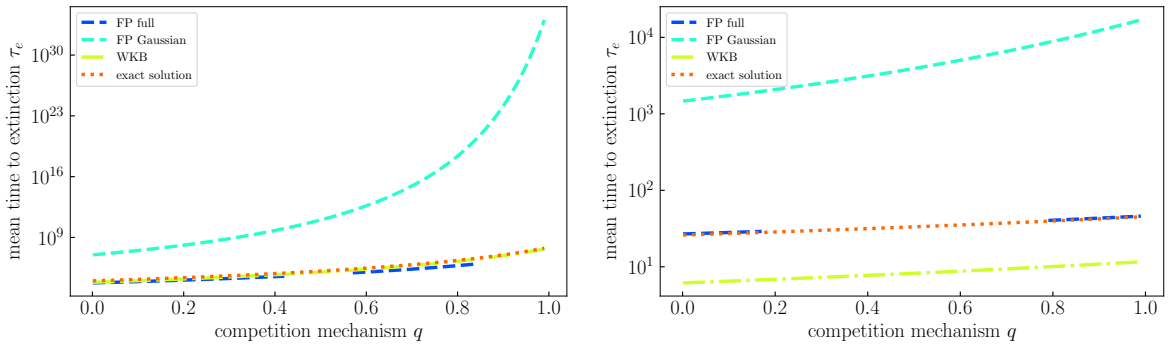

Figure 7.3: *Approximation techniques as they depend on the competition mechanism.* Carrying capacity $K = 16$, q varying, and $\delta = 0.4$ (left) or 4 (right). Whether an approximation technique is correct or not does not depend on q.

where

$$q_0 = \frac{1}{b(0)} \quad q_1 = \frac{1}{d(1)}, \tag{7.3}$$

$$q_i = \frac{b(i-1)\cdots b(1)}{d(i)d(i-1)\cdots d(1)} = \frac{1}{d(i)} \prod_{j=1}^{i-1} \frac{b(j)}{d(j)}, \; i > 1,$$

and

$$S_i = \frac{d(i)\cdots d(1)}{b(i)\cdots b(1)} = \prod_{j=1}^{i} \frac{d(j)}{b(j)}. \tag{7.4}$$

If the process does indeed go extinct and in finite time then the extinction time can be written as follows [78]:

$$\tau[n_0] = \sum_{i=1}^{\infty} q_i + \sum_{j=1}^{n_0-1} S_j \sum_{i=j+1}^{\infty} q_i. \tag{7.5}$$

Evaluating this sum with $b(n) = rn$, $d(n) = rn^2/K$ and the initial condition $n_0 = K \gg 1$ with the help of the integral tables of Mathematica gives

$$r\,\tau \simeq -\gamma - \Gamma[0, -K] - \ln[K].$$

which has the asymptotic limit [95, 113]

$$r\,\tau \simeq \frac{1}{K} e^K \tag{7.6}$$

to leading order. Including δ (but $q = 0$) gives $r\,\tau \sim \frac{K\,{}_pF_q[1,1,2,2+\delta K,(1+\delta)K]}{1+\delta K}$ and inclusion of both δ and q gives

$$r\,\tau \sim \frac{K\,{}_pF_q[1, 1, 1 - K/q - (\delta K)/q, 2, -(2/(-1+q)) - (\delta K)/(-1+q) + (2q)/(-1+q), q/(-1+q)]}{1 + \delta K - q}, \tag{7.7}$$

where ${}_pF_q$ is the generalized hypergeometric function, the sum of a series of ratios of increasing products. If the summation in the MTE (also in equation **??**) goes to some finite N the result is a difference of hypergeometric functions, but numerically evaluating the single hypergeometric or the difference of the two gives practically similar results.

Single logistic model with Fokker-Planck and WKB approximations

The Fokker-Planck equation for extinction time is [78]

$$-\frac{1}{r} = \frac{n}{K}(K-n)\frac{\partial \tau_{FP}}{\partial n} + \frac{1}{2}\frac{n}{K}(K+n)\frac{\partial^2 \tau_{FP}}{\partial n^2}. \tag{7.8}$$

The solution to this equation is

$$r\,\tau_{FP}[n_0] = \int_0^{n_0} dn \frac{\int_n^\infty dm \frac{2K}{m(K+m)} \exp[\int_0^m dn' \frac{2(K-n')}{(K+n')}]}{\exp[\int_0^n dm \frac{2(K-m)}{(K+m)}]}. \tag{7.9}$$

It is difficult to solve analytically. If we approximate the underlying population distribution as Gaussian [78], however, an analytic solution for $\delta, q = 0$ is easy to obtain:

$$r\,\tau_{FP} \approx 2\sqrt{2\pi K}e^{K/2}. \tag{7.10}$$

Let me sketch out a derivation of all these approximations, in brief, following Nisbet and Gurney [78]. Assume that, after an initial time of relaxing from the initial condition, the probability density function decays to extinction exponentially. That is,

$$p(0,t) = 1 - \exp\{-t/\tau_e\}, \tag{7.11}$$

$$p(n,t) = \mathcal{P}_0(n)\exp\{-t/\tau_e\}. \tag{7.12}$$

The distribution $\mathcal{P}_0(n)$ acts as a sort of initial distribution after relaxation from the real initial condition has occurred. We assume it is normalized between 0^+ and ∞. But note that

$$p^c(n,t) \equiv \frac{p(n,t)}{1-p(0,t)} = \frac{\mathcal{P}_0(n)\exp\{-t/\tau_e\}}{1-(1-\exp\{-t/\tau_e\})} = \mathcal{P}_0(n) = \widetilde{p}^c(n). \tag{7.13}$$

Substituting $p(n,t)$ into the Fokker-Planck equation 7.8 and integrating from 0^+ to ∞ gives

$$\frac{1}{\tau_e} = \left[f(n)\widetilde{p}^c(n) - \frac{1}{2}\frac{\partial}{\partial n}[g(n)\widetilde{p}^c(n)]\right]\Bigg|_{n=0}^{n=\infty}, \tag{7.14}$$

recalling $f(n) = b_n - d_n$ and $g(n) = b_n + d_n$. Since $f(0) = 0$, $g(0) = 0$, $\widetilde{p}^c(n=\infty) = 0$, and typically $\frac{d\widetilde{p}^c(n=\infty)}{dn} = 0$, the above equation reduces to

$$\tau_e = 2\left(\widetilde{p}^c(0)\frac{dg(n)}{dn}\bigg|_{n=0}\right)^{-1}. \tag{7.15}$$

Solving this requires the extrapolation of $\widetilde{p}^c(n)$ to $n = 0$. By linearizing about the fixed point the quasi-stationary distribution can be replaced by a Gaussian [78]

$$\widetilde{p}^c(n) = \frac{1}{\sqrt{2\pi\sigma^2}}\exp\Big\{-\frac{(n-K)^2}{2\sigma^2}\Big\}, \tag{7.16}$$

the variance of which is given by $\sigma^2 = -g(K)/\left(2\frac{df}{dn}\Big|_{n=K}\right)$ Then

$$\tau_e = 2\sqrt{2\pi\sigma^2}\left(\frac{dg(n)}{dn}\Big|_{n=0}\right)^{-1}\exp\left\{\frac{(K)^2}{2\sigma^2}\right\}, \tag{7.17}$$

which gives equation 7.10 for $\delta, q = 0$ and equation **??** more generally.

The WKB approximation can also estimate the mean time to extinction [103]. It assumes a quasi-steady state population probability distribution of

$$P_n \propto \exp\left[-K\sum_{i=0}^{\infty}\frac{S_i(n)}{K^i}\right], \tag{7.18}$$

but properly normalized. The extinction time is estimated from the quasi-steady state distribution as $\tau \approx 1/(d(1)P_1)$ [78, 103]. Including only the $S_0\int_{n=0}^{K}\ln\left(\frac{b_n}{d_n}\right)$ term for $\delta, q = 0$ gives

$$r\,\tau_{WKB} = \sqrt{2\pi K}e^{-1}e^{K}. \tag{7.19}$$

Comparing to the asymptotic solution of equation 7.6, the Fokker-Planck equation with the further Gaussian approximation does not get the exponential scaling correct, being off by a factor of 1/2 on a log-linear plot. The WKB approximation at least gets the correct exponential scaling. However, it gets an incorrect prefactor, being $\propto \sqrt{K}$ rather than $\propto K^{-1}$ as shown to be asymptotically correct for equation 7.6. I include these considerations for $\delta, q = 0$ to clarify the way in which these approximation methods fail.

Time step correspondence between the Moran and coupled logistic models

Given that the Moran model time step corresponds to one birth and one death event, I make the comparison between it and the generalized stochastic Lotka-Voterra model with the estimate

$$\Delta t \approx \frac{1}{\big(b_1\left(x_1, K-x_1\right) + b_2\left(x_1, K-x_1\right)\big)/2 + \big(d_1\left(x_1, K-x_1\right) + d_2\left(x_1, K-x_1\right)\big)/2} \tag{7.20}$$

where b_i and d_i are the birth and death rates of the coupled logistic model. The line $x_2 = K - x_1$ is the Moran line, on which the system spends most of its time. The average time of one Moran time step is the sum of the average of one birth and one death. This gives $\Delta t \approx 1/K$ as found in the main text.

The 2D Fokker-Planck equation is not a potential system

The most common approximation to the master equation is Fokker-Planck, which assumes the state space is continuous. I attempt its use here to get an analytic estimate of the dependence of fixation time on K and a. We shall see that its utility is only marginal, though with some further approximations and an application of Kramers' theory I get my desired estimate.

The Fokker-Planck approximation to the coupled logistic system studied herein takes its traditional

form [78]:

$$\begin{aligned}\frac{dP}{dt} &= -\partial_1[(b_1-d_1)P] - \partial_2[(b_2-d_2)P] + \frac{1}{2}\partial_1^2[(b_1+d_1)P] + \frac{1}{2}\partial_2^2[(b_2+d_2)P] \\ &= -\sum_i \partial_i F_i P + \sum_{i,j}\partial_i\partial_j D_{ij} P \end{aligned} \tag{7.21}$$

where F is the force vector and D is the diffusion matrix (in this case diagonal). Here, under symmetric conditions and nondimensionalization by r, $F_1 = \frac{x_1}{K}(K - x_1 - ax_2)$ and $D_{11} = \frac{x_1}{K}(K + x_1 + ax_2)$, with similar terms for species 2.

We want to write these force terms using a scalar potential, $F = -\nabla U$. If this were possible, it would imply that $\nabla \times F = -\nabla \times \nabla U = 0$. However,

$$\begin{aligned}|\nabla \times F| &= |\partial_1 F_2 - \partial_2 F_1| \\ &= |-a_{21}x_2/K + a_{12}x_1/K| \\ &\neq 0.\end{aligned}$$

The steady state solution of equation 3.24 would solve

$$\partial_i \log P = \sum_k (D^{-1})_{ik}\big(2F_k - \sum_j \partial_j D_{kj}\big) \equiv -\partial_i U,$$

where the final equivalence would define a potential for the system. However, for consistency this requires $\partial_j(-\partial_i U) = \partial_i(-\partial_j U)$ and it is easy to show that this is not upheld for the two directions unless $a_{12} = a_{21} = 0$ and the system can be decomposed into two one-dimensional logistic systems. Effectively there is a non-zero curl in the system which disallows the writing of a potential unless it is simply a product of two independent systems.

Though a potential cannot be written in our system, similar quantities can be constructed. In particular, we want to define

$$U(x_1, x_2) \equiv -\ln\left[P(x_1, x_2, t \to \infty)\right]. \tag{7.22}$$

Rather than getting this quasi-steady state probability from numerics, I approximate it by linearizing the Fokker-Planck equation (3.24) about the deterministic coexistence fixed point [79]. This linearized equation is

$$\partial_t P = -\sum_{i,j} A_{ij}\partial_i x_j P + \sum_{i,j} B_{ij}\partial_i\partial_j x_i x_j P \tag{7.23}$$

where $A_{ij} = \partial_j F_i|_{\vec{x}=\vec{x}^*}$ and $B_{ij} = D_{ij}|_{\vec{x}=\vec{x}^*}$. The solution to Equation 3.26 is $P = \frac{1}{2\pi}\frac{1}{|C|^{1/2}}\exp[-(\vec{x} - \vec{x}^*)^T C^{-1}(\vec{x} - \vec{x}^*)/2]$, a Gaussian centered on the coexistence point and with a variance given by the covariance matrix C. For the $a_{12} = a_{21} = a$, $K_1 = K_2 = K$ symmetric case the diagonal term of C is $\frac{1}{1-a^2}K$ and the off-diagonal, which corresponds to the correlation between the two species, is $-\frac{a}{1-a^2}K$. Since we now have a probability density, I can write our pseudo-potential from equation 3.25.

With a pseudo-potential we can employ Kramers' theory, which states that the logarithm of the exit time should be proportional to the depth of this potential [107]. By defining our starting point as the coexistence fixed point and estimating the exit to happen at one of the axial fixed points (eg. $(0, K)$) I

get a well depth of

$$\Delta U = \frac{(1-a)}{2(1+a)}K. \tag{7.24}$$

As expected, the well depth is proportional to carrying capacity K. Even the Gaussian approximation to the already approximate Fokker-Planck equation shows the extinction time scaling exponentially with K. What is more, the exponential scaling disappears as niche overlap a approaches unity, just as with the ansatz (shown in the left panel of figure 3.5). The correlation between the two species diverges in this parameter limit, such that they are entirely anti-correlated. Whereas the well has a single lowest point at the coexistence fixed point for partial niche overlap, at $a = 1$ the potential shows a trough of equal depth going between the two axial fixed points. This is the Moran line, along which diffusion is unbiased; diffusion away from the Moran line is restored, as the system is drawn toward the bottom of the trough.

Dynamical properties of Moran model with immigration

Define the temporary extinction probability E_i as the probability that the focal species goes extinct in this modified system with absorbing states at $n = 0$ and $n = N$, *i.e.* the system reaches the former before the latter, given that it starts at $n = i$. Then $E_i = \frac{b(i)}{b(i)+d(i)}E_{i+1} + \frac{d(i)}{b(i)+d(i)}E_{i-1}$. Further define $S_i = \frac{d(i)\cdots d(1)}{b(i)\cdots b(1)}$. Then

$$E_i = \frac{\sum_{j=i}^{K-1} S_j}{1+\sum_{j=1}^{K-1} S_j}. \tag{7.25}$$

As with the stationary distribution, the extinction probabilities can be written explicitly in terms of K, ν, and g, but the solution has an even less nice form. The numerator $\sum_{j=i}^{K-1} S_j$ is

$$\begin{aligned} &{}_3F_2\left[\{1,2,\frac{2-K-2\nu+gK\nu}{1-\nu}\},\{2-K,\frac{2-2\nu+gK\nu}{1-\nu}\},1\right]\frac{K-1+\nu-gK\nu}{(K-1)(1-\nu+gK\nu)} \\ &-\Gamma[K+1]{}_2F_1\left[K+1,\frac{1-\nu-K\nu+gK\nu}{1-\nu},\frac{1+K-\nu-K\nu+gK\nu}{1-\nu},1\right] \\ &\times\frac{Pochhammer[(1-\nu-K+gK\nu)/(1-\nu),K]}{Pochhammer[1-K,K]Pochhammer[1+(gK\nu)/(1-\nu),K]} \end{aligned} \tag{7.26}$$

where $Pochhammer[a,n] = (a)_n = \Gamma(a+n)/\Gamma(a)$, $\Gamma(n) = (n-1)! = \int_0^\infty t^{n-1}e^{-t}dt$, and the generalized hypergeometric function ${}_pF_q$ is defined as normal. The denominator is just the numerator plus one, and together these define the extinction probability.

Similar to the extinction probabilities, we can write the unconditioned mean first passage time to either temporary fixation or extinction of the focal species [78]:

$$\tau[j] = \sum_{k=1}^{K-1} q_k + \sum_{i=1}^{j-1} S_i \sum_{k=i+1}^{K-1} q_k. \tag{7.27}$$

Mathematica with its tables of sums gives

$$\begin{aligned}\tau[j] =& -\frac{K^2}{-\nu+K(g\nu-1)+1}\\ &+\sum_{j=2}^{n-1}\frac{\Lambda}{(1-K)_j\left(1-\frac{gK\nu}{\nu-1}\right)_j}+\frac{M}{(g-1)g\nu(-\nu+K(g\nu-1)+1)\Gamma(K)\left(\frac{-g\nu K+K+\nu-1}{\nu-1}\right)_{K-1}}\\ &+\frac{W}{(g-1)g(K-1)\nu((gK-1)\nu+1)(-\nu+K(g\nu-1)+1)\Gamma(K)\left(\frac{-g\nu K+K+\nu-1}{\nu-1}\right)_{K-1}}\end{aligned}$$

where

$$\begin{aligned}\Lambda =&\Gamma(j+1)\left(\frac{-g\nu K+K+\nu-1}{\nu-1}\right)_j\\ &\times\Big(\frac{\Psi}{(g-1)g\nu(-\nu+K(g\nu-1)+1)\Gamma(K)\left(\frac{-g\nu K+K+\nu-1}{\nu-1}\right)_{K-1}}\\ &-\frac{\Phi}{g(j+1)\nu(-\nu+K(g\nu-1)+1)(-\nu j+j-\nu+K(g\nu-1)+1)\Gamma(j+1)\left(\frac{-g\nu K+K+\nu-1}{\nu-1}\right)_j}\Big)\end{aligned}$$

and

$$\begin{aligned}\Psi =&g(-\nu+K(g\nu-1)+1)(1-K)_{K-1}\left(1-\frac{gK\nu}{\nu-1}\right)_{K-1}\\ &+(g-1)\Gamma(K)\left(g\nu K^2-g\nu K+K+\nu+(-\nu+K(g\nu-1)+1)\,{}_2F_1\left(-K,-\frac{gK\nu}{\nu-1};\frac{-g\nu K+K+\nu-1}{\nu-1};1\right)-1\right)\\ &\times\left(\frac{-g\nu K+K+\nu-1}{\nu-1}\right)_{K-1}\end{aligned}$$

and

$$\begin{aligned}\Phi =&gK^2\nu(-\nu+K(g\nu-1)+1)\\ &\times{}_3F_2\left(1,j-K+1,\frac{\nu j-j+\nu-gK\nu-1}{\nu-1};j+2,\frac{\nu j-j+2\nu+K-gK\nu-2}{\nu-1};1\right)(1-K)_j\left(1-\frac{gK\nu}{\nu-1}\right)_j\\ &-(j+1)(-g\nu K+K+j(\nu-1)+\nu-1)\Gamma(j+1)\left(\frac{-g\nu K+K+\nu-1}{\nu-1}\right)_j\\ &\times\left(g\nu K^2-g\nu K+K+\nu+(-\nu+K(g\nu-1)+1)\,{}_2F_1\left(-K,-\frac{gK\nu}{\nu-1};\frac{-g\nu K+K+\nu-1}{\nu-1};1\right)-1\right),\end{aligned}$$

$$\begin{aligned}M =&g(-\nu+K(g\nu-1)+1)(1-K)_{K-1}\left(1-\frac{gK\nu}{\nu-1}\right)_{K-1}\\ &+(g-1)\Gamma(K)\left(g\nu K^2-g\nu K+K+\nu+(-\nu+K(g\nu-1)+1)\,{}_2F_1\left(-K,-\frac{gK\nu}{\nu-1};\frac{-g\nu K+K+\nu-1}{\nu-1};1\right)-1\right)\\ &\times\left(\frac{-g\nu K+K+\nu-1}{\nu-1}\right)_{K-1}.\end{aligned}$$

and

$$W = (-g\nu K + K + \nu - 1)\Bigg(g(-\nu + K(g\nu - 1) + 1)(1 - K)_{K-1}\left(1 - \frac{gK\nu}{\nu - 1}\right)_{K-1} + (g-1)\Gamma(K)$$
$$\times \left(g\nu K^2 - g\nu K + K + \nu + (-\nu + K(g\nu - 1) + 1)\,{}_2F_1\left(-K, -\frac{gK\nu}{\nu - 1}; \frac{-g\nu K + K + \nu - 1}{\nu - 1}; 1\right) - 1\right)$$
$$\times \left(\frac{-g\nu K + K + \nu - 1}{\nu - 1}\right)_{K-1}\Bigg)$$